

ระบาดวิทยา การพัฒนาการตรวจวินิจฉัยระดับโมเลกุลของเชื้อฮิวแมนเอนเทอโรไวรัส และการเกิด  
รีคอมบิเนชันและวิวัฒนาการของเชื้อฮิวแมนคอกแซกกีไวรัส เอ6



นางสาวจิรัชญา พันผา

จุฬาลงกรณ์มหาวิทยาลัย  
CHULALONGKORN UNIVERSITY

บทคัดย่อและแฟ้มข้อมูลฉบับเต็มของวิทยานิพนธ์ตั้งแต่ปีการศึกษา 2554 ที่ให้บริการในคลังปัญญาจุฬาฯ (CUIR)  
เป็นแฟ้มข้อมูลของนิสิตเจ้าของวิทยานิพนธ์ ที่ส่งผ่านทางบัณฑิตวิทยาลัย

The abstract and full text of theses from the academic year 2011 in Chulalongkorn University Intellectual Repository (CUIR)  
are the thesis authors' files submitted through the University Graduate School.

วิทยานิพนธ์นี้เป็นส่วนหนึ่งของการศึกษาตามหลักสูตรปริญญาวิทยาศาสตรดุษฎีบัณฑิต

สาขาวิชาวิทยาศาสตร์การแพทย์

คณะแพทยศาสตร์ จุฬาลงกรณ์มหาวิทยาลัย

ปีการศึกษา 2558

ลิขสิทธิ์ของจุฬาลงกรณ์มหาวิทยาลัย

Epidemiology, development of molecular diagnostic of human enterovirus and  
recombination and evolutionary dynamics of human coxsackievirus A6

Miss Jiratchaya Peunpa



A Dissertation Submitted in Partial Fulfillment of the Requirements  
for the Degree of Doctor of Philosophy Program in Medical Science

Faculty of Medicine

Chulalongkorn University

Academic Year 2015

Copyright of Chulalongkorn University

Thesis Title	Epidemiology, development of molecular diagnostic of human enterovirus and recombination and evolutionary dynamics of human coxsackievirus A6
By	Miss Jiratchaya Peunpa
Field of Study	Medical Science
Thesis Advisor	Professor Yong Poovorawan, M.D.

---

Accepted by the Faculty of Medicine, Chulalongkorn University in Partial Fulfillment of the Requirements for the Doctoral Degree

..... Dean of the Faculty of Medicine  
(Professor Suttipong Wacharasindhu, M.D.)

THESIS COMMITTEE

..... Chairman  
(Associate Professor Padet Siriyasatien, M.D.)

..... Thesis Advisor  
(Professor Yong Poovorawan, M.D.)

..... Examiner  
(Professor Duangporn Werawatganon, M.D.)

..... Examiner  
(Assistant Professor Sunchai Payungporn)

..... External Examiner  
(Associate Professor Teeraporn Chinchai)

วิจัยญา พื้นผา : ระบาตวทยา การพัฒนาการตรวจวจนิจฉัยระดับโมเลกุลของเชื้ออ้วแมนเอนเทอโรไวรัส และการเกดรีคอมบเนชัน และวฒนาการของเชื้ออ้วแมนคอกแซกกีไวรัส เอ6 (Epidemiology, development of molecular diagnostic of human enterovirus and recombination and evolutionary dynamics of human coxsackievirus A6) อ.ที่ปฏึกษาวทยาพนธ์หลัก : ศ. นพ. ยง ภู่วรรณ, 117 หน้า.

โรคมือ เท้า ปาก มีสาเหตุเกดจากเชื้อไวรัสในกลุ่มเอนเทอโรไวรัส สปีชีเอ ซึ่งมออยู่มากกว่า 20 สายพันธุ์ที่เป็นบญหาใหญ่ทาง เศรษฐกค สังคม ในประเทศไทยและทั่วโลก หนึ่งนไวรัสที่มีบพบาทล้าคญตอการเกดโรคค้อ เชื้อเอนเทอโรไวรัส 71 สามารถก่อให้เกดโรคแทรก ซ้อนทางระบบประสาทและสมองที่รุนแรงจนเป็นเหตุให้เสยชีวิตได้ บัจจุบันยังไม่มีวัคซีนและยารักษาที่มีประสิทธิภพ งานวจนิจมีวัตถุประสงค์ เพื่อศีกษาระบาตวทยาและการเปลยนแปลงสายพันธุ์ไวรัส มือ เท้า ปาก ที่เกดการระบาตในประเทศไทยในปี พ.ศ. 2555 เปรียบเทียบกับการ ระบาตในอดีตที่ผ่านมา โดยทำการตรวจวจนิจเคราะห์ตัวอย่างจากกลุ่มผู้ป่วยโรคมือ เท้า ปาก, โรคเฮอร์แปงไจนา และผู้ป่วยติดเชื้อในระบบ ทางเดินหายใจ ทำการตรวจหาเชื้ออ้วแมนเอนเทอโรไวรัส โดยอาศัยวจนิจการ semi-nested RT-PCR ผลการวจนิจพบว่ามีสามารถตรวจพบเชื้ออ้ว แมนเอนเทอโรไวรัสทั้งสิ้น 17 สายพันธุ์ (คอกซากกีไวรัส เอ 4, เอ 5, เอ 6, เอ 8, เอ 9, เอ 10, เอ 12, เอ 16, เอ 21, บี 1, บี 2, บี 4, บี 5, เอกโคไวรัส 7, 16, 25 และเอนเทอโรไวรัส 71) โดยเชื้อคอกซากกีไวรัส เอ 6 เป็นสายพันธุ์ที่พบมากที่สุดในกลุ่มผู้ป่วยโรคมือ เท้า ปากและผู้ป่วยติดเชื้อในระบบ ทางเดินหายใจ คิดเป็นร้อยละ 33.5 และร้อยละ 1.5 ตามลำดับ เชื้อคอกซากกีไวรัส เอ 8 พบมากที่สุดในกลุ่มผู้ป่วยโรคเฮอร์แปงไจนา คิด เป็นร้อยละ 19.3 ลักษณะการระบาตของเชื้อเอนเทอโรไวรัสในช่วงที่มีศีกษานี้พบว่ามีการกระจายตัวของเชื้อเอนเทอโรไวรัสตลอดทั้งปี และพบ มากที่สุดในเดือนกรกฎาคม ในกลุ่มผู้ป่วยทั้งสามกลุ่มเมื่อตรวจการติดเชื้อเอนเทอโรไวรัสมากที่สุดในเด็กอายุมากกว่าหรือเท่ากับ 1 ปี จากนั้นได้ ทำการพัฒนาการตรวจวจนิจฉัยระดับโมเลกุลของเชื้ออ้วแมนเอนเทอโรไวรัสโดยเฉพาะสายพันธุ์ที่พบในประเทศไทย ด้วยเทคนิค multiplex real-time RT-PCR ผลการศีกษาพบว่ามีในการทดสอบความจำเพาะและความไวของเทคนิค multiplex real-time RT-PCR พบว่า ไม่เกด cross reactivity ตอเชื้อไวรัสชนิดอื่นที่ก่อโรคทั้งในระบบทางเดินอาหารและทางเดินหายใจ แสดงให้เห็นว่าไพรเมอร์และโพรบในงานวจนิจนี้มีความจำเพาะสูงตอเชื้อเป้าหมาย และผลความไวของเทคนิคตอเชื้อเป้าหมาย พบว่า สามารถตรวจจับได้ในปริมาณ 10 copies/μl เมื่อ เปรียบเทียบประสิทธิภาพของเทคนิค multiplex real-time RT-PCR กับ conventional RT-PCR ในการตรวจหาเชื้อเอนเทอโรไวรัสจำนวน 1,313 ตัวอย่าง จากกลุ่มผู้ป่วยโรคมือ เท้า ปาก, โรคเฮอร์แปงไจนา ผลการวจนิจพบว่าเทคนิค multiplex real-time RT-PCR มีความไวและความจำเพาะในการตรวจจับเชื้ออ้วแมนเอนเทอโรไวรัสมากกว่าเทคนิค conventional RT-PCR ดังนั้น เทคนิค multiplex real-time RT-PCR ในงานวจนิจนี้มีประโยชน์สูงทั้งในด้านความเร็วในการตรวจวจนิจฉัยของโรค มีความจำเพาะและมีความไวตอเชื้ออ้วแมนเอนเทอโรไวรัส ซึ่งเป็นวิธี ที่เหมาะสมที่สุดที่จะนำมาใช้ในการควบคุมและป้องกันการระบาตของโรคมือเท้าปาก นอกจากนี้ ในช่วงระยะเวลาใกล้เคียงกันหลายๆ ประเทศก็ได้มีการรายงานอุบัติการณ์การเพิ่มขึ้นของการติดเชื้อคอกซากกีไวรัส เอ 6 ที่เกี่ยวข้องกับการเกดโรคมือ เท้า ปาก ซึ่งเริ่มมีรายงานการ ระบาตใหญ่ครั้งแรกที่ประเทศฟินแลนด์ในปี พ.ศ. 2551 พบว่าการติดเชื้อไวรัสสายพันธุ์นี้ มีแนวโน้มที่ผู้ป่วยจะแสดงอาการรุนแรงมากกว่าการ ติดเชื้ออ้วแมนเอนเทอโรไวรัสสายพันธุ์อื่นๆ งานวจนิจนี้ทำการศีกษาวฒนาการและการเกดรีคอมบเนชันของเชื้อคอกซากกีไวรัส เอ 6 โดยเก็บ ตัวอย่างจาก 5 ประเทศ ได้แก่ ไทย สวีเดน เดนมาร์ค สเปน และ เยอรมัน ผลการวจนิจพบว่า อัตราของการเปลยนแปลงทางวฒนาการของเชื้อ ไวรัสนี้เท่ากับ  $8.1 \times 10^{-3}$  จำนวนนิวคลีโอไทด์ที่ถูกแทนที่ตอหนึ่งตำแหน่งตอปี ในการเกดรีคอมบเนชันของเชื้อไวรัสนี้ในช่วงระยะเวลาต่างๆ พบว่าเกี่ยวข้องกับการแทนที่ของยีนที่ไม่ใชยีนโครงสร้าง เมื่อด้านนระยะเวลาที่ครั้งหนึ่งของเชื้อไวรัสนี้จะเกดรีคอมบเนชัน มีค่าเท่ากับ 3.1 ปี สรุปได้ว่าเกดการเกดความหลากหลายทางพันธุกรรมของเชื้อไวรัสนี้ใช้เวลาที่สั้นกว่าเชื้อเอนเทอโรไวรัส 71 นอกจากนี้ จุดที่เกดการรวมของจีโนมไทย (recombination breakpoint) ของเชื้อไวรัสนี้พบว่าเกดขึ้นที่บริเวณยีน 2A-2C และ 5' untranslated region กล่าวโดยสรุปงานวจนิจนี้แสดงให้เห็นถึงการเกดสายพันธุ์ใหม่ของเชื้อคอกซากกีไวรัส เอ 6 และทำให้เกิดการระบาตของโรคมือ เท้า ปากทั่วโลก

## 5574903830 : MAJOR MEDICAL SCIENCE

KEYWORDS: EPIDEMIOLOGY/ RECOMBINATION/ EVOLUTIONARY DYNAMICS/ HUMAN ENTEROVIRUS/ HUMAN COXSACKIEVIRUS A6

JIRATCHAYA PEUNPA: Epidemiology, development of molecular diagnostic of human enterovirus and recombination and evolutionary dynamics of human coxsackievirus A6. ADVISOR: PROF. YONG POOVORAWAN, M.D., 117 pp.

Hand, foot, and mouth disease (HFMD) is a common infectious disease caused by several genotypes of human enterovirus species A and represent a significant global public health concern. Enterovirus 71 (EV71) infections cause a deadly neurological disease for which no specific anti-viral drugs or vaccines has received regulatory approval. Published reports have described a dramatically increased incidence of coxsackievirus A6 (CV-A6) infections associated with HFMD since their occurrence in 2008 in Finland. The aim of this study was to evaluate the burden of human enteroviruses associated to HFMD and herpangina in patients and establish epidemiological profiles of these viruses in Thailand in 2012. Detection and genotype determination of enteroviruses were accomplished by reverse transcription-polymerase chain reaction and sequencing of the VP1 region. Enterovirus-positive samples were differentiated into 17 genotypes (CV-A 4, A5, A6, A8, A9, A10, A12, A16, A21, B1, B2, B4, B5, echovirus 7, 16, 25 and EV71). The result showed CV-A6 (33.5%), followed by CV-A 16 (9.4%) and EV71 (8.8%) as the most frequent genotypes in HFMD, CV-A 8 (19.3%) in herpangina and CAV6 (1.5%) in influenza like illness. Enterovirus infections were most prevalent during July with 34.4% in HFMD, 39.8% in herpangina and 1.6% in ILI. The higher enterovirus infection associated with HFMD and herpangina occurred in infants over one year-old. This represents the first report describing the circulation of multiple enteroviruses in Thailand. Furthermore, multiplex real-time PCR using TaqMan probes for broad detection of EVs and differentiation of EV71, CV-A6 and CV-A16 were developed and validated. The multiplex real-time PCR system which was run in two separate tubes was capable of screening and specific detection of the three selected enteroviruses, without cross-reactions with the other examined RNA viruses. The detection limit of the assays was 10 copies/μl for EV71, CV-A6, CV-A16 and panenterovirus. The overall diagnostic sensitivity, specificity, positive predictive value (PPV) and negative predictive value (NPV) of the multiplex rRT-PCR assay were greater than those of conventional RT-PCRs. The multiplex rRT-PCR assays provide the highly sensitive detection and rapid simultaneous typing of EV71, CV-A6 and CV-A16 thus rendering it feasible and attractive for large scale surveillance of EVs associated with HFMD outbreaks. Moreover, this study also investigated the relationship between these disease outbreaks with the evolutionary dynamics of CV-A6 and the appearance of novel recombinant forms (RFs) of the virus. Based on the analysis of the VP1 gene, the substitution rates of CV-A6 was estimated at  $8.1 \times 10^{-3}$  substitutions/site/year. There was an increasing likelihood between CV-A6 genome recombination and VP1 sequence divergence, with an estimated half-life of the RFs of 3.1 years. Bayesian phylogenetic analysis of the data showed that recently occurring recombination groups (RF-E, -F, -H, -J and -K) shared a common ancestor (RF-A). Recombination breakpoints were frequently observed between the 2A-2C gene and the 5' untranslated region. This study revealed the potential for new CV-A6 variants to emerge and potentially modify disease outcomes of this major etiologic agent for HFMD affecting children worldwide.

Field of Study: Medical Science

Academic Year: 2015

Student's Signature .....

Advisor's Signature .....

## ACKNOWLEDGEMENTS

First and foremost, I would like to express my deepest gratitude to my academic advisor, Professor Yong Poovorawan. Without his guidance and continuous engagement with me in new ideas, I couldn't have completed this journey in time. I would also like to thank my committee members Professor Duangporn Werawatganon, Associate Professor Padet Siriyasatien, Associate Professor Teeraporn Chinchai and Assistant Professor Sunchai Payungporn for their interest in my work.

I am also indebted to Professor Peter Simmonds who wholeheartedly supported me for six months during my course of work with their research group at Roslin Institute, University of Edinburgh, Edinburgh, UK. I benefited a lot from his knowledge about recombination and evolution of enteroviruses. I would also like to thank various members of Peter's group for providing samples and invaluable discussions: Dr. Matti Waris, Dr. Riikka Osterback, Dr. Eva Eriksson, Dr. Jan Albert, Dr. Sophie Midgley, Dr. Thea K Fischer, Dr. Anna M Eis-Hübinger and Dr. Maria Cabrerizo.

I would also like to show my appreciation to the following funding sources that allowed me to pursue my thesis projects: The Royal Golden Jubilee Ph.D. program (PHD/0087/2554), the National Research Council of Thailand, The Centre of Excellence in Clinical Virology Chulalongkorn University and King Chulalongkorn Memorial Hospital. I am thankful to all lab staffs at Center of Excellence in Clinical Virology for all the instances in which their assistance helped me along the way and provided a friendly smile in my daily work. I am grateful to Dr. Kamol Suwannakarn for reading my reports, commenting on my views and helping me understand and improve my knowledge in the area. I would like to thank everyone who has supported and helped me through the work described in this thesis.

I would like to express my gratitude to my family for their support throughout my studies. Finally, I would like to thank my best friend, Mr. Jie Hao Ng who aided and encouraged me throughout this endeavor.

## CONTENTS

	Page
THAI ABSTRACT .....	iv
ENGLISH ABSTRACT .....	v
ACKNOWLEDGEMENTS.....	vi
CONTENTS.....	vii
LIST OF TABLES.....	ix
LIST OF FIGURES .....	x
LIST OF ABBEVIATIONS.....	xiii
CHAPTER I GENERAL INTRODUCTION .....	1
CHAPTER II LITERATURE REVIEW.....	3
2.1 Introduction .....	3
2.2 Structure of Enterovirus Particles.....	4
2.3 Viral genome organization .....	6
2.4 Replication cycle.....	8
2.5 Enterovirus Receptors.....	9
2.5.1 Human scavenger receptor class B member 2.....	10
2.5.2 Human P-selectin glycoprotein ligand-1.....	10
2.5.3 Anx2.....	11
2.5.4 Sialic acid .....	11
2.6 Viral Pathogenesis .....	12
2.7 Virus entry and spread.....	12
2.6.2 Tropism.....	12
2.6.3 EV-A71 infection induce apoptosis .....	14

	Page
2.8 Clinical Manifestation and Outbreak .....	15
2.9 Antiviral Compounds .....	16
Part 1: Prevalence and characterization of enterovirus infections among pediatric patients with hand foot mouth disease, herpangina and influenza like illness in Thailand, 2012 .....	17
Materials and Methods .....	20
Results .....	27
Part 2: Development of single step multiplex real-time RT-PCR for screening (panEV) and typing (EV-A71/CV-A6/CV-A16) of Enterovirus .....	45
Materials and Methods .....	47
Results .....	52
Part 3: Molecular epidemiology and the evolution of human Coxsackievirus A6 .....	63
Materials and Methods .....	65
Results .....	68
Discussion and conclusion .....	83
APPENDIX A .....	90
REFERENCES .....	98
VITA .....	117



## LIST OF TABLES

	Page
Table 1. Characteristics and functions of several genes of enterovirus. ....	7
Table 2. Enterovirus receptors and their functions.....	13
Table 3. Examples of preventative and therapeutic approaches targeting EV infections. ....	16
Table 4. Primers used for conventional RT-PCR assays. ....	26
Table 5. Demographic characteristics of all patients. ....	27
Table 6. Comparison between frequency of enterovirus genotypes in patients with hand, foot, mouth disease, herpangina and influenza-like illness, in 2012. ....	32
Table 7. Details of patients with ILI positive for enterovirus during investigation in 2012.....	33
Table 8. Nucleotide identity matrix obtained for the alignment of the partial VP1 region of CV-A6 strains from Thailand and reference strains of CV-A6 and other members of enterovirus species A. ....	43
Table 9. Multiplex PCR primers and TaqMan probes. ....	49
Table 10. Specificity test of multiplex real-time RT-PCR. ....	55
Table 11. Intra- and inter-assay reproducibility of monoplex and multiplex real-time RT-PCR. ....	61
Table 12. Diagnostic performance of one step multiplex real-time PCR and conventional RT-PCR identification of hand foot mouth viruses.....	62
Table 13. Recombination groups (RF-A to -K) based on phylogenetic analysis of the 3Dpol region. ....	71
Table 14. Rates of sequence change and TMRCA by MCMC analysis.....	76

## LIST OF FIGURES

	Page
Figure 1. Members of the Picornaviridae family as classified based on Maximum likelihood tree in capsid proteins. ....	4
Figure 2. The 3D structure of the Enterovirus particle .....	5
Figure 3. A Schematic representing the enteroviral genome composition and organization. ....	6
Figure 4. Overview of the Enterovirus life cycle.....	9
Figure 5. The structure of human P-selectin glycoprotein ligand-1 (PSGL-1). ....	11
Figure 6. Location of sample collection sites during outbreak of hand, foot, and mouth disease, Thailand, 2012. ....	21
Figure 7. Clinical manifestations in children with coxsackievirus A6 infection during outbreak of hand, foot, and mouth disease and herpangina, Thailand, 2012. ....	28
Figure 8. Seasonal distribution of hEV in Thailand 2012. ....	29
Figure 9. Age distribution of hEV infected subjects. ....	30
Figure 10. Distribution of human enteroviruses among hospitalized a) HFMD b) herpangina and c) influenza like illness cases in Thailand, 2012. ....	34
Figure 11. Phylogeny of human enterovirus specie A based on the partial VP1 region constructed by the neighbor-joining (NJ) algorithm implemented in MEGA version 5.0 using the Kimura two-parameter substitution model and 1000 bootstrap pseudo-replicates. ....	37
Figure 12. Phylogeny of human enterovirus specie B and C based on the partial VP1 region constructed by the neighbor-joining (NJ) algorithm implemented in MEGA version 5.0 using the Kimura two-parameter substitution model and 1000 bootstrap pseudo-replicates. ....	38

Figure 13. Phylogeny of a) CV-A6 and b) EV-A71 based on the partial VP1 region constructed by the neighbor-joining (NJ) algorithm implemented in MEGA version 5.0 using the Kimura two-parameter substitution model and 1000 bootstrap pseudo-replicates. ....	40
Figure 14. Phylogeny of a) CV-A8 and b) CV-B2 based on the partial VP1 region constructed by the neighbor-joining (NJ) algorithm implemented in MEGA version 5.0 using the Kimura two-parameter substitution model and 1000 bootstrap pseudo-replicates. ....	42
Figure 15. Genome signatures in amino acid residues at the alignment position of BC surface-exposed loop of a) CV-A6 and b) CV-A8 in Thailand in 2012. ....	44
Figure 16. Interpretation of panEV (A) and hEV (B) detection by multiplex real-time RT-PCR assay.....	54
Figure 17. Sensitivity of the multiplex real-time RT-PCR assay for EV-A71 (A), CV-A16 (B), CV-A6 (C) and panEV (D), obtained from the amplification of 10-fold serially diluted the transcribed RNA standards. ....	58
Figure 18. Standard curves of multiplex one-step real-time RT-PCR assays. ....	59
Figure 19. Phylogenetic analysis of VP1 sequences of CVA6 for study subjects and those previously determined. The tree display the color code for different countries.....	70
Figure 20. Phylogenetic analysis of VP1 sequences of CVA6 for study subjects and those previously determined (RF-B, -C, -D, and -E).....	72
Figure 21. Phylogenetic analysis of 3D sequences of CVA6 for study subjects and those previously determined (RF-B, -C, -D, and -E).....	73
Figure 22. Phylogenetic analysis of 5'UTR of CVA6 for study subjects and those previously determined (RF-B, -C, -D, and -E).....	77
Figure 23. Phylogenetic analysis of VP4/2 sequences of CVA6 for study subjects and those previously determined (RF-B, -C, -D, and -E).....	78

Figure 24. Histogram of genetic distances between CVA6 sequences. ....	79
Figure 25. (A) Association between VP1 sequence divergence (shown on the x-axis) and the proportion of recombinant comparisons. (B) Comparison of mean half-lives of CVA6 with previously estimated by the same method. ....	79
Figure 26. A dated phylogeny of VP1 sequences of CVA6 variants in this study and published sequences. ....	81
Figure 27. Divergence scan of nucleotide sequence between RF-A with other recombination groups (RF-F, H, G, K and J). ....	82



## LIST OF ABBREVIATIONS

$\alpha$	Alpha
$\beta$	Beta
$\mu$	Micro
$\mu\text{g}$	Microgram
$\mu\text{l}$	Microliter
%	Percent
$^{\circ}\text{C}$	Degree Celsius
3'UTR	3' untranslated region
5'UTR	5' untranslated region
aa	Amino acid
AFP	Acute flaccid paralysis
Anx2	Annexin 2
BHQ	Black hole quencher
BLAST	Basic local alignment search tool
bp	Base pairs
BrCr	Enterovirus 71 prototype strain
CAR	Coxsackie-adenovirus receptor
CEB	Chick embryo cells
CI	Confidence intervals
CODEHOP	Consensus degenerate hybrid oligonucleotide primer
CV	Coefficients of variation
CV-A	Coxsackievirus A
CV-B	Coxsackievirus B
cDNA	Complementary deoxyribonucleic acid
CNS	Central nervous system
CSF	Cerebrospinal fluid
Ct	Threshold cycle

DAF	The decay-accelerating factor
DC	Dendritic cell
DNA	Deoxyribonucleic acid
dNTP	Deoxynucleotide triphosphates
E	Echovirus
EMCV	Encephalomyocarditis virus
ER	Endoplasmic reticulum
EV	Enterovirus
FMDV	Foot-mouth disease virus
g	grams
GAPDH	Glyceraldehyde 3-phosphate dehydrogenase
HA	Herpangina
hEV	Human enterovirus
hEV-A	Human enterovirus group A
hEV-B	Human enterovirus group B
hEV-C	Human enterovirus group C
hEV-D	Human enterovirus group D
HFMD	Hand, foot and mouth disease
Hr	Hour
HRVs	Human rhinoviruses
HS	Heparan sulphate
ICAM-1	Intercellular adhesion molecule-1
ICTV	International Committee on the Taxonomy of Viruses
ILI	Influenza-like illness
IRES	Internal ribosome entry site
Kb	Kilobases
LDL-R	The low-density lipoprotein receptor
M	Molar
MEGA	Molecular evolutionary genetics analysis

NCBI	The National Center for Biotechnology Information
NPV	Negative predictive value
nt	Nucleotide
NS	Non-structural protein
NTP	Nucleotide triphosphate
ORF	Open reading frame
PCR	Polymerase chain reaction
Poly(A)	Polyadenylated
PPV	Positive predictive value
PSGL-1	Human P-selectin glycoprotein ligand-1
PV	Poliovirus
PVR	Poliovirus receptor
RD	Rhabdomyosarcoma (cells)
RdRp	RNA-dependent RNA polymerase
RF	Recombination form
RNA	Ribonucleic acid
RNAse	Ribonuclease
RSV	Respiratory syncytial virus
RT	Reverse transcription
SA	Sialic acid
SCARB2	Human scavenger receptor class B member 2
ss	Single-stranded
VCAM-1	Vascular adhesion molecule-1
VP	Viral protein
VPg	Viral protein genome-linked

## CHAPTER I GENERAL INTRODUCTION

### Background and rationale

Enterovirus (EV) infections are the immense health issue worldwide, affect both children and adults, and causing a wide spectrum of diseases ranging from mild (common cold) to life-threatening (poliomyelitis, hepatitis, meningitis, myocarditis and encephalitis). In particular, hand, foot, and mouth disease (HFMD) can be caused by various EV species A, most of them are coxsackievirus A4 (CV-A4), CV-A5, CV-A6, CV-A7, CV-A10, CV-A12, CV-A16 and EV-A71 (1). Although most of these virus infections are not serious in healthy individual, but HFMD caused by EV-A71 is occasionally leading to fatal neurological diseases (2). Recent repeated outbreak of EV-A71 subgenogroup C4 associated with severe encephalitis with cardiovascular collapse has occurred in Cambodia in 2012, resulting in more than 50 deaths (3).

This thesis will focus mainly on EV species A (especially EV-A71, CV-A6 and CV-A16) which are the predominant causes of HFMD and herpangina in the human population, with an incidence rate up to 500,000 - 1,000,000 cases per year (4). Therefore, epidemiological surveillance of EV infections in the population will help understand the pattern of EV transmission, and the epidemic background of circulating EVs, which could help interpret the EV trend and prevent the spread of these viruses. These informative data will provide major implications for future research on the pathogenic roles of EVs in HFMD and herpangina disease. In addition, this study has developed the multiplex real-time PCR panel allowing simultaneous detection of EV-A71, CV-A6 and CV-A16 by comparing with standard conventional diagnostic (RT)-PCR assays. This panel provides a rapid, specific and sensitive diagnostic approach and will be useful for routine diagnostics, epidemiological detection of EV infections and



preventing and controlling of the progress of disease. Moreover, the study provides clear evidence for recombination events in the founding of new CV-A6 lineages over an evolutionary time scale which remain a major etiologic agent for HFMD affecting children worldwide, comparable to that previously observed among EV species B.

### Objectives

It is hypothesized that there are other enteroviruses play an important role during the large scale outbreaks of HFMD and herpangina in Thailand during the rainy season in 2012. Although previous studies have shown that the viruses predominately associated with disease were EV-A71 and CV-A16 (5, 6). This study hypothesizes that CV-A6 may be the most frequent viral agent associated with the diseases. And there are some virus-specific factors that contribute to changes in clinical phenotype of CV-A6. Therefore the objectives of this study were to:

- (i) To evaluate the burden of human enteroviruses associated to HFMD and herpangina in patients and establish epidemiological profiles of these viruses during the study period.
- (ii) To develop a rapid, sensitive and specific assay based on one-step multiplex RT-PCR for use in Enterovirus 71, Coxsackievirus A6, Coxsackievirus A16 and panenterovirus detection.
- (iii) To investigate the evolutionary dynamics and molecular epidemiology of circulating strains of Coxsackievirus A6 from different countries (Germany, Spain, Sweden, Denmark, and Thailand) between 2013 and 2014 through analysis of structural and non-structural genome regions.

## CHAPTER II

### LITERATURE REVIEW

#### 2.1 Introduction

In general, human enterovirus (EV) species A (especially EV-A71, CV-A6 and CV-A16) is one of the most common etiological agents of hand, foot, mouth disease (HFMD) and herpangina. They have been classified in the genus *Enterovirus* belonging to the family *Picornaviridae* which contains crucial pathogenic viruses such as poliovirus, human enterovirus (hEV), hepatitis A virus (HAV) and foot-and-mouth disease virus (FMDV). The Picornaviridae is one of the largest family and currently comprises 29 genera (50 species), seven of which include human pathogens (1) (Figure 1).

Enteroviruses were originally identified more than 100 immunologically distinct serotypes in the 1950s. These viruses can be classified by several parameters including the clinical manifestations observed in human infection, their pathogenesis in suckling mice, evolutionary relationships, antiviral drug susceptibility, and receptor specificity (7). By using the basis of a molecular classification system, human enteroviruses have been taxonomically categorized into 12 species: previously defined species EV-A (25 types), EV-B (63 types), EV-C (23 types), EV-D (5 types), HRV-A (80 serotypes), HRV-B (32 serotypes), and the new species HRV-C (55 types proposed based on determinant-encoded gene), and five EV species that only detect in animals (EV-E to EV-J). Although the polioviruses fall within the same genetic cluster as species C, they are currently assigned to a distinct species in recognition of their biological uniqueness as agents of poliomyelitis. The classification of new types or strains within a species is based on the similarity of nucleotides and amino acid sequences of the capsid coding regions. A new type of EV is commonly defined by less than (<) 75% nucleotide and <85% amino acid sequence identity with known members across the VP1 (1).

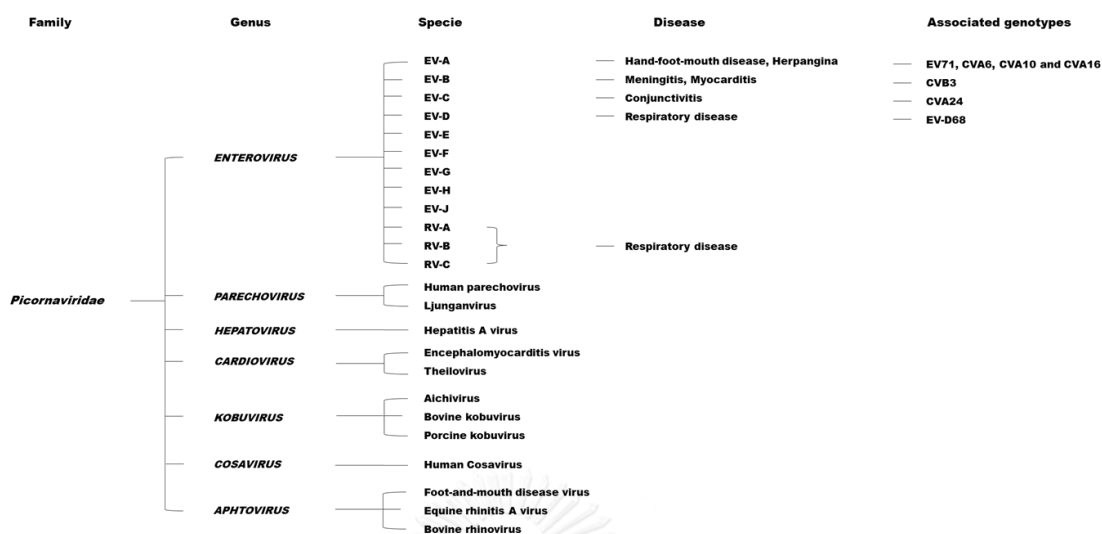


Figure 1. Members of the Picornaviridae family as classified based on Maximum likelihood tree in capsid proteins by Knowles (1) (Modified from van der Linden (8)).

## 2.2 Structure of Enterovirus Particles

Enterovirus capsids are encoded by the P1 region of the genome, serves multiple functions in many stages of the virus life cycle such as cell surface receptor binding, capsid internalization and destabilization, and transferring the viral genome into host cell (9). The mature virions containing 60 copies each of four viral polypeptides (VP1-VP4) and associate to form an icosahedral shell. The outer shell of the capsid is formed of parts of the three large proteins VP1, VP2 and VP3 that comprise wedge-shaped eight stranded  $\mu$ -barrels. A large twisted beta sheet comprising of four strands B, D, I and G form the front and bottom sections of the barrel while a flatter sheet comprising four strands C, H, E and F form the rear section. Each capsid protein taking the form of four loops (BC, HI, ED and FG) connect with these eight strands. The small VP4 molecules is located completely on the inner surface of the capsids (10) (Figure 2).

Many reports have documented the particle structures of enterovirus including poliovirus (11), rhinovirus (12), CV-A21 (13), CV-B3 (14), and CV-A16 (15). Recently, (16-18) reporting the structural resolution of the mature virions of EV-A71 (subgenogroups B3, C2 and C4) revealed the capsid expansion without RNA encapsidation and the stabilization of virus by the presence of pocket factor which unlike in other enteroviruses. There is canyon surrounding the five-fold axes, which serve as the receptor binding site for enterovirus. Furthermore, the hydrophobic pocket within VP1 (the floor of canyon) has been recognized to be the directed binding site of several antiviral compounds including disoxaril (WIN 51711), WIN 54954, WIN 61209, WIN 68934, WIN 65099 and pleconaril (WIN 63843) (19).

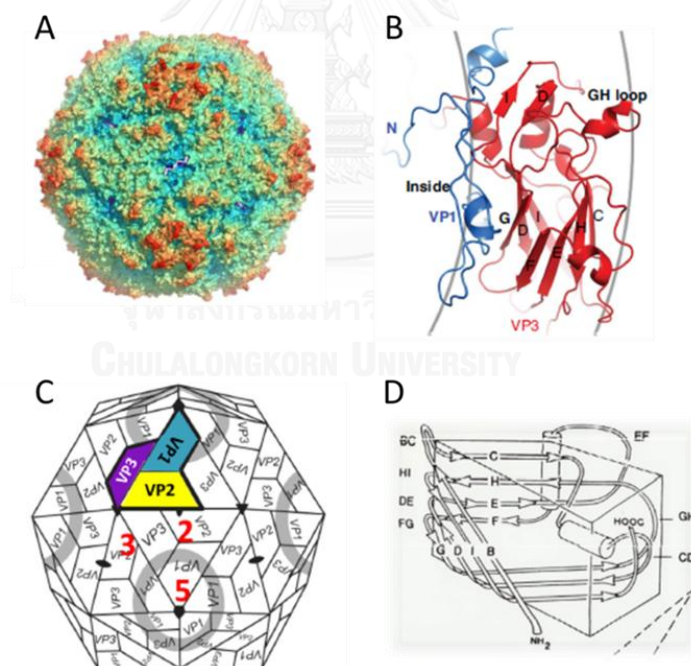


Figure 2. The 3D structure of the Enterovirus particle. (A) The crystal structure shows the surface of the 80S-like EV-A71 particle colour coded by radius. (B) The mature EV-A71 virion show structural regions in VP1 (blue) and VP3 (red) due to capsid expansion. (C and D) Icosahedral structure and schematic representation showing the positions of an enteroviral major capsid protein (VP1, VP2 and VP3), associate with eight stranded antiparallel beta sheet structures. (Modified from Jiang (20) and Ren (15))

### 2.3 Viral genome organization

Enterovirus is a small non-enveloped virus (30 nm) which comprises a positive single-stranded RNA genome (+ssRNA) of approximately ~7.2 to 8.4 kb long, which are encased by a highly structured icosahedral capsid. The viral genome is covalently linked to the small viral peptide VPg (22 to 25 amino acids) at the 5'-uridine of the genome (Tyr-p-U) (21). It is translated into a large polyprotein with a single open reading frame (ORF) flanked by 5' untranslated regions (UTR) containing replication signals and the internal ribosome entry site (IRES), and 3'UTR with polyadenylated tail of variable length as shown in figure 3. The virus polyprotein is proteolytically cleaved by viral protease into structural protein P1 (viral capsid protein (VP) 1 to VP4) and nonstructural proteins P2 (2A to 2C) and P3 (3A to 3D) which have different functions important for virus survival, shown in table 1. VP1 has been recognized as an essential part of the viral antigenic determinant, and it is also utilized as binding sites of many cellular receptors and neutralization antibodies (9).

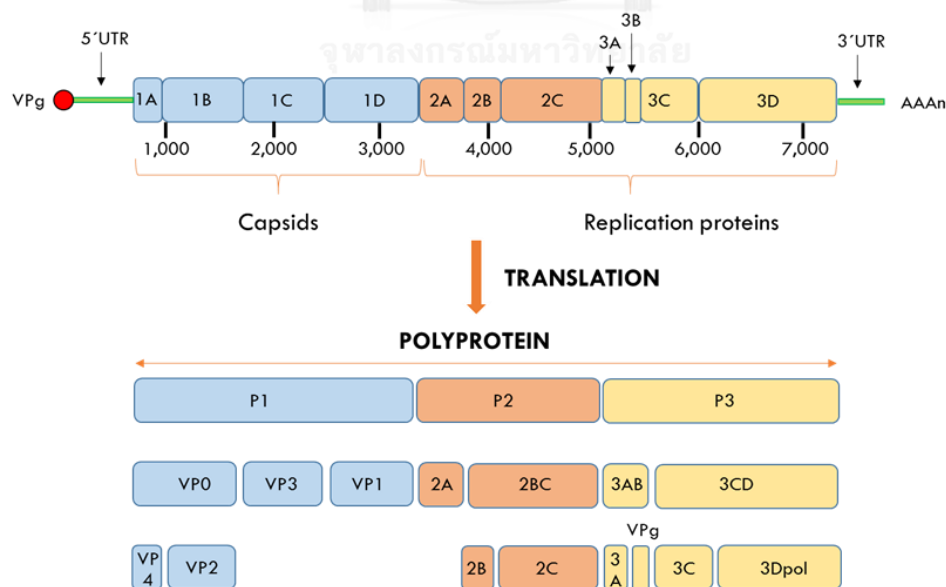


Figure 3. A Schematic representing the enteroviral genome composition and organization.

Table 1. Characteristics and functions of several genes of enterovirus.

Genomic Region	Length (bp)	Protein designation	Protein Function
P1	~200	VP4	Small capsid protein implicated in virion uncoating
	~800	VP2	Major capsid protein
	~700	VP3	Major capsid protein
	~900	VP1	Receptor binding site
P2	~400	2A	Chymotrypsin-like cysteine protease releasing capsid precursor from the nascent polypeptide, inhibit host transcription and maturate viral protein
	~300	2B	Increased membrane permeability, inhibition of cellular secretory pathways
	~1,000	2C	Vesicle formation and NTPase
P3	~200	3A	Inhibition of intracellular transport
	~100	3B	VPg primes RNA synthesis
	~500	3C	Protease
	~1,400	3D	RNA-dependent RNA polymerase

The P2 and P3 regions are comprised of 7 viral genes which 2A is included into 2C, and 3A is included into 3D. 2A<sup>pro</sup>, 3C<sup>pro</sup> and 3CD<sup>pro</sup> are encoded as viral protease, and play essential roles in viral polyprotein processing. The first cleavage reaction in all enteroviral polyproteins is catalyzed by the 2A<sup>pro</sup>. Viral proteases not only cleave viral polypeptides, but also inhibit various host machineries (22-24). Viral protein 2B contain two hydrophobic regions, which is crucial for multimerization, integrating into the membrane of the host Golgi and ER complex, producing virus-induced vesicles, and forming the viroporin complex (25). The 2C protein is a multifunctional protein comprising 329 amino acid residues. The protein contains many inter-species conserved motifs including membrane, RNA, and NTP binding sites which are crucial for decapsidation process, host cell membrane rearrangement, genome replication and virus particle encapsulation (26, 27). Protein 3A which is a membrane binding protein plays a role in inhibiting cellular protein secretion and mediating presentation of membrane proteins during viral infection (28, 29). The enteroviral 3B protein (VPg) is small peptides (21-23 aa), which is utilized as a primer in both positive- and negative-strand RNA synthesis (30, 31). The viral RNA-dependent RNA polymerase 3D is one of the major components of the viral RNA replication complex (32, 33).

#### 2.4 Replication cycle

EV is transmitted predominantly via oral-fecal route, but also through contact with virus-contaminated oral secretions and vesicular fluid, surfaces and fomites as well as through direct contact of patient's respiratory droplets (34). EV can infect a wide range of different cells with the different in the viral replication capacity. Virus entry into susceptible host cells involves several processes, including viral surface attachment, receptor binding and then the virus particles are uptake into host cell through endocytic pathway (Figure 4). Subsequently, the viral RNA is released into the cytoplasm after the

virus is uncoated. After that, the ORF is translated in the cytoplasm to produce a single, large polyprotein of approximately 2,200 amino acid residues, which may be co- and post-translationally cleaved into P1, P2 and P3 precursors upon the synthesis of virus encoded protease (2A<sup>pro</sup> and 3C<sup>pro</sup>). During replication initiation with a secondary RNA structure in the genome as a template, 3D<sup>pol</sup> and 3C protease uridylylates the VPg protein by uridylylation process (VPg-pUpU) (30). After that, the newly made viral RNA is replicated and translated prior to form new infectious virus particles which exits the host cell either after cell lysis.

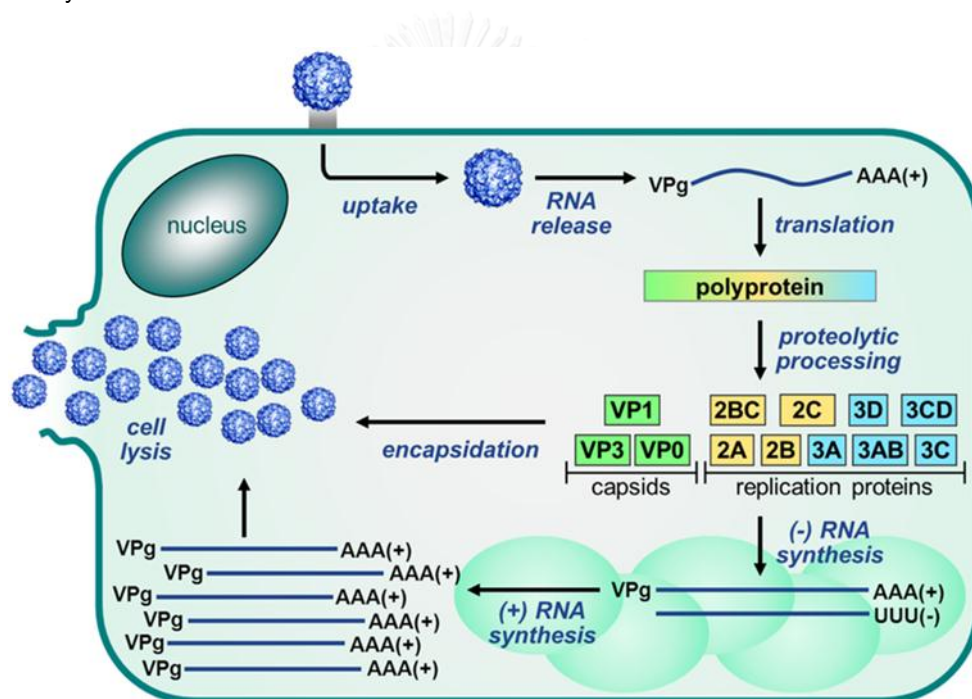


Figure 4. Overview of the Enterovirus life cycle.

From van der Linden, 2015 (8).

## 2.5 Enterovirus Receptors

By attaching on the surface of host cell, Enterovirus receptors play an crucial role in the internalization and destabilization of the capsid. Several viruses in this family have similar receptor molecules. Table 2 provides an overview of the receptors identified among enteroviruses and their functions. However, the specific host cellular receptor for



EV remains unknown. Until recently, there are at least four different types of human cellular receptors specific to EV-A71 and CV-A16 infection such as human scavenger receptor class B member 2 (SCARB2), Human P-selectin glycoprotein ligand-1 (PSGL-1), ANX2, and Sialylated Glycans.

### 2.5.1 Human scavenger receptor class B member 2

The first characterized receptor is human scavenger receptor class B member 2 (SCARB2), which also known as lysosomal integral membrane protein II, CD36b like-2 or HLG85. SCARB2 is a large family of the scavenger receptor family. They are involved in physiological function including transfer  $\beta$ -glucocerebrosidase from the endoplasmic reticulum to lysosomes and reorganize the endosomal/lysosomal compartment (35). SCARB2 is expressed on many cells including neurons in the central nervous system, lung pneumocytes, hepatocytes, renal tubular epithelium, splenic germinal centers and intestinal epithelium and expression can enhance efficient viral replication (36). SCARB2 is used by EV-A71 for cell attachment through the binding of  $\alpha 5$  helix within the head region (amino acids 142-204) (37). The interaction of EV-A71 with SCARB2 induces a conformational changes which lead to the uncoating of the virion at acidic pH (below 6.0) (38). In addition, SCARB2 also functions as a receptor for Coxsackievirus A7 (CV-A7), CV-A14 and CV-A16, which are in the same species with EV-A71 in *Enterovirus* genus (39).

### 2.5.2 Human P-selectin glycoprotein ligand-1

Human P-selectin glycoprotein ligand-1 (PSGL-1) is a second characterized receptor for EV-A71 (40). It is a membrane protein expressed by leukocytes and involve in inflammatory responses including tethering and rolling of leukocytes due to the recruitment of cells from blood vessels (41). The expression of PSGL-1 is essentially ubiquitous, with expression found on myeloid, lymphoid, dendritic lineages and platelets.

The binding of PSGL-1 on EV-A71 was determined to be close to the five-fold vertex via an electrostatic interaction (42) (Figure 5).

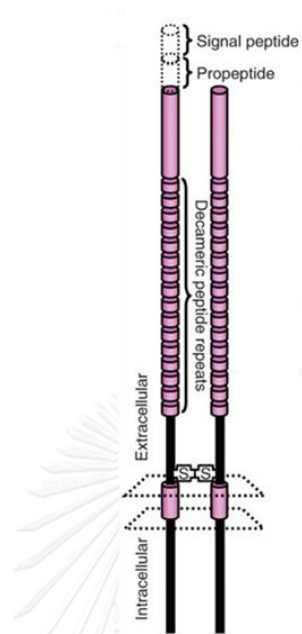


Figure 5. The structure of human P-selectin glycoprotein ligand-1 (PSGL-1).

From Nishimura Y, 2009 (40).

### 2.5.3 Anx2

Anx2 is the member of the annexin family, the members of which are involved in a range of functions including a profibrinolytic coreceptor for tissue plasminogen activator and plasminogen on endothelial cells (43). The Anx2 binding site on EV-A71 was mapped by yeast two-hybrid analysis to be close to VP1 amino acids 40–100, which comprise  $\beta$ -sheet B and the partial BC loop and not in the canyon region (44).

### 2.5.4 Sialic acid

The expression of sialic acid (SA)-linked glycan on intestinal epithelial cells corresponds to the known tropism of the viruses that use this molecule as a receptor (45). The direct interaction between sialylated glycans and EV-A71 is still unclear

## 2.6 Viral Pathogenesis

### 2.7 Virus entry and spread

Initial viral replication is presumed to occur in the lymphoid tissues of the tonsils and Peyer's patches and further multiplication in the regional lymph nodes. Subsequently, the virus particles begin to appear in the respiratory and alimentary tracts leading to prolonged virus shedding up to 2 weeks post infection. EV-A71 can persistently present in the alimentary tract up to 11 weeks after the symptoms recovered (46). Furthermore, studies in mice indicated that CNS invasion may occur at this point through retrograde axonal spread along cranial or peripheral nerves (47). Secondary site of infection is the central nervous system (CNS) and dissemination of EV-A71 could also be found in the reticulo-endothelial system (liver, spleen, bone marrow and lymph nodes), heart, lung, pancreas, skin, and mucous membrane, leading to cause mild viremia (46).

#### 2.6.2 Tropism

Despite the genome and life cycle of EV-A71 is similar to other picornaviruses, the associated pathological conditions differ significantly. Coxsackievirus B3 (CVB3) induces myocarditis and cardiomyocyte apoptosis (48). Various factors could affect severe disease or pathogenesis, including age, viral genotype, viral proteins, the host genetic background, the host immunity and co-infection with other viruses such as adenovirus 21 (49). The host immune response may induce serious complications of EV-A71 patients. Additionally, inflammation of the CNS has been proposed as the underlying pathogenic mechanism of EV-A71-associated severe neurological complication. Recent studies suggest that EV-A71 can infect several types of immune cells, such as DCs, monocytes and Jurkat T-cell lines (50). Infected immune cells may contribute to pathogenesis by secreting cytokines and chemokines, which mediate effector cells. Moreover, EV-A71

infection causes the up-regulation of FasL expression and thus promotes the apoptosis of Jurkat cells (51).

Table 2. Enterovirus receptors and their functions (52-63).

Receptors	Function	Receptor / Virus domain binding	Viruses	Reference
1. Immunoglobulin Superfamily				
1.1 ICAM-1 (CD54)	Inflammatory responses		Major group of HRVs, CVA13, A17, A18, A20, A21 and A24	(52)
1.2 VCAM-1	Not reported	The amino-terminal domain, D1 / Canyon	EMCV	(53)
1.3 PVR (CD155)	The formation of adherens junctions		Poliovirus	(54)
1.4 CAR	Cell adhesion molecule in developing brain		CVB1 - B6	(55)
2. LDL-R	Serum cholesterol and vitamin homeostasis	the 2 <sup>nd</sup> and 3 <sup>rd</sup> domains / HI & BC surface loops	Minor group of HRVs	(56)
3. DAF (CD55)	Regulate complement activation and protect cells from autologous lysis	Several binding patterns	CVB1, B3, B5, Echoviruses and EV70	(57)
4. Integrins	Regulate cell-to-cell / cell-to-matrix contacts, tissue repair, angiogenesis and inflammation	Several binding patterns	CVA9, CVB1, B3, B5, Echoviruses	(58-60)
5. Heparan sulphate	Embryonic development, wound healing and homeostasis	(+) charged amino acid residues on surface particle interact with (-) charged sulphates	CVB3, Echovirus, HRV89, FMDV	(61-63)

ICAM-1, Intercellular adhesion molecule-1; VCAM-1, Vascular adhesion molecule-1; PVR, Poliovirus receptor; CAR, Coxsackie-adenovirus receptor; LDL-R, The low-density lipoprotein receptor; DAF, The decay-accelerating factor; HRVs, Human Rhinoviruses; EMCV, Encephalomyocarditis virus and FMDV, Foot-mouth disease virus

### 2.6.3 EV-A71 infection induce apoptosis

Although the pathogenesis of EV-A71 infection remains unclear, the induction of cell death by EV-A71 may be a crucial factor contributing to its pathogenesis. Host-virus interactions studies suggested that many types of virus in the *Picornaviridae* family have ability to induce apoptotic cell deaths such as poliovirus, and coxsackievirus type B3 (64, 65). EV-A71 infection results in apoptosis for a wide range of cells, including rhabdomyosarcoma (RD) cells, Jurkat cells, SK-N-MC cells, glioblastoma SF268 cells, Vero cells, the human microvascular endothelial cell line and Hela cells (51, 66, 67). Cell apoptosis is necessary to induce EV-A71 viral protein synthesis. Animal studies showed that neuronal loss and apoptosis were evident in the brainstem and spinal cord of EV-A71-infected mice (68).

Several studies indicated that the proteolytic cleavage of EV-A71 3C and 2A can trigger apoptosis by activating of caspases (66, 69). A previous study identified that SUMO-modified 3C delayed the onset of cell apoptosis, providing evidence that EV-A71-3C plays a crucial role in apoptosis induction (70). The synergistic effect of many EV-A71 proteins might contribute to the pathogenesis of disease severity. Many picornaviral proteins including VP1, VP2, VP3, 2A, and 3C are reported to interact with host cellular factor by associating with apoptosis induction (71). For example, the 2C protein is a multifunctional protein comprising 329 amino acid residues. The protein contains many conserved motifs including membrane-, RNA-, and NTP-binding sites which are crucial for host cell membrane rearrangement, genome replication and virus particle encapsulation (26, 27, 72). The 2C protein also has two important functions during viral RNA synthesis: NTPase activity and directing replication complexes to the cell membrane (73). The 2C protein can specifically bind to the 3'-end of viral RNA itself (74). It also has specific interaction with structural protein (VP3), which implicates in the genome

encapsulation (75). Furthermore, evidence from *in vitro* studies suggested that apoptosis process could be induced in chick embryo cells (CEB) and Cos-7 cells through an activation of the cytochrome-c-caspase 9 pathway by the 2C protein of avian encephalomyelitis virus (76). Recent studies also suggest that the 2C protein of EV-A71 can interact with host protein reticulon 3 to form protein complex which is important for viral replication (77). Moreover, EV-A71-2C can function as an antagonist of the TNF- $\alpha$ -mediated activation of NF- $\kappa$ B signaling pathway, which is responsible for the secretion of numerous cytokines. Through interaction with IKK $\beta$ , EV-A71 can modulate host immune reactions via its 2C protein (78). The EV-A71-2C has also been implicated as a virulence factor and regulation of host response.

## 2.8 Clinical Manifestation and Outbreak

EV-A71 was first isolated from the feces of a female encephalitis patient in 1969 in California (79). However, a retrospectively analysis suggested that the virus could have emerged in the Netherlands as early as 1963 (80). Infection by EV-A71 is often asymptomatic or may manifest as a self-limiting influenza-like illness. EV-A71 has been recognized as the most common pathogen of hand, foot, and mouth disease (HFMD), which are one of the most infectious diseases frequently affecting children below 5 years of age. EV-A71 can also occasionally cause serious neurological manifestations including aseptic meningitis, acute flaccid paralysis (AFP), brainstem encephalitis as well as pulmonary edema, which may lead to mortality due to the complications (81, 82). EV-A71-associated HFMD have become a major public health concern in many countries especially in the Asia-Pacific countries including China (83), Taiwan (84), Malaysia (85), Japan (86), Singapore (87), and Thailand (6). Among the epidemic of HFMD in these countries, China has experienced many large scale outbreaks of EV-A71-associated HFMD. The largest outbreak occurred in 2008 with an estimated 25.71 cases per 100,000

populations with a high fatality rate in young children (126 death cases among 490,000 HFMD confirmed cases). Auhui province was the most affected area during the outbreak period (83). Until recently, neither effective antiviral therapy nor vaccine for EV-A71 is yet available.

## 2.9 Antiviral Compounds

Several antiviral compounds directed against EVs have been developed as shown in table 3.

Table 3. Examples of preventative and therapeutic approaches targeting EV infections (88-93).

Type	Therapeutic agent	Action	Effect
Capsid binders	Pleconaril (WIN 63843 or Picovir)	Bind Canyon	Broad-spectrum activity against a variety of HRV and enterovirus serotypes
	BTA798	Bind Canyon	Treated HRV infections in asthmatic patients
	Pocapavir	Bind Canyon	Against EVs and poliovirus
	Rupintrivir (AG7088)	3C protease inhibitor	Potent activity against all HRV serotypes in vitro whereas insignificant impact in human trial.
Protease Inhibitor	AG7404	3C protease inhibitor	Analog of rupintrivir with improved oral bioavailability compared to rupintrivir
	<i>PI4KIIIβ</i> inhibitors	3A protease inhibitor	Inhibited effect on CVB4 replication and CVB4-induced pathology
	TTP-8307	3A protease inhibitor	Against CVB3 and inhibited viral RNA synthesis
Polymerase Inhibitor	Ribavirin	3D <sup>pol</sup> inhibitor	Increases the error rate of 3D <sup>pol</sup>
	GPC-N114	3D <sup>pol</sup> inhibitor	Interferes with productive binding of the template-primer to 3D <sup>pol</sup>

## Part 1: Prevalence and characterization of enterovirus infections among pediatric patients with hand foot mouth disease, herpangina and influenza like illness in Thailand, 2012

Hand, foot, and mouth disease (HFMD) and herpangina are common causes of morbidity among children particularly, elementary school children below 10 years of age. HFMD is a febrile viral illness with oral ulceration on the anterior tonsillar pillars, soft palate, buccal mucosa and uvula and vesiculo-papular rashes over the hands, feet, elbows, knees or buttocks, while pathological hallmarks of HA are fever and oral ulcers without any progression of vesicular eruption on the skin (2, 94-96). HFMD and herpangina are generally considered as asymptomatic or self-limiting infectious diseases with patients having mild clinical complications which can be resolved completely within 5-7 days post infection. Various species and genotypes of enterovirus have been recognized as etiological agents for HFMD and herpangina including human enterovirus 71 (EV-A71), coxsackievirus A genotypes 1 (CV-A1) to CV-A10, A12, A16 and A22 and coxsackievirus B genotype 2 (CV-B2) to CV-B5 and echovirus 18 (97-100).

Recent viral etiological surveillance studies have suggested that viral profiles implicated in herpangina are less complex than HFMD; notably, members of enterovirus species A have been reported to be common viruses of herpangina. Nevertheless, among these, EV-A71 and CV-A16 are the most frequent viral agents associated with the diseases (101-103). Although different types and species of enteroviruses are somewhat different in their genetic background, the clinical manifestation and severity are identical and therefore, hamper the differentiation between specific virus infections and their clinical consequences based on the sole observation of clinical signs. Some epidemiological studies have suggested that, unlike other viruses, EV-A71-induced HFMD may cause severe life-threatening neurological and systemic complications,



accompanied by brainstem encephalitis, aseptic meningitis, encephalomyelitis, poliomyelitis-like paralysis and cardiopulmonary failure, and may consequently lead to death, resulting in the recognition of EV-A71 as the most important neurotropic virus since the prevention of poliovirus by vaccine (104, 105). Furthermore, EV-A71-caused HFMD and herpangina have largely emerged and continuously led to deaths due to complications in many Asia-Pacific countries including China (83, 106-108), Taiwan (84, 109), Malaysia (85, 110), Japan (86), Singapore (87, 95), and Vietnam (105, 111). Accordingly, understanding the risk factors that may exacerbate clinical complications and establishing effective molecular detection and enterovirus serotyping methods in clinical specimens are critical for disease surveillance and public health intervention.

Studies on clinical complications caused by specific types of enteroviruses have been reported. Among multiple enterovirus types associated with recent HFMD and herpangina outbreaks, CV-A6 has been recognized as an emerging causative virus since the epidemics in Finland and Singapore in 2008 (112-114) and its global dissemination thereafter in Taiwan in 2010 (115), Japan and Spain in 2011 (116, 117) and the United State in 2012 (118). In our previous study, we have reported on large scale outbreaks of HFMD and herpangina in Thailand during the rainy season in 2012 with approximately 40,000 suspected cases all over the country, and shown that CAV6 played an important role during the outbreak in 2012 (119). Our previous enterovirus detection assays in clinical specimens targeted the consensus sites in the 5' UTR combined with the specific primer sets for the most common viruses EV71 and CV-A16 and the recently emerged CV-A6 (5, 6, 119). Nonetheless, as the 5' UTR site has highly conserved sequences shared by all enterovirus members, our molecular serotyping based on 5' UTR sequences alone could not unequivocally distinguish between the genetic types of enterovirus and accordingly, only 65.7% of all pan-enterovirus positive specimens could be assigned to

any specific type (119). In addition, the underlying reasons for these changes in clinical phenotype of CV-A6 are unknown. Therefore, cohort epidemiologic studies and pathogenic role of this virus should be concerned.

Recently, many PCR techniques mainly targeting the hypervariable capsid encoding VP1 region using a consensus degenerate hybrid oligonucleotide primer (CODEHOP) have been developed to further increase sensitivity and specificity of detection as its classification results resembled the result from seroneutralization assays (120). To encounter the nonspecific amplification problem, the CODEHOP consists of two regions Degenerate Core and Consensus clamp. The degenerate core region uses inosine to make the region highly degenerative, designed from conserved motif when amino acid sequences are aligned, allowing broad target specificity while consensus clamp are non-degenerate driven the hybridization of primer to template, therefore increases the stability allowing higher annealing temperature to be use and in turn diminish nonspecific amplification. These observations prompted us to conduct a study to further our insight into the genetic diversity of enteroviruses and document their epidemiological profiles associated with HFMD and herpangina diseases in Thailand in 2012.

In the present study, we investigated the involvement of multiple enterovirus types by a molecular typing method using CODEHOP primers targeting the VP1 gene in order to establish an effective method which could be directly applied for clinical specimen testing. Parallel screening for enteroviruses in influenza-like illness (ILI) patients over the same period was also performed in order to compare the viral activities in different subjects with clinical symptoms.

## Materials and Methods

### Ethical considerations

The research protocol was approved by the institutional review board of the Ethical Committee of the Faculty of Medicine, Chulalongkorn University, Thailand (approval number IRB390/55). All information and patient identifiers were kept anonymous to protect patient confidentiality. The stored data included age, location of hospitals or medical centers, any recorded symptoms or clinical information, referral source, month of sample collection, and, if any, the results of other virological tests for each sample. Since the data obtained in this study were de-identified, written consent from the patients was waived. Permission for specimen utilization had been granted by the Director of King Chulalongkorn Memorial hospital.

### Population study

The studied population in this research was inpatients and outpatients from different parts of Thailand (Bangkok, Khonkaen, Suphanburi, Saraburi Rayong and Chantaburi) in 2012, diagnosed as suspected cases for HFMD, herpangina and influenza-like illness (Figure 6). These clinical specimens will be subjected for routine enteroviruses and respiratory viruses diagnostic and keep at the Center of Excellent in Clinical Virology, Faculty of Medicine, Chulalongkorn University, Bangkok, Thailand.

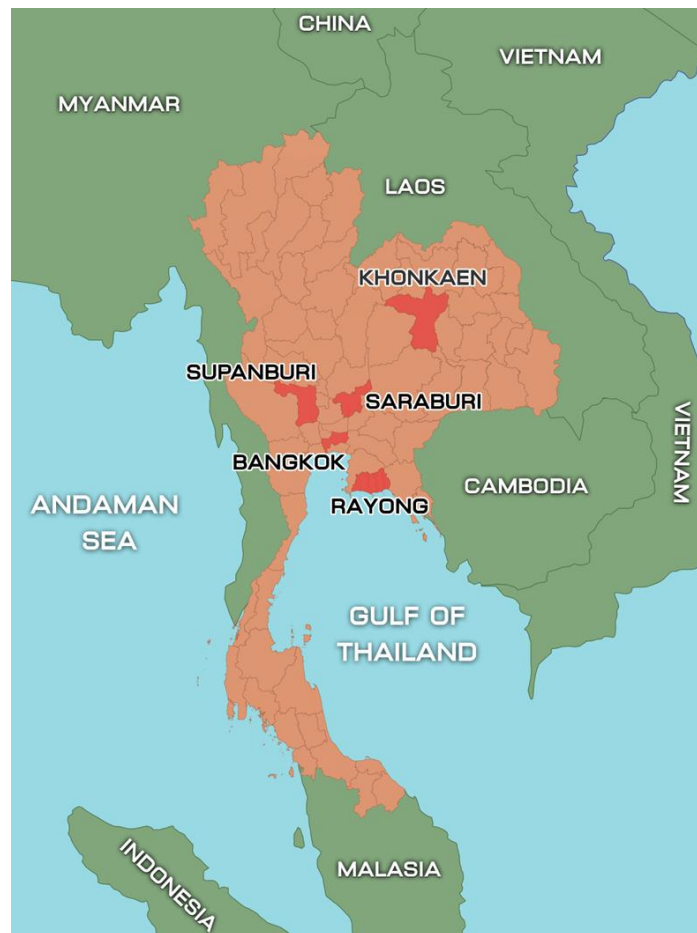


Figure 6. Location of sample collection sites during outbreak of hand, foot, and mouth disease, Thailand, 2012.

จุฬาลงกรณ์มหาวิทยาลัย  
CHULALONGKORN UNIVERSITY

#### Case definition and sample collection

##### *Herpangina*

Herpangina was defined as well-characterized multiple vesicular exanthema and ulcers of the soft palate with presentation of fever, sore throat, and decreased appetite. In addition, a total of 172 clinical specimens from 166 cases were collected from herpangina cases including 133 rectal swabs, 26 throat swabs, 9 serum samples, 2 stool samples, 1 vesicle fluid, and 1 nasal swab (119).

### *HFMD*

HFMD suspected cases were defined as having oral ulcers but chiefly on the buccal mucosa, tongue, hard and soft palate accompanied by typical vesicular rashes most commonly on the extensor surfaces of the hands, feet, knees and/ or buttock. A total of 730 clinical specimens were taken from 704 HFMD suspected patients including 578 rectal swabs, 75 stool samples, 36 throat swabs, 15 serum samples, 8 cerebrospinal fluid samples, 8 nasal swabs, 8 vesicle fluids, 1 sputum and 1 saliva (119).

### *Influenza like illness (ILI)*

The inclusion criteria for ILI were as follows: pediatric patient aged less than 12 years with the onset of high temperature (more than 38°C) and respiratory tract symptoms such as sore throat, cough, and runny nose with difficulty to breathe. In addition, a total of 1,094 nasal and throat swab specimens had been collected from both hospitalized and non-hospitalized patients having presented with ILI symptoms and admitted to hospital between January and December 2012.

All patient samples were collected from outpatients during visit and from inpatients within 48 h of admission and were transferred in 2 ml viral transport media (VTM) modified according to recommendations by the World Health Organization to the Center of Excellence of Clinical Virology, Chulalongkorn Hospital and immediately stored at -70°C until RNA extraction.

### **Sample size estimation**

The prevalence of enteroviruses infection in patients has been reported by several countries and years with variation considerably. As for examples, the EV prevalence values are as follows: Spain, 66%; Singapore, 62%; Korea, 43%; Hong Kong, 67%. With regard to the precise of identifying epidemic data, average values of the prevalence of

EV in patients with HFMD will be used in the experimental designs as 59.5%. The sample size required will be calculated according to the following formula:

$$n = \frac{Z\alpha^2 P(1-P)}{e^2}$$

n	=	required sample size
Z $\alpha$	=	confidence level at 95% (standard Z value of 1.96(two-tail))
P	=	Incidence proportion EV infection in patients with HFMD and herpangina estimated from the previous study
e	=	acceptable margin of error at 3% (standard value of 0.03)

Therefore, 1,029 samples will be required for the EV surveillance, respectively, in order to achieve the statistically supported results with 3% acceptable error.

#### **Viral nucleic acid preparation**

Total viral nucleic acid was extracted from 200  $\mu$ l of the clinical specimens using a Viral Nucleic Acid Extraction Kit according to the manufacturer's recommendation (RBC Bioscience, Taipei, Taiwan) and the extracted solution was stored at -70°C. All experiments were performed in a Bio-safety Level 2 plus environment. RNA from individual specimens was reverse transcribed into cDNA using the ImProm-II Reverse Transcription System (Promega, Madison, WI) with random hexamer primers (First BASE Laboratories, Selangor Darul Ehsan, Malaysia).

#### **Laboratory diagnosis for enterovirus using RT-PCR**

##### **Pan-Enterovirus detection using PCR amplification for 5'UTR**

RNA from individual specimens was reverse transcribed into cDNA using the ImProm-II Reverse Transcription System (Promega, Madison, WI) with random hexamer

primers (First BASE Laboratories, Selangor Darul Ehsan, Malaysia). The primer details are listed in table 4. The PCR reaction mixture contained the following: 1 µl of cDNA, 15 µl of PerfectTaq Plus Mastermix (5Prime, Hamburg, Germany), 0.5 µM forward and reverse primers, MgCl<sub>2</sub> and nuclease free water. The PCR for detection of enterovirus was carried out on a thermal cycler (Eppendorf, Hamburg, Germany) under the following conditions: 3 min at 94°C for initial denaturation, followed by 40 amplification cycles consisting of denaturation at 94°C for 30 sec, primer annealing at 60°C for 45 sec followed by 1 min at 72°C for extension, and a final extension at 72°C for 10 min. The expected 317-bp PCR products were visualized under UV light upon gel electrophoresis and staining with ethidium bromide.

#### **Enterovirus typing using PCR amplification of VP1 region**

Amplification of the VP1 encoding regions was performed using three different primer sets including specific primers for EV-A71/CV-A16, CV-A6 and CODEHOP.

To identify the type of Pan-enterovirus, samples were amplified using CODEHOP primer VP1 semi-nested PCR as previously described. Briefly, cDNA were synthesized from total RNA using four different primers (AN32-35). Enteroviruses were detected by nested-PCR with primers 222 and 224 as first-round primers and primers AN88 and AN89 for nested amplification. The CODEHOP PCR product was 350-400 bp in length.

#### **Sequence Analysis**

The amplified products from the conventional PCR reactions were purified using the HiYield Gel DNA Fragment Extraction kit (RBC Bioscience, Taipei, Taiwan). All sequences were amplified bidirectionally using the primers of the 2nd round PCR and subjected to sequencing by automated DNA cycle sequencer (First BASE Laboratories, Selangor Darul Ehsan, Malaysia). The nucleotide sequences were edited using the

Seqman program of DNASTAR Software (v5.0). Multiple sequence alignment was achieved by using the ClustalW multiple alignment programs, primer sequences were trimmed out and percent identities between pairs of sequences were calculated using the BioEdit Sequence Alignment Editor package (v7.0.9.0). To determine the genetic variation and the relationships with other reference viruses, phylogenetic trees were constructed using the neighbor-joining (NJ) method and Kimura's two-parameter distance model with 1,000 bootstrap pseudo-replicated and pair-wise deletions for missing data implemented in the MEGA software package (v5.0) (121). According to the 9th ICTV report, members of enterovirus species which share more than 75% nucleotide identity within the VP1 capsid gene, those with amino acid identities exceeding 85% would be considered as lineages of the previously defined enterovirus types (1). In this study, we maintained the criteria for type assignment originally described by ICTV and followed by some publications contributing to the discussion on phylogenetically evolving viruses.

The nucleotide sequences obtained from this study have been stored in GenBank database under accession numbers JX556422–JX556564, KF383346–KF383383 and KF661098–KF661255.



Table 4. Primers used for conventional RT-PCR assays (6, 119, 120).

Specificity	Primer name	Nucleotide sequence 5' - 3'	Strand	Target gene	Product size (bp)	Reference
panenterovirus	panEV-F1	CAA GCA CTT CTG TTT CCC CGG	Sense	5'UTR	317	(6, 119)
	panEV-R1	ATT GTC ACC ATA AGC AGC CA	Antisense	5'UTR		
	panEV-F2	AAG CAC TTC TGT TTC C	Sense	5'UTR		
	panEV-R2	CAT TCA GGG GCC GGA GGA	Antisense	5'UTR		
EV71/CAV16	EV-F2760	ATG GKT ATG YWA AYT GGG ACA T	Sense	VP1	418 (EV71), 306 (CAV16)	(6, 119)
	EV71/F2788	AAC WGG TTA YGC RCA AAT GCG	Sense	VP1		
	CA16/F2900	ACT GCA GTA CAT GTA TGT CCC	Sense	VP1		
CAV6	EV-R3206	CCT GAC RTG YTT MAT CCT CAT	Antisense	VP1	420	(6, 119)
	CA6-F2632	TGT GTG ATG AAT CGA AAC GGG GT	Sense	VP1		
	CA6-R3288	TGC AGT GTT AGT TAT TGT TTG GCT	Antisense	VP1		
CAV8	CA6-R3053	GGG TAA CCA TCA TAA AAC CAC TG	Antisense	VP1	440	-
	CA8-F2690	GAC CAT TTC TTT TCA AGA GCA GG	Sense	VP1		
	CA8-R3203	GCG CAC GTG YTT SAG GCG CAT	Antisense	VP1		
Enterovirus (CODEHOP)	CA8-R3127	GCG AAT GTR CCC ATC ATG TTA TT	Antisense	VP1	350-400	(120)
	222	CIC CIG GIG GIA YRW ACA T	Antisense	VP1		
	224	GCI ATG YTI GGI ACI CAY RT	Sense	VP3		
	AN89	CCA GCA CTG CAG CAG YNG ARA YNG G	Sense	VP1		
	AN88	TAC TGG ACC ACC TGG NGG NAY RWA CAT	Antisense	VP1		
	AN32	GTYTGCCA	Antisense	VP1		
	AN33	GAYTGCCA	Antisense	VP1		
AN34	CCRTCRTA	Antisense	VP1			
AN35	RCTYTGCCA	Antisense	VP1			

## Results

### Patient characteristics

From January 1st to December 31st, 2012, cases of HFMD (704 cases), herpangina (166 cases) and influenza-like illness (1,094 cases) were enrolled in this study. The median (range) age at the time of infection diagnosed as HFMD, herpangina and ILI were 2.0 years (from 1 month to 54 years), 2.3 years (from 3 months to 16 years) and 3.0 years (from 1 month to 12 years), respectively. Most suspected cases of HFMD (92.5%), herpangina (89.7%) and ILI (74.6%) occurred in children aged 5 years or younger. Patients with HFMD (59.9%), herpangina (53.6%) and ILI (56.5%) were male, with a M/F ratio of approximately 1.5, 1.2 and 1.3, respectively. 74.1% patients with HFMD were from urban, 25.9% from suburban areas of Thailand (Khonkaen, Suphanburi, Saraburi, Rayong and Chantaburi) (Table 5).

Table 5. Demographic characteristics of all patients.

Characteristic	HFMD (N = 704)		Herpangina (N = 166)		ILI (N = 1,094)		
	No.	%	No.	%	No.	%	
	<b>Gender</b>						
	Male	422	59.9	89	53.6	618	56.5
	Female	282	40.1	77	46.4	476	43.5
<b>Area</b>							
	Urban	522	74.1	91	54.8	864	79.0
	Suburb	182	25.9	75	45.2	230	21.0
<b>Age median (yrs.)</b>		2.0		2.25		3.0	
<b>Age</b>							
	0 – 2 yrs.	454	64.5	101	60.8	541	49.5
	3 – 5 yrs.	197	28.0	48	28.9	275	25.1
	6 – 12 yrs.	39	5.5	15	9.0	278	25.4
	13 – 15 yrs.	4	0.6	1	0.6	0	-
	>15 yrs.	10	1.4	1	0.6	0	-

Generally, the clinical manifestations of HFMD were fever; drooling, and refusal to eat (among young children); painful lesions in the mouth, especially on the soft palate (Figure 7, panel A); and vesicular rashes on the palms and feet (Figure 7, panels B, C). For patients affected by this outbreak, physicians from reporting sites reported anecdotally that they observed more severe skin manifestations than usual, especially on the buttocks and perianal area (Figure 7, panel D), knees, and elbows. Two cases with neurologic involvement (convulsion, altered consciousness) were caused by EV71 and were treated with intravenous immunoglobulin. No patients died.



Figure 7. Clinical manifestations in children with coxsackievirus A6 infection during outbreak of hand, foot, and mouth disease and herpangina, Thailand, 2012.

A) Lesions on the soft palate of the mouth; B) vesicular rash on the hands; C) vesicular rash on the foot; D) lesions on the buttocks and perianal area.

### Temporal Distribution

The temporal distribution of enteroviruses from HFMD, herpangina and ILI patients showed that the prevalence of enteroviruses in different months was distinctly different (Figure 8). As for HFMD, EV were distributed throughout the year except for February and showed a pronounced increase in the incidence during the rainy season; 14.6% in June (103/704), 34.4% in July (242/704) and 9.9% in August (70/704). As for herpangina, EV showed seasonal variation with a peak during the rainy season. The pattern of outbreak was similar to HFMD spanning a time period of 3 months; 16.3% in June (27/166), 39.8% in July (66/166) and 6.6% in August (11/166). As for ILI, EV was detected throughout the year except for May, November and December. The prevalent months for EV were 1.0% in June (11/1094) and 1.6% in July (18/1094).

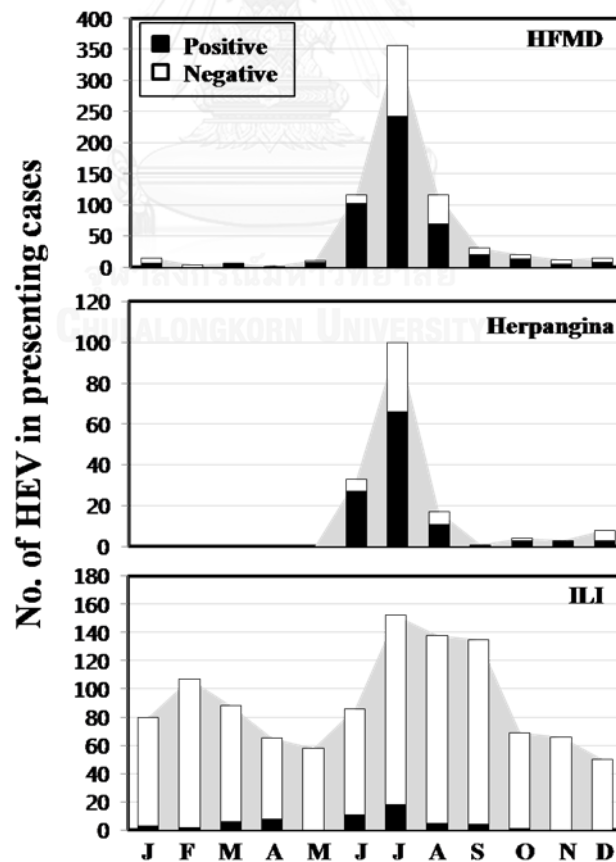


Figure 8. Seasonal distribution of hEV in Thailand 2012.

### Age Distribution

Three patient groups (HFMD, herpangina and ILI) showed a high prevalence of enterovirus infection in young children below the age of 5 years (Figure 9). As for the age of HFMD patients with enterovirus infection, extremely high infection rates were observed in 1-year-old infants (24.3%). The result showed the lowest incidence of enterovirus among the 0-6-month olds accounting for 1.6% and a peak incidence among the 7-12-month olds. Moreover, the oldest HFMD patient in this study was 36 years old. As for herpangina, the age distribution pattern was similar to HFMD. The result showed the lowest incidence of enterovirus among the 0-6-month olds accounting for 1.2% and a peak incidence among 1-year olds (18.1%). As for ILI, 1.0% of EV infections were observed in 2-year-old children. In addition, the result showed that the distribution patterns in each age group were comparable.

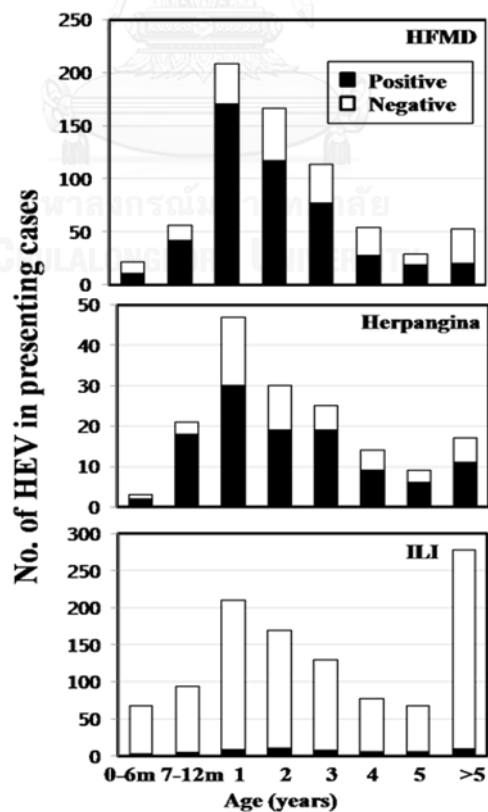


Figure 9. Age distribution of hEV infected subjects.

### Enterovirus detection

Of the 704 HFMD suspected cases, 485 were virus-positive, indicating a prevalence of 68.9%. Of these, 402 samples typed positive for 15 different human enterovirus types. They are: 386 samples (54.8%) were identified as species A (CV-A4, A5, A6, A8, A10, A12, A16 and EV-A71), 15 samples (2.1%) as species B (CV-A9, CV-B1, B2, B4, B5 and Echo7), and one sample (0.1%) as species C (CV-A21). The remaining 83 samples initially tested positive (11.8%) were could not be typed. Of the 166 herpangina samples tested for hEV, 68 could be fully typed. Of those, 64 samples (94.1%) were identified as species A (CV-A4, A5, A6, A8, A10, A12 and A16), 4 samples (5.9%) as species B (CV-B2 and E25) and 46 samples (27.7%) as non-identified genotypes. hEV-species C was not detected in herpangina patients (Table 6).

Of the 1,094 influenza-like illness cases, a total of 58 samples were EV positive upon initial screening, indicating a prevalence of 5.3%. We found that 38 out of the 58 samples typed positive for 11 different human enterovirus types, including 26 samples (2.4%) identified as species A (CV-A5, A6, A8, A10 and EV-A71), 11 samples (1.0%) as species B (CV-A9, CV-B1, B2, Echo7 and Echo16), and one sample (0.09%) as species C (CV-A21). Twenty samples (1.8%) were of non-identified genotypes (Table 6). We note in table 7 that co-infection by respiratory viruses was found in 2 cases. First, a 5-year-old girl was infected by CV-A8/respiratory syncytial virus (RSV) and a 2-year-old girl was infected by CV-B2/seasonal influenza virus (H3).

The majority of enterovirus detected in three patient groups (HFMD, herpangina and ILI) belonged to human enterovirus species A. In the largest outbreak of HFMD in Thailand in 2012, CV-A6 was identified as the most prevalent virus followed by CV-A16 and EV-A71. A small outbreak of herpangina in the same year was caused in most patients

by infection with CV-A8 followed by CV-A6. Moreover, we found CV-A6 was the most predominant pathogen in ILI patients followed by CV-A8 (Figure 10).

Genotypes of human enterovirus species A present in all HFMD, herpangina and ILI groups were CV-A5, CV-A6, CV-A8 and CV-A10. Genotypes of hEV-species A detected in HFMD and herpangina were CV-A4, CV-A12 and CV-A16. Not a single herpangina patient was infected by EV-A71. Moreover, one of the herpangina patients demonstrated co-infection by CV-A8/ CV-A10 (data not show). The most common type of human enterovirus species B in HFMD and herpangina patients was CV-B2. Both CV-A9 and CV-B2 were mainly found in ILI patients. Types of hEV-species B only detected in HFMD and ILI patients were CV-A9, CV-B1 and Echo7. Furthermore, CBV4 and CBV5 were only detected in HFMD, Echo16 in ILI and Echo25 in herpangina. Moreover, CV-A21 (human enterovirus species C) was detected in both HFMD and ILI patients.

Table 6. Comparison between frequency of enterovirus genotypes in patients with hand, foot, mouth disease, herpangina and influenza-like illness, in 2012.

Virus	Influenza-like illness		Hand, foot, mouth disease		Herpangina	
	No.	%	No.	%	No.	%
Coxsackievirus A4	0	-	2	0.3	3	1.8
Coxsackievirus A5	1	0.1	2	0.3	1	0.6
Coxsackievirus A6	16	1.5	236	33.5	22	13.3
Coxsackievirus A8	6	0.5	7	1.0	32	19.3
Coxsackievirus A9	4	0.4	3	0.4	0	-
Coxsackievirus A10	1	0.1	8	1.1	3	1.8
Coxsackievirus A12	0	-	3	0.4	2	1.2
Coxsackievirus A16	0	-	66	9.4	1	0.6
Coxsackievirus A21	1	0.1	1	0.1	0	-
Coxsackievirus B1	1	0.1	2	0.3	0	-
Coxsackievirus B2	4	0.4	6	0.9	3	1.8
Coxsackievirus B4	0	-	2	0.3	0	-
Coxsackievirus B5	0	-	1	0.1	0	-
Echovirus 7	1	0.1	1	0.1	0	-
Echovirus 16	1	0.1	0	-	0	-
Echovirus 25	0	-	0	-	1	0.6
Enterovirus 71	2	0.2	62	8.8	0	-
Untypable	20	1.8	83	11.8	46	27.7
Negative	1036	94.7	219	31.1	52	31.3
<b>Total</b>	<b>1094</b>	<b>100</b>	<b>704</b>	<b>100</b>	<b>166</b>	<b>100</b>

Table 7. Details of patients with ILI positive for enterovirus during investigation in 2012.

Strain	Sampling Date	Gender	Age	Virus detected	Place	Accession no.	Co-infection
Echo16_THA/B6018/2012	25/1	M	3 y	Echovirus 16	Bangkok	KF383381	-
Echo7_THA/C2541/2012	26/1	F	2 y	Echovirus 7	Khon Kaen	KF383383	-
CV-A6_THA/C2607/2012	16/2	F	7 y	Coxsackievirus A6	Khon Kaen	KF383347	-
CV-A6_THA/C2697/2012	14/3	F	3 y	Coxsackievirus A6	Khon Kaen	KF383348	-
CV-A6_THA/C2710/2012	22/3	M	10 y	Coxsackievirus A6	Khon Kaen	KF383349	-
CV-A6_THA/C2711/2012	22/3	M	10 y	Coxsackievirus A6	Khon Kaen	KF383350	-
CV-A6_THA/C2717/2012	22/3	M	5 y	Coxsackievirus A6	Khon Kaen	KF383351	-
CV-A6_THA/C2723/2012	29/3	F	4 y	Coxsackievirus A6	Khon Kaen	KF383352	-
CV-A6_THA/C2737/2012	29/3	F	2 y	Coxsackievirus A6	Khon Kaen	KF383353	-
CV-A6_THA/C2744/2012	3/4	M	7 m	Coxsackievirus A6	Khon Kaen	KF383354	-
CV-A6_THA/C2745/2012	3/4	F	1 y	Coxsackievirus A6	Khon Kaen	KF383355	-
CV-A6_THA/C2747/2012	3/4	F	3 y	Coxsackievirus A6	Khon Kaen	KF383356	-
CV-A6_THA/C2769/2012	11/4	F	10 m	Coxsackievirus A6	Khon Kaen	KF383357	-
CV-A6_THA/C2773/2012	11/4	M	5 m	Coxsackievirus A6	Khon Kaen	KF383358	-
CV-A6_THA/C2785/2012	25/4	F	13 d	Coxsackievirus A6	Khon Kaen	KF383359	-
CV-A6_THA/C2788/2012	25/4	F	2 y	Coxsackievirus A6	Khon Kaen	KF383360	-
CV-A6_THA/C2791/2012	25/4	F	1 y	Coxsackievirus A6	Khon Kaen	KF383361	-
EV-A71_THA/C2904/2012	7/6	M	1 y	Enterovirus 71	Khon Kaen	KF383376	-
CBV2_THA/C2909/2012	7/6	M	1 y	Coxsackievirus B2	Khon Kaen	KF383374	-
CAV8_THA/C2921/2012	21/6	M	1 y	Coxsackievirus A8	Khon Kaen	KF383367	-
CAV8_THA/C2928/2012	21/6	F	1 y	Coxsackievirus A8	Khon Kaen	KF383366	-
CBV2_THA/C2929/2012	21/6	M	2 y	Coxsackievirus B2	Khon Kaen	KF383373	-
CBV2_THA/C2938/2012	21/6	F	7 y	Coxsackievirus B2	Khon Kaen	KF383372	-
CAV8_THA/B6294/2012	27/6	M	8 y	Coxsackievirus A8	Bangkok	KF383362	-
CAV8_THA/B6328/2012	6/7	M	8 m	Coxsackievirus A8	Bangkok	KF383363	-
CAV5_THA/C3007/2012	10/7	M	3 y	Coxsackievirus A5	Khon Kaen	KF383380	-
CV-A6_THA/B6347/2012	14/7	M	2 y	Coxsackievirus A6	Bangkok	KF383346	-
CAV8_THA/C3021/2012	17/7	F	5 y	Coxsackievirus A8	Khon Kaen	KF383365	-
CBV1_THA/C3025/2012	17/7	F	4 y	Coxsackievirus B1	Khon Kaen	KF383382	-
CAV10_THA/B6446/2012	24/7	M	5 y	Coxsackievirus A10	Bangkok	KF383378	-
CAV8_THA/C3035/2012	24/7	F	5 y	Coxsackievirus A8	Khon Kaen	KF383364	RSV
EV-A71_THA/C3051/2012	24/7	M	2 y	Enterovirus 71	Khon Kaen	KF383377	-
CBV2_THA/B6463/2012	25/7	F	2 y	Coxsackievirus B2	Bangkok	KF383375	Seasonal influenza
CAV9_THA/C3055/2012	8/8	M	1 y	Coxsackievirus A9	Khon Kaen	KF383371	-
CAV9_THA/B6761/2012	26/8	F	3 y	Coxsackievirus A9	Bangkok	KF383368	-
CAV9_THA/B6763/2012	26/8	M	2 y	Coxsackievirus A9	Bangkok	KF383369	-
CAV9_THA/B6773/2012	28/8	M	2 y	Coxsackievirus A9	Bangkok	KF383370	-
CAV21_THA/B6982/2012	21/9	M	10 y	Coxsackievirus A21	Bangkok	KF383379	-



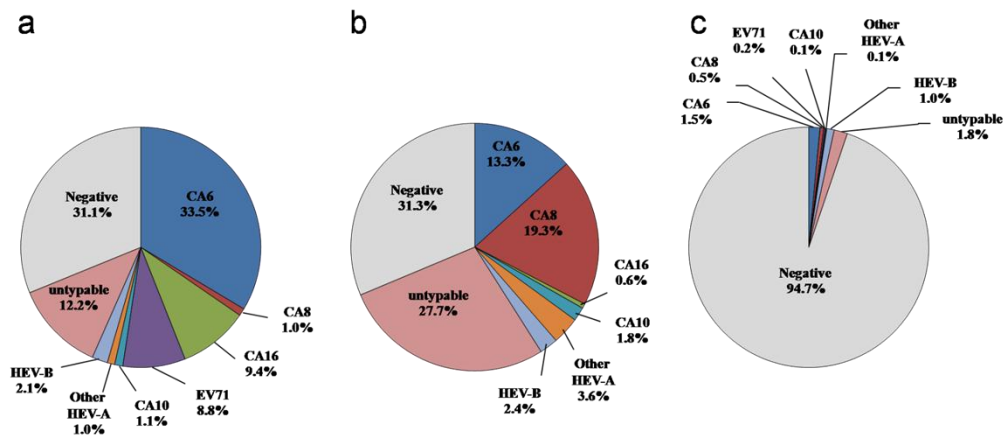


Figure 10. Distribution of human enteroviruses among hospitalized a) HFMD b) herpangina and c) influenza like illness cases in Thailand, 2012.

#### Phylogenetic and sequence analysis of enterovirus

Two phylogenetic trees were constructed comprising all human enterovirus species A, B and C strains from the present study along with their respective prototype strains with bootstrap values higher than 85% (Figures 11 and 12).

Phylogenetic analyses of the representative Thai CV-A6 strains are shown in figure 13a. Overall, the partial VP1 sequences were classified into ten clusters (A-J) with obvious geographical distribution patterns. All representatives CV-A6 strains identified in Thailand in 2012 segregated into cluster A and displayed a close genetic relationship with other strains from Shanghai, China 2012. They were also similar to strains from Finland and Spain in 2008 (cluster B and E) and Japan in 2011 (cluster C), which were associated with onychomadesis subsequent to HFMD (112, 113, 116, 117). The partial VP1 genes of all CV-A6 strains determined in this study exhibited 88.3% to 100% similarity. The Thai CV-A6 strains share 81.7-83.5% nucleotide identity with the prototype strain 'Gdula' and 55.7-66.7% with other members of enterovirus species A (Table 8).

The molecular epidemiology of the Thai EV-A71 strains was investigated applying a phylogenetic tree, with the representative strains selected from GenBank as known subgenotype references (A, B1-B5, C1-C5) (Figure 13b). The results have shown that all EV-A71 strains determined in this study were categorized into two genotypes, with the majority clustered with genotype B, and closely related to subgenotype B5. Interestingly, two EV-A71 strains from HFMD patients cluster with subgenotype C4a (CU562 and CU947), closely related to strains circulating in Ho Chi Minh City, Vietnam (2011) and China (2009-2010). Genetic differences within the VP1 gene of these two Thai C4a and B5 strains were 3.8% and 6.8%, respectively. Genetic differences within the VP1 gene between genotypes C4a and B5 were 14.6-16.5%. The bootstrap supported phylogenetic tree showed that EV-A71 (subgenotype B5) strains from Thailand clustered into 3 clades, namely, clades I, II and III. The results showed that most of them including two strains from ILI patients (from June to December 2012) belonged to clade I, closely related to strains circulating in Malaysia in 2008. Seven strains (the majority from January 2012) were classified into clade II, which is closely related to strains identified in Singapore in 2008. Finally, 12 strains (from June to December 2012) in clade III were closely related to strains detected in Taiwan (2007-2008).

As shown in figure 14a, the CV-A8 strains were assigned to six major clusters, denoted A, B, C, D, E, F and G based on criteria described above. The partial VP1 genes of all CV-A8 strains (n = 45) in this study exhibited 74.4% to 100% similarity. The Thai CV-A8 strains were divided into two distinct groups; the majority of which grouped with cluster A and four strains grouped with cluster C. The majority of the CV-A8 strains showed a close genetic relationship with 2007-2009 Indian strains associated with non-polio acute flaccid paralysis (122) and a minority of strains showed a close genetic relationship with the 2013 Japanese strains associated with herpangina, 2012 Chinese strains associated

with HFMD and 2008 Chinese strains associated with acute respiratory tract infection (123).

The phylogenetic relationship between CV-B2 strains was also assessed based on partial VP1 regions (Figure 14b). The nucleotide sequence identities within all Thai CV-B2 strains (n = 13) amounted to approximately 94.8% to 100% in partial VP1 regions. Comparison with the prototype strain (AF081485/Ohio strain) showed that the Thai CV-B2 strains in 2012 had less than 85% nucleotide sequence identities. CV-B2 strains were assigned to seven major clusters based on the criteria described above (A-G). All CV-B2 strains (n = 13) were grouped in cluster A, which is most closely related to strains in China (1994-2003). Cluster B comprising the strains from Russia, Bangladesh, Australia, India and United Kingdom: cluster C from USA: cluster D from China: cluster E from Denmark, Finland, Germany and France: cluster F from Denmark, Finland and Germany and cluster G from Japan. No significant clustered relationship was observed based on clinical syndromes and temporal specific distribution. In addition, the aligned amino acid positions of the BC-surface loops of CV-A6 and CV-A8 are shown in figure 15.

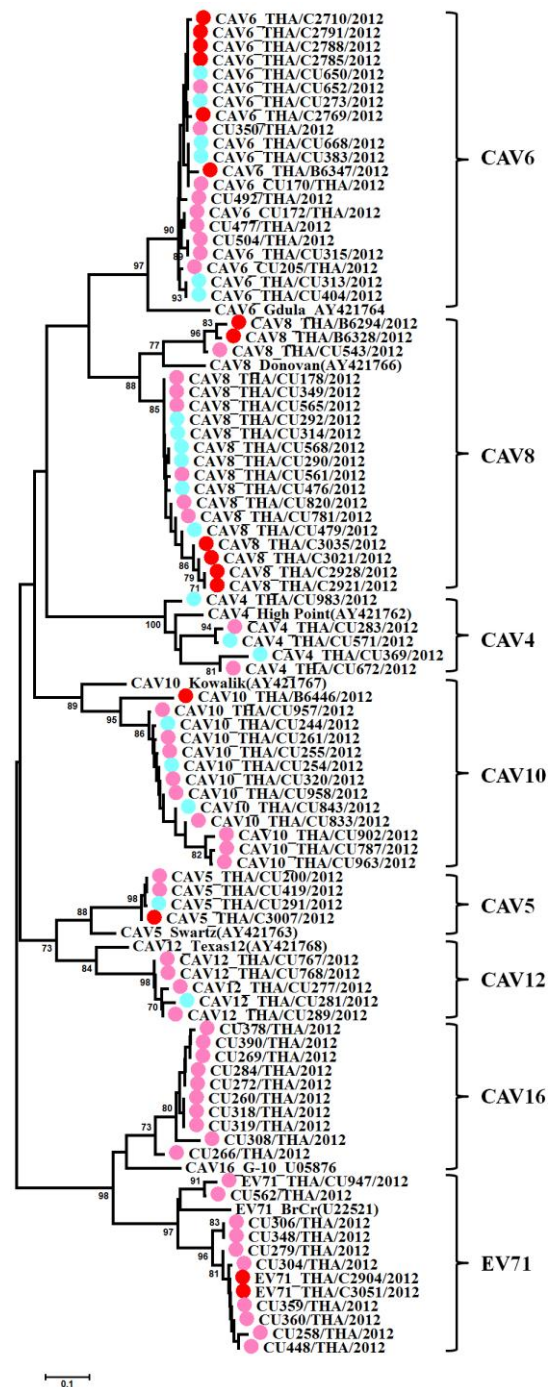


Figure 11. Phylogeny of human enterovirus specie A based on the partial VP1 region constructed by the neighbor-joining (NJ) algorithm implemented in MEGA version 5.0 using the Kimura two-parameter substitution model and 1000 bootstrap pseudo-replicates. Strains from HFMD patients are indicated in pink, herpangina patients in blue, and influenza like illness patients in red.

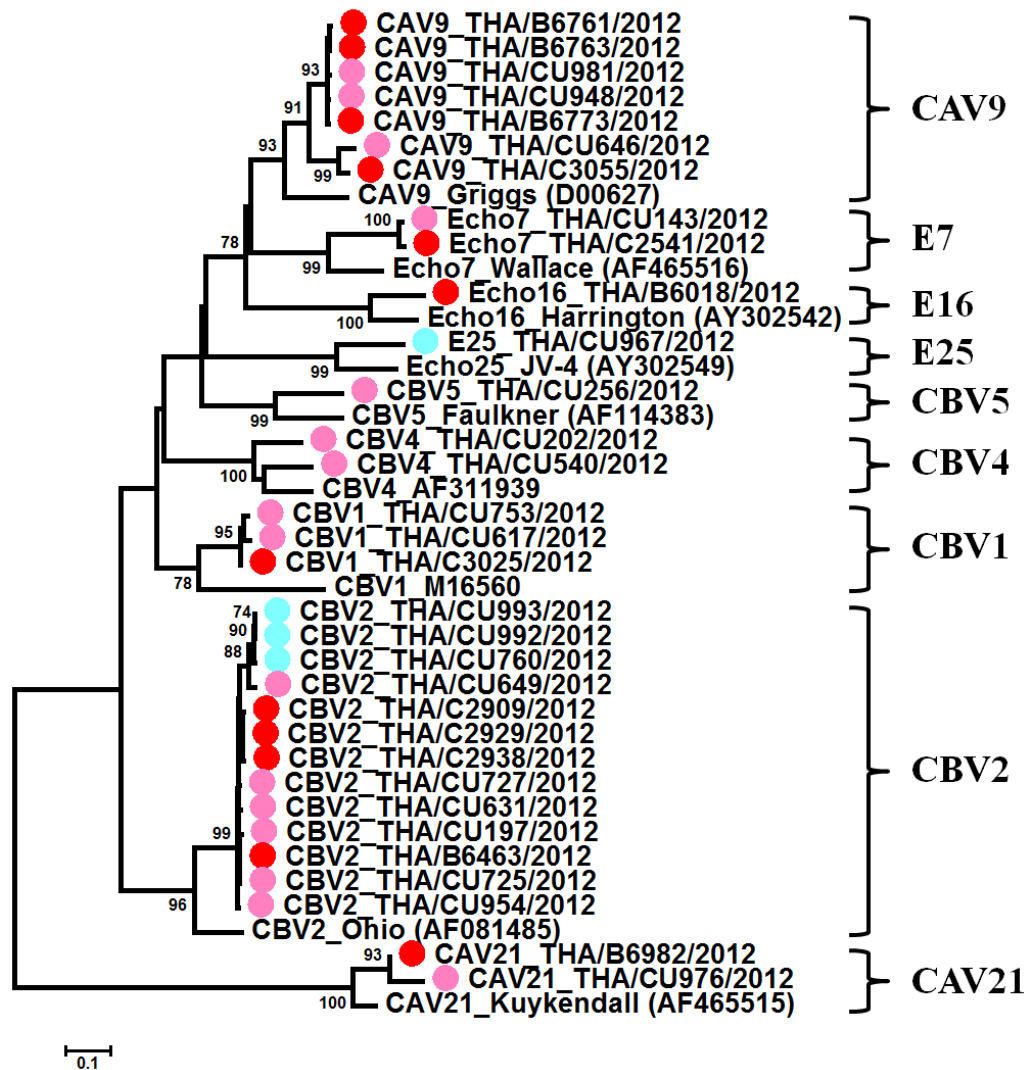


Figure 12. Phylogeny of human enterovirus specie B and C based on the partial VP1 region constructed by the neighbor-joining (NJ) algorithm implemented in MEGA version 5.0 using the Kimura two-parameter substitution model and 1000 bootstrap pseudo-replicates. Strains from HFMD patients are indicated in pink, herpangina patients in blue, and influenza like illness patients in red.

(a)



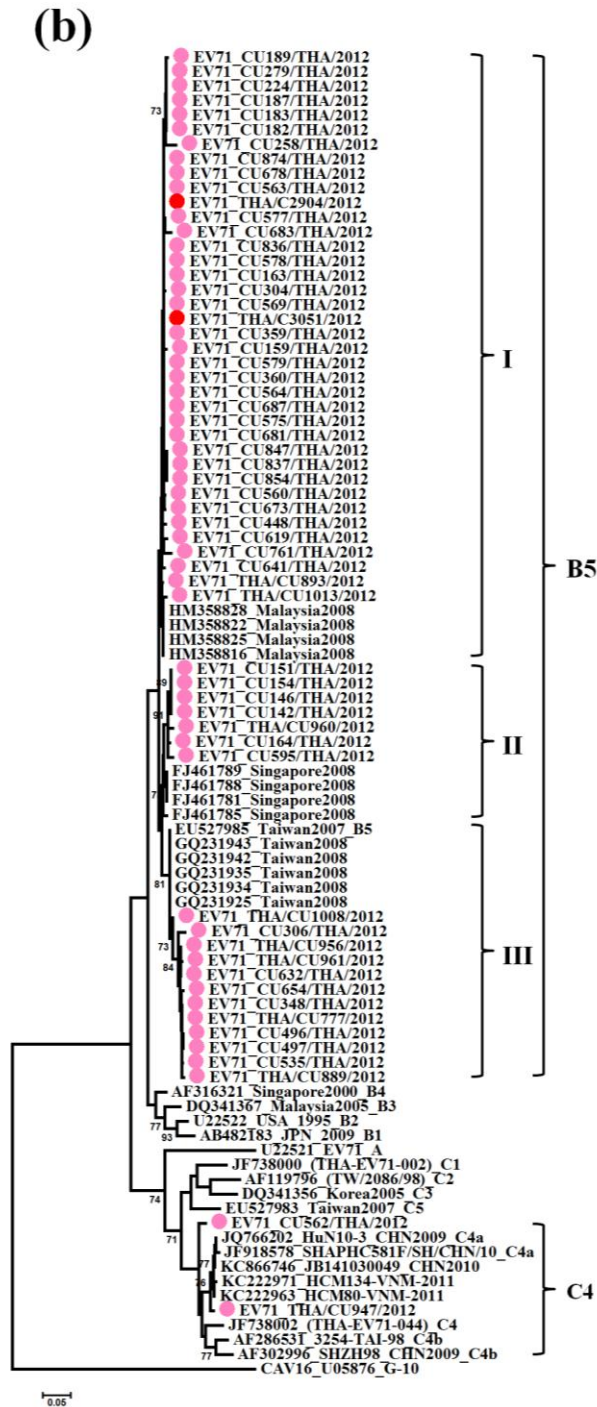
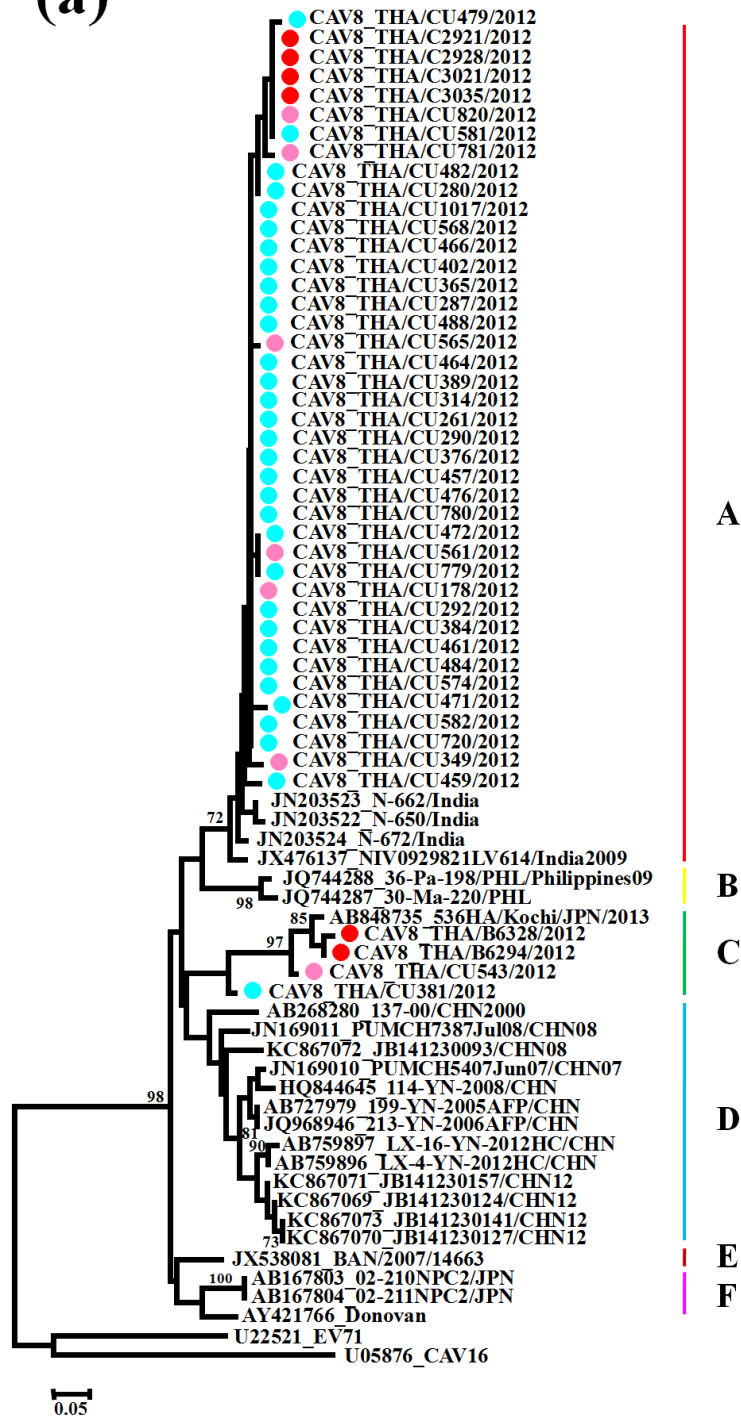


Figure 13. Phylogeny of a) CV-A6 and b) EV-A71 based on the partial VP1 region constructed by the neighbor-joining (NJ) algorithm implemented in MEGA version 5.0 using the Kimura two-parameter substitution model and 1000 bootstrap pseudo-replicates. Strains from HFMD patients are indicated in pink, herpangina patients in blue, and influenza like illness patients in red.

(a)





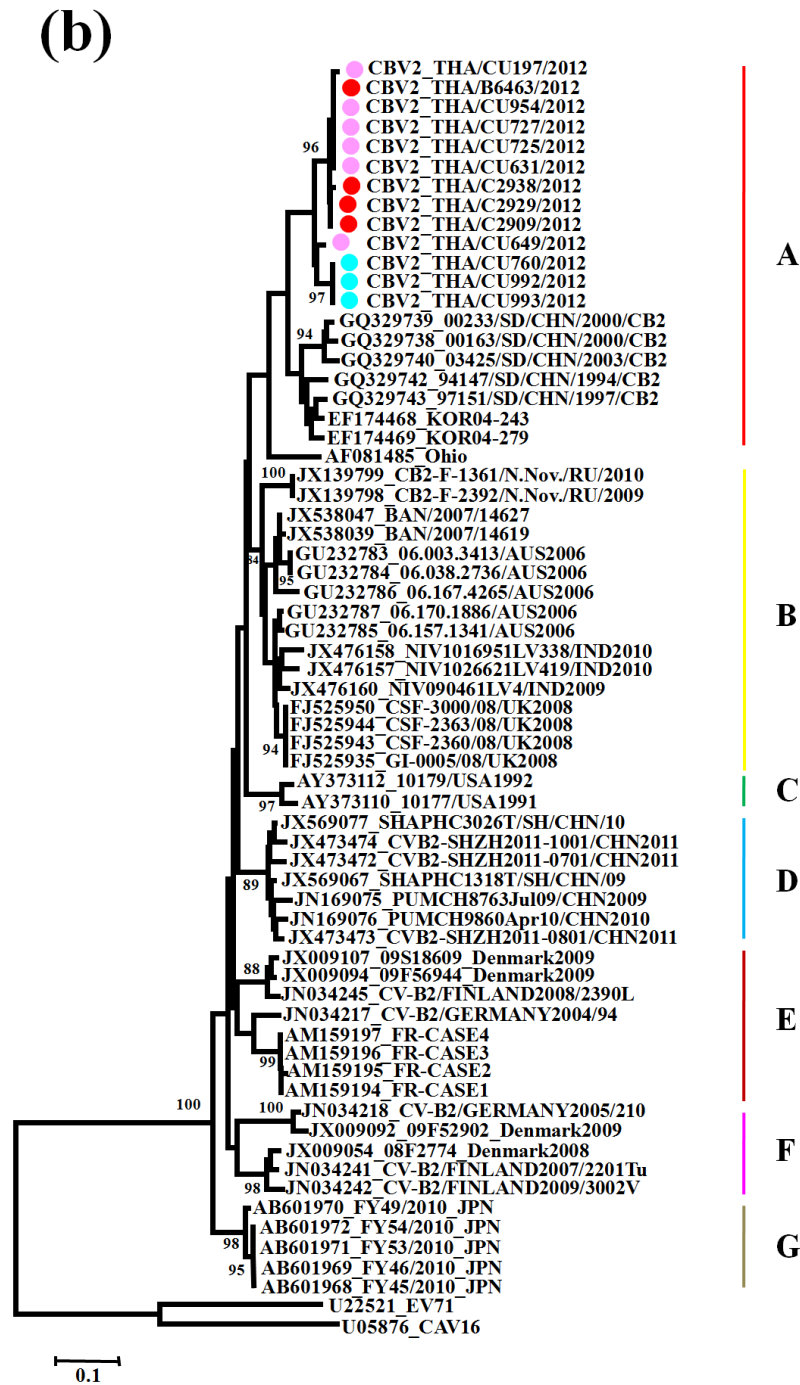


Figure 14. Phylogeny of a) CV-A8 and b) CV-B2 based on the partial VP1 region constructed by the neighbor-joining (NJ) algorithm implemented in MEGA version 5.0 using the Kimura two-parameter substitution model and 1000 bootstrap pseudo-replicates.

Strains from HFMD patients are indicated in pink, herpangina patients in blue, and influenza like illness patients in red.

Table 8. Nucleotide identity matrix obtained for the alignment of the partial VP1 region of CV-A6 strains from Thailand and reference strains of CV-A6 and other members of enterovirus species A.

Sequence	KF383346	KF383348	KF383351	KF383355	KF383358	KF383361	Gdula	Donovan	BrCr	Kowalic
<b>KF383348</b>	94.3									
<b>KF383351</b>	94.8	99.4								
<b>KF383355</b>	94.3	99.4	99.4							
<b>KF383358</b>	94.5	99.7	99.7	99.7						
<b>KF383361</b>	94.5	99.7	99.7	99.7	100.0					
<b>Gdula</b>	83.5	82.2	82.2	81.7	81.9	81.9				
<b>Donovan</b>	66.4	66.7	66.7	66.7	66.4	66.4	68.8			
<b>BrCr</b>	57.8	56.0	55.7	55.7	55.7	55.7	57.2	59.0		
<b>Kowalic</b>	62.8	63.6	63.9	63.9	63.9	63.9	64.1	68.5	60.6	
<b>Swartz</b>	65.7	66.4	66.4	65.9	66.2	66.2	65.2	62.8	56.5	67.5

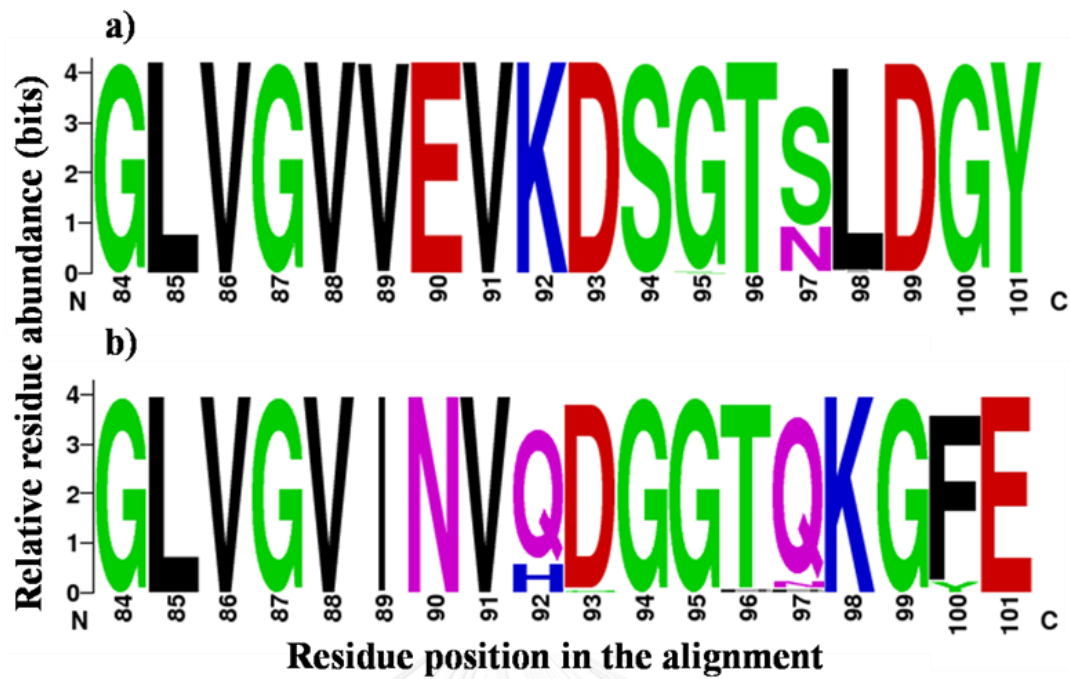


Figure 15. Genome signatures in amino acid residues at the alignment position of BC surface-exposed loop of a) CV-A6 and b) CV-A8 in Thailand in 2012.

The graphical presentation was performed using WebLogo. The height of symbol indicates the relative frequency of the corresponding amino acid at that position. Residue positions are given based on the nucleotide positions of the Gdula strain (AY421764) and the Donovan strain (AY421766).

## Part 2: Development of single step multiplex real-time RT-PCR for screening (panEV) and typing (EV-A71/CV-A6/CV-A16) of Enterovirus

HFMD is one of the most infectious diseases commonly found in infant and children aged <5 years. Series of molecular surveillance study have been reported that large-outbreaks of HFMD were frequently found in Western Pacific and Southeast Asia countries with endemic findings in America and Europe countries. Since the discovery of a large outbreak of HFMD associated with CV-A6 in Finland in 2008, the virus has spread worldwide including China, Japan, Spain, Taiwan, the United State and Scotland (115-118, 124, 125). Unlike EV-A71 and CV-A16, infection with CV-A6 often causes uncommon symptoms in HFMD patients including cutaneous eruption, perioral lesions, large vesicles affecting the palms, soles, face, trunk and buttock, and also onychomadesis (nail shedding). In the past few years, HFMD has been recognized as endemic disease in Thailand and the dominant causative pathogens change every endemic season. In recent, a large CV-A6 outbreak was documented in 2012 and eclipsing EV-A71 and CV-A16 as causative agents (126). As the outbreak of CV-A6 increases, there is a requirement for early and rapid diagnostic techniques to differentiate EV-A71, CV-A16 and CV-A6, prevent the spread of these viruses and for initial treatment as soon as possible.

As these enteroviruses usually cause very similar clinical symptoms, there is a requirement for accurate diagnostic techniques to differentiate EV-A71, CV-A16 and CV-A6, prevent the spread of these viruses and for initial treatment as soon as possible. Monospecific PCR assays have been described to identify EV-A71, CV-A16 and CV-A6 of each target and are therefore expensive and resource intensive (119, 120, 127, 128). Multiplex PCR assays have a significant advantage for clinical diagnosis, as several viruses can be detected in a single reaction mixture, and also been reported for

differentiating EV-A71 and CV-A16. However, the viral targets commonly can be distinguished after electrophoresis by PCR product size or hybridization with probes after completion of the PCR reaction (129). The multiplex real-time RT-PCR (rRT-PCR) is a powerful tool used for improving the sensitivity of hEV detection and one-tube assay for multi-pathogen detection. Many assays based on multiplex rRT-PCR had been applied to the differential detection of EV-A71 and CV-A16, but none of them were targeted CV-A6 (130-133). Recently, another rRT-PCR assay was also developed for the specific detection of CV-A6 (134). However, this assay is single rRT-PCR methods that detect VP1 genes of CV-A6.

In this study, a rapid and convenient one-step multiplex real-time RT-PCR using TaqMan probes for simultaneous detection and serotypes differentiation of circulating EV in Thailand was developed and evaluated. Consequently, two separate assays were developed for screening EV and concurrently identifying their serotypes. The first assay consists of primers and probes corresponding to the viral protein gene (VP1) of EV-A71, CV-A16 and CV-A6 in order to identify the three most prominent genotypes of enterovirus capable of infecting humans. The other assay employed primers and probes target to the 5'UTR of almost all EVs specifically and GAPDH gene of host cells for screening of enterovirus and serving as an internal control, respectively.

## Materials and Methods

### Ethical considerations

The research protocol was approved by the institutional review board of the Ethical Committee of the Faculty of Medicine, Chulalongkorn University, Thailand (approval number IRB286/58). Patient identifiers including personal information (name, address) and hospitalization number were removed from these samples to protect patient confidentiality and neither did they appear in any part of document in this study. Permission for specimen utilization had been granted by the Director of King Chulalongkorn Memorial hospital. IRB waived the need for consent because the samples were de-identified.

### Virus and samples

The specificity of the multiplex rRT-PCR assay was evaluated by cross reaction tests with known viral isolates and different panels of sequence confirmed known clinical samples with other genotypes of EV including: CV-A4 ( $N = 4$ ), CV-A5 ( $N = 2$ ), CV-A8 ( $N = 7$ ), CV-A9 ( $N = 3$ ), CV-A10 ( $N = 10$ ), CV-A12 ( $N = 2$ ), CV-A21 ( $N = 1$ ), echovirus 25 ( $N = 1$ ), CV-B1 ( $N = 2$ ), CV-B2 ( $N = 6$ ), CV-B4 ( $N = 2$ ) and CV-B5 ( $N = 1$ ). The assays were also evaluated against other viral pathogens as reference material including: influenza A (H3N2;  $N = 5$  and H1N1;  $N = 5$ ), influenza B ( $N = 5$ ), respiratory syncytial virus (RSV) ( $N = 5$ ), adenovirus ( $N = 4$ ), rotavirus ( $N = 5$ ), parechovirus ( $N = 5$ ), and the non-specific pathogen specimens ( $N = 100$ ), which were negative for pan-enterovirus, EV-A71, CV-A16 and CV-A6.

A total of 1,312 clinical specimens (stool/rectal swab, throat swab, vesicle fluid, serum, CSF) collected from HFMD suspected patients in Thailand during the period from

2012-2016 were utilized to test the multiplex real-time PCR. The samples were stored at -70 °C until testing.

### Design of primers and probes

In this study, a rapid and sensitive single-step multiplex real-time RT-PCR was developed and evaluated by using primers and TaqMan probes in two assays. The first assay comprises of primers and probes specific to VP1 genes of EV-A71, CV-A16 and CV-A6 in order to identify the three most predominant genotypes of enterovirus that cause of HFMD in Thailand. Primers and probes for differentiation between EV-A71, CV-A16 and CV-A6 were designed from conserved nucleotide sequences specific for the VP1 gene of EV-A71 for EV-A71 detection, specific for the VP1 gene of CV-A16 for CV-A16 detection and specific for the VP1 gene of CV-A6 for CV-A6 detection. For the other assays aimed at screening other HEV, the specific regions of 5'UTR hEV were chosen for designation of primers and probes to identify other hEV. Primers and probes for GAPDH detection were designed previously to correspond to the glyceraldehyde-3-phosphate dehydrogenase (GAPDH) nucleotide sequence.

In order to design primers and probes for the screening and typing of HEV, the nucleotide sequences of the VP1 genes of EV-A71, CV-A16 and CV-A6 and 5'UTR of other HEV available from the Genbank database were aligned using the CLUSTALX multiple alignment program. Both of primers and probes were analyzed using the primer design software (OLIGOS, Version 9.1 by Ruslan Kalendar, Institute of Biotechnology, University of Helsinki, Finland) and the software Primer Express 5.0 (Applied Biosystems) to ensure that they could be combined in a multiplex format and subjected to identical PCR conditions. The probes were labeled with minor groove binding black hole quencher (BHQ) at the 3' end, and three different fluorescent reporter dyes (FAM, HEX and ROX) at the 5' end, so that multiple pathogens of EV (EV-A71, CV-A16, CV-A6) could be

identified simultaneously in one-tube assay. All data related to the primers and probes are shown in table 9.

### Nucleic acid extraction and reverse transcription

Viral genomic RNA was extracted from cell cultures infected with EV-A71 or clinical samples using a Viral Nucleic Acid Extraction Kit (RBC Bioscience, Taipei, Taiwan) according to the manufacturer's instructions and the extracted solution was stored at -70°C.

Reverse transcription was performed as follows: 5 µl of the extracted viral genomic RNA was mixed with 0.5 µg random primer, denatured at 70 °C for 5 min, and immediately cooled on ice for a final volume of 20 µl reaction mixture. For complementary DNA (cDNA) synthesis, 7.3 µl of nuclease-free water, 4 µl of 5x reaction buffer, 1.5 mM MgCl<sub>2</sub>, 0.5 mM dNTP Mix, 20 U of RNase inhibitor and 1 µl of ImProm-II™ (Promega) reverse transcriptase were mixed.

Table 9. Multiplex PCR primers and TaqMan probes (135).

Target region	Primer/Probe	Sequence (5'-3')	Position	Strand	Reference
GAPDH	GAPDH-F85	GTGAAGGTCGGAGTCAACGG	85 – 104	Sense	(135)
	GAPDH-P121	HEX-CGCTGGTCACCGGGCTGC-BHQ1	121 – 140	Sense	
	GAPDH-R191	TCAATGAAGGGGTCATTGATGG	191 – 169	Antisense	
5'UTR	pan-F453	TCCTCCGGCCCCTGAATG	453 - 470	Sense	-
	pan-P590	FAM-GCAGCGGAACCGACTACTTT-BHQ1	537 - 556	Sense	
	pan-R1	ATTGTCACCATAAGCAGCCA	587 - 606	Antisense	
VP1	EV-A71_F3079	ATGATGGGYACRTTCTCRGTG	3079 - 3099	Sense	-
EV-A71	EV-A71_P3153	FAM-GAGRATGAAGCAYGTCAGGGCRTGG -BHQ1	3153 - 3177	Sense	
	EV-A71_R3326	TTG CCC ACG TAA ATG GCC	3309 - 3326	Antisense	
VP1	CV-A16_F2830	ATGCGCTTTGATGCTGAATTCA	2830 - 2851	Sense	-
CV-A16	CV-A16_P2913	HEX-CCC RCC AGG GGC TCC RAA ACC-BHQ1	2913 - 2933	Sense	
	CV-A16_R3032	GACATGAARGGGACTGACACTTG	3010 - 3032	Antisense	
VP1	CVA6-F2586	GAGCRAGTTCYAATGCTAGTG	2586 - 2606	Sense	-
CV-A6	CVA6-P2642	ROX-CGAAACGGGGTYAATGARGCGAGTGTGG-BHQ2	2642 - 2669	Sense	
	CVA6-R2802	GAYAGCTCTAGTTGCGCCG	2783 - 2802	Antisense	



### **Construction of plasmids as a positive control**

Standard plasmids containing specific viral target fragments were used as template for optimization of each of the assays for screening pan-enterovirus and typing (EV-A71/CV-A6/CV-A16) of enteroviruses. Plasmid DNAs were constructed by insertion of the VP1 gene of EV-A71 (nt 832-1079; EV-A71B5\_THA/CU1048/2012 and EV-A71C4\_THA/CU562/2012), VP1 gene of CV-A6 (nt 146-359; CV-A6\_THA/CU788/2012, KF661213), VP1 gene of CV-A16 (nt 2825-3027; CV-A16\_THA/CU1012/2012, KF661132), GAPDH gene (nt 85-191), 5'UTR region (nt 453-R1; EV-A71B5\_THA/CU1048/2012) into the pGEM-T Easy Vector (Promega, Madison, WI) by TA-cloning strategy. The resulting plasmid constructs were confirmed by PCR and DNA sequencing (First BASE Laboratories, Selangor Darul Ehsan, Malaysia).

### **RNA standard for sensitivity test**

RNA standard for the sensitivity test was generated using the RiboMAX™ Large Scale RNA Production System-T7 (Promega, Madison, WI) according to the manufacturer's instructions. After DNase digestion to remove residues of RT-PCR products, the transcribed RNA was purified twice using a Viral Nucleic Acid Extraction Kit according to the manufacturer's recommendation (RBC Bioscience, Taipei, Taiwan). The concentration of the transcribed RNAs was calculated by measuring absorbance at 260 nm. The RNAs standards of serial diluted concentrations ( $10^8$  - 10 copies/ $\mu$ l) were used to evaluate the sensitivities and detection limits of the one-step multiplex rRT-PCR assay.

### **One-step multiplex rRT-PCR assay**

To use differentially for each pathogen, five monoplex real-time RT-PCR assays were initially performed and followed by multiplexing. All real-time RT-PCR reactions were carried out in the LightCycler® Nano instrument capable of simultaneous detection of up

to three different fluorescence dyes. Thus, two multiplex assays were created and run separate in each of two tubes: screening (pan-EV, GAPDH) were tested in reaction 1; typing (EV-A71, CV-A16, CV-A6) were tested in reaction 2. The reaction mixture of a monoplex real-time RT-PCR in a total volume of 10  $\mu$ l contained: RNA template, one-step RT-PCR reaction mix including RNase Inhibitor,  $Mg^{2+}$ , primers and probe. The reaction mixture of a multiplex real-time RT-PCR in a total volume of 20  $\mu$ l contained: RNA template, one-step RT-PCR reaction mix including RNase Inhibitor,  $Mg^{2+}$ , two or three pairs of primers and two or three probes. Cycling was performed as follows: 30 min at 42°C to activate RT, followed by initial denaturation for 3 min at 95°C with a subsequent 40-45 cycles of amplification (denaturation at 95°C for 15 s and annealing as well as extension at 55-62°C for 20 s). Multiple fluorescent signals were obtained once per cycle upon completion of the extension step with detectors corresponding to FAM (518 nm), HEX (553 nm) and ROX (607 nm). Fluorescent signals were collected during annealing and extension steps and amplification data were analyzed using the Light Cycler<sup>®</sup> Nano SW1.1 software according to the manufacturer's instructions. To obtain the highest fluorescence signals and lowest threshold cycle (Ct), the final concentration of primers, probes and  $Mg^{2+}$  were optimized.

### Statistical analysis

Reproducibility was computed using the Ct values, standard deviations, coefficients of variation of the standard curves and confidence intervals (CI) separately for each RNA dilution. Sensitivity, specificity, and positive and negative predictive values of the two assays were calculated from two-by-two contingency tables for each test with their 95 % confidence intervals (CIs). Data analysis was done using the Statistical Package for Social Sciences version 17.0 (SPSS Inc., Chicago, IL).

## Results

### Optimization of mono- and multiplex real-time RT-PCR conditions

To optimize monoplex and multiplex real-time RT-PCR panels, several factors including primers and probes concentration, additional  $Mg^{2+}$  concentration and thermocycling condition were subjected by using the transcribed RNAs as positive control. A monoplex real-time RT-PCR assay and a multiplex assay for simultaneous detection of pan-enterovirus, EV-A71, CV-A16 and CV-A6 were carried out in use of SensiFAST Probe No-ROX One-Step kit (Bioline, Australia). The optimized reaction system of each monoplex real-time RT-PCR assay of 10  $\mu$ l total volume consisted of 5  $\mu$ l of 2x PCR buffer, 0.3  $\mu$ M of forward and reverse primer, 0.1  $\mu$ M of each probe, 0.1  $\mu$ l of Reverse transcriptase and 0.2  $\mu$ l of RNase inhibitor. The optimized reaction system of each tube reaction of multiplex real-time RT-PCR of 20  $\mu$ l total volume consisted of 10  $\mu$ l of 2x PCR buffer, 0.3  $\mu$ M of forward and reverse primer, 0.075  $\mu$ M of each probe, 0.1  $\mu$ l of Reverse transcriptase and 0.2  $\mu$ l of RNase inhibitor. The optimal reaction conditions of a one-step assay were used as follows: 42 °C for 30 min, 95 °C for 3 min, then 45 cycles of 15 s at 95 °C and 20 s at 60 °C. Fluorescence data was collected at 60 °C.

### Interpretation of multiplex real-time RT-PCR detection

In first assay aimed at screening of panEV, the results were obtained by using multiple Taqman probes label with the FAM and HEX fluorescent signals corresponding to 5'UTR of panEV and GAPDH gene, respectively. The fluorescent signals obtained from the screening assay can be interpreted as shown in figure 16a. The results obtained from each detection channel revealed a clear signal without any unanticipated noises. PanEV yielded an amplification signal in the FAM channel and the internal control gene yielded detected in the HEX channel.

In the typing assay, the presence of EV-A71, CV-A16 and CV-A6 genotypes was detected by using TaqMan probes labeled with the FAM, HEX and ROX fluorescent dyes, respectively (figure 16b). Samples yielding a positive FAM signal have been interpreted as EV-A71 genotype, samples yielding a positive HEX signal as CV-A16 genotype and samples yielding a positive ROX signal as CV-A6 genotype.

#### **Specificities and qualitative ability of assays**

To estimate the specificity of the multiplex real-time RT-PCR assay, the cross-reactivity of the primers and probes was tested against other RNA viruses including influenza A virus (H3N2 and H1N1), influenza B virus, respiratory syncytial virus (RSV), adenovirus, rotavirus, human parechovirus, human rhinovirus and the unknown specimens, which were negative for enteroviruses. The results did not show any cross amplification signal when testing against other RNA viruses (data not shown).

Moreover, other genotypes of enterovirus including CV-A4, CV-A5, CV-A8, CV-A9, CV-A10, CV-A12, CV-A21, CV-B1, CV-B2, CV-B4, CV-B5 and echovirus 25 were also included in order to validate the assays in terms of specificity. The results show yielded only a FAM fluorescent signal of 5'UTR indicating panenterovirus but not typing EV-A71, CV-A16 and CV-A6 genotypes (Table 10), indicative of absence of cross-reactivity to other genotypes of enterovirus. These findings indicate high specificity of the primers and probes used in the multiplex real-time RT-PCR assay.

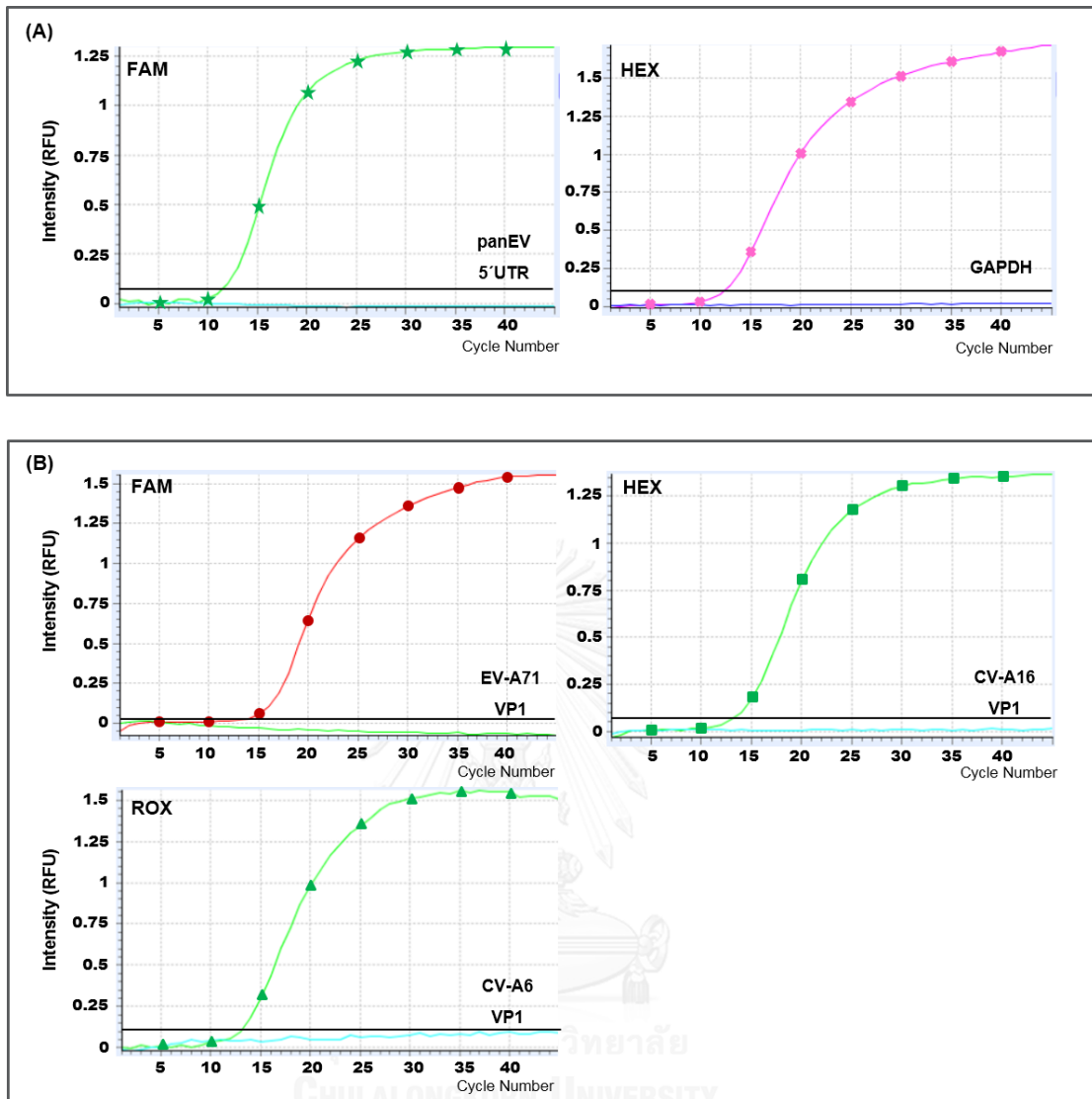


Figure 16. Interpretation of panEV (A) and hEV (B) detection by multiplex real-time RT-PCR assay. The panEV screening (A) shows fluorescent signals of FAM and HEX corresponded to 5UTR of panEV and GAPDH, respectively. The typing of hEV detection (B) shows fluorescent signals of FAM, HEX and ROX corresponded to EV-A71, CV-A16 and CV-A6, respectively.

Table 10. Specificity test of multiplex real-time RT-PCR.

Virus	Code	Fluorescent signal			
		FAM (panEV)	FAM (EV-A71)	HEX (CV-A16)	ROX (CV-A6)
Influenza A virus (H3N2)	B7858	-	-	-	-
Influenza A virus (H3N2)	B7885	-	-	-	-
Influenza A virus (H3N2)	B7914	-	-	-	-
Influenza A virus (H3N2)	B7919	-	-	-	-
Influenza A virus (H3N2)	B7922	-	-	-	-
Influenza A virus (H1N1)	B7256	-	-	-	-
Influenza A virus (H1N1)	B7491	-	-	-	-
Influenza A virus (H1N1)	B7652	-	-	-	-
Influenza A virus (H1N1)	B7678	-	-	-	-
Influenza A virus (H1N1)	B7731	-	-	-	-
Influenza B virus	B7283	-	-	-	-
Influenza B virus	B7284	-	-	-	-
Influenza B virus	B7294	-	-	-	-
Influenza B virus	B7508	-	-	-	-
Influenza B virus	B7636	-	-	-	-
Respiratory syncytial virus (RSV)	CU99	-	-	-	-
Respiratory syncytial virus (RSV)	CU161	-	-	-	-
Respiratory syncytial virus (RSV)	H3090	-	-	-	-
Respiratory syncytial virus (RSV)	CU205	-	-	-	-
Respiratory syncytial virus (RSV)	CU215	-	-	-	-
Adenovirus	B1435	-	-	-	-
Adenovirus	B1500	-	-	-	-
Adenovirus	B1522	-	-	-	-
Adenovirus	B1535	-	-	-	-
Rotavirus	B1755	-	-	-	-
Rotavirus	B1756	-	-	-	-
Rotavirus	B1757	-	-	-	-
Rotavirus	B1760	-	-	-	-
Rotavirus	B1762	-	-	-	-

Human parechovirus	B1304	-	-	-	-
Human parechovirus	B1415	-	-	-	-
Human parechovirus	B1610	-	-	-	-
Human parechovirus	B1630	-	-	-	-
Human parechovirus	B1652	-	-	-	-
Coxsackievirus A4 (KF661251)	CU283	+	-	-	-
Coxsackievirus A4 (KF661252)	CU369	+	-	-	-
Coxsackievirus A4 (KF661253)	CU571	+	-	-	-
Coxsackievirus A4 (KF661254)	CU672	+	-	-	-
Coxsackievirus A4 (KF661255)	CU983	+	-	-	-
Coxsackievirus A5 (KF661151)	CU200	+	-	-	-
Coxsackievirus A5 (KF661152)	CU291	+	-	-	-
Coxsackievirus A8 (KF661169)	CU178	+	-	-	-
Coxsackievirus A8 (KF661170)	CU261	+	-	-	-
Coxsackievirus A8 (KF661175)	CU314	+	-	-	-
Coxsackievirus A8 (KF661176)	CU349	+	-	-	-
Coxsackievirus A8 (KF661179)	CU381	+	-	-	-
Coxsackievirus A8 (KF661181)	CU389	+	-	-	-
Coxsackievirus A8 (KF661183)	CU457	+	-	-	-
Coxsackievirus A9 (KF661148)	CU646	+	-	-	-
Coxsackievirus A9 (KF661149)	CU948	+	-	-	-
Coxsackievirus A9 (KF661150)	CU981	+	-	-	-
Coxsackievirus A10 (KF661155)	CU254	+	-	-	-
Coxsackievirus A10 (KF661156)	CU255	+	-	-	-
Coxsackievirus A10 (KF661158)	CU320	+	-	-	-
Coxsackievirus A10 (KF661159)	CU833	+	-	-	-
Coxsackievirus A10 (KF661160)	CU843	+	-	-	-
Coxsackievirus A10 (KF661161)	CU902	+	-	-	-
Coxsackievirus A10 (KF661162)	CU957	+	-	-	-
Coxsackievirus A10 (KF661163)	CU958	+	-	-	-
Coxsackievirus A10 (KF661164)	CU787	+	-	-	-
Coxsackievirus A10 (KF661165)	CU963	+	-	-	-
Coxsackievirus A12 (KF661144)	CU281	+	-	-	-

Coxsackievirus A12 (KF661146)	CU767	+	-	-	-
Coxsackievirus A21 (KF661250)	CU976	+	-	-	-
Coxsackievirus B1 (KF661141)	CU617	+	-	-	-
Coxsackievirus B1 (KF661142)	CU753	+	-	-	-
Coxsackievirus B2 (KF661133)	CU760	+	-	-	-
Coxsackievirus B2 (KF661135)	CU197	+	-	-	-
Coxsackievirus B2 (KF661137)	CU727	+	-	-	-
Coxsackievirus B2 (KF661138)	CU954	+	-	-	-
Coxsackievirus B2 (KF661139)	CU992	+	-	-	-
Coxsackievirus B2 (KF661140)	CU993	+	-	-	-
Coxsackievirus B4 (KF661166)	CU202	+	-	-	-
Coxsackievirus B4 (KF661167)	CU540	+	-	-	-
Coxsackievirus B5 (KF661168)	CU256	+	-	-	-
Echovirus 25 (KF661108)	CU967	+	-	-	-

#### Sensitivities and detection limits of assays

To examine the actual detection limit of the multiplex real-time PCR assays, *in vitro* RNA transcripts of EV-A71, CV-A6, CV-A16 and panenterovirus were carried out with T7 RNA polymerase. A ten-fold serial dilution of each EVs RNA standard was then tested in the multiplex real-time PCR assays. The actual detection limit of the assay was determined to be 10 copies of synthetic RNA per reaction for EV-A71, CV-A6, CV-A16 and panenterovirus (Figure 17). The standard curves were generated using Ct values of each multiplex real-time RT-PCR assay and showed a linear relationship between the log of the viral titer and the Ct values for all assays (Figure 18). The multiplex rRT-PCR assays were linear with a dynamic range of detection between  $10^8$  and 10 copies/ $\mu$ l in 45 cycles for the standards of EV-A71 (correlation coefficient  $R^2 = 0.9982$ ; slope = -3.57), CV-A6 ( $R^2 = 0.9974$ ; slope = -3.53), CV-A16 ( $R^2 = 0.9863$ ; slope = -3.26) and panenterovirus ( $R^2 = 0.9740$ ; slope = -3.68). The amplification efficiency of developed multiplex rRT-PCR



assays for EV-A71, CV-A6, CV-A16 and panenterovirus was 90.6%, 92.0%, 100% and 87.0% respectively.

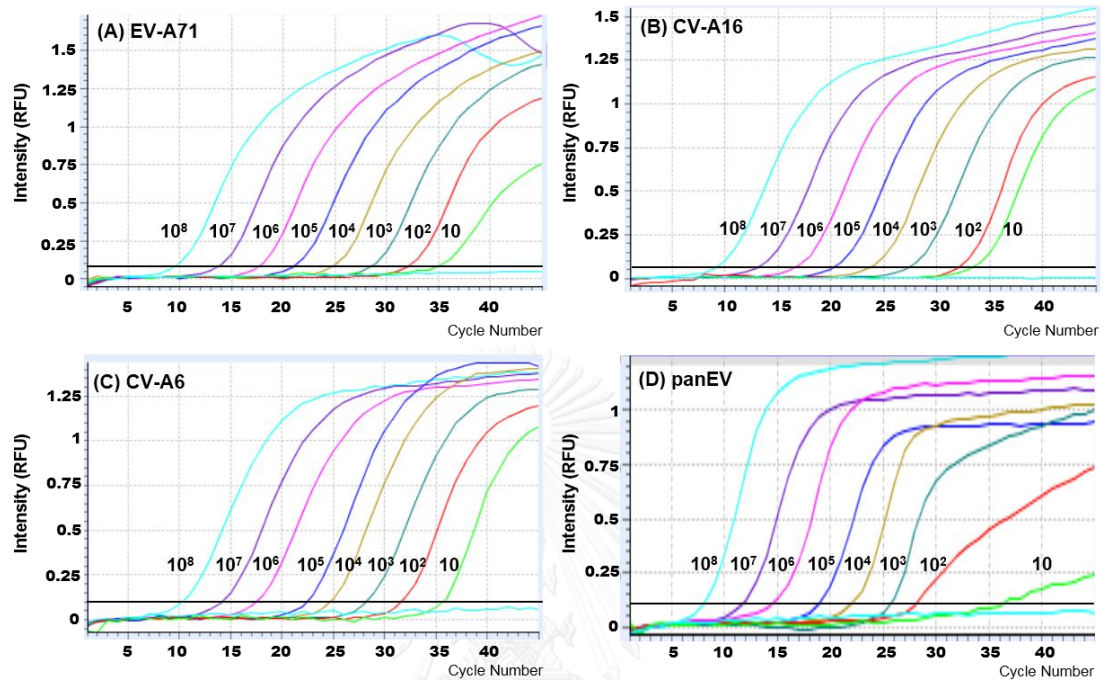


Figure 17. Sensitivity of the multiplex real-time RT-PCR assay for EV-A71 (A), CV-A16 (B), CV-A6 (C) and panEV (D), obtained from the amplification of 10-fold serially diluted the transcribed RNA standards.

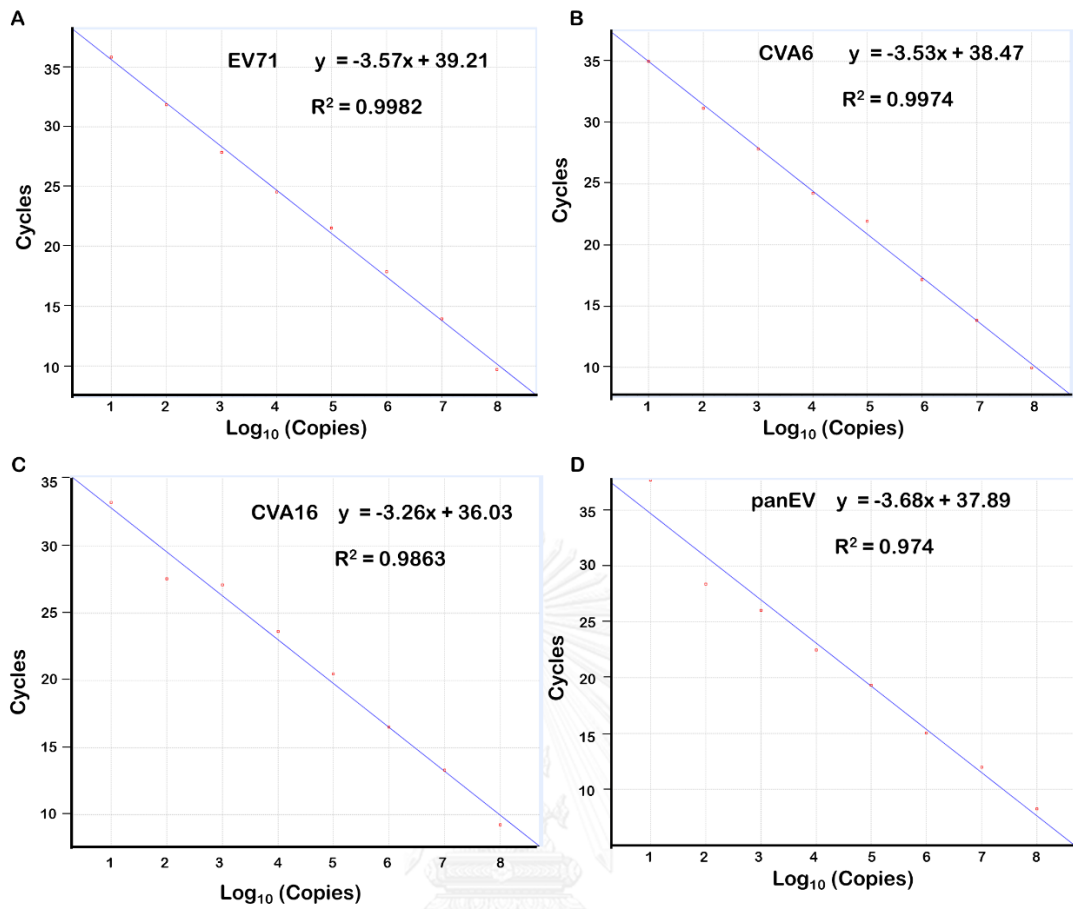


Figure 18. Standard curves of multiplex one-step real-time RT-PCR assays.

The multiplex one-step realtime TaqMan RT-PCR assays were tested using synthesized in vitro target viral RNA transcripts ranging from  $10^1$  to  $10^8$  copies/ $\mu\text{L}$ .

### Reproducibility of real-time RT-PCR assays

To determine intra-assay variation of the monoplex and multiplex rRT-PCR assay, serial dilution viral RNA standards (from  $10^6$  -  $10^3$  copies/reaction) were tested in triplicate within a single run (Table 11). The coefficients of variation (CV) and confidence intervals (CI) were calculated separately for each dilution. The mean CVs of intra-assay variability of the monoplex rRT-PCR were 0.98% (95% CI, -0.56–2.52%) for EV-A71, 1.30% (95% CI, 0.22–2.38%) for CVA6, 1.43% (95% CI, -1.09–3.94%) for CVA16 and 0.95% (95% CI, -0.11–2.01%) for panenterovirus. The mean CVs of intra-assay variability of the multiplex rRT-PCR were 1.63% (95% CI, 0.47–2.79%) for EV-A71, 1.92% (95% CI, 0.31–3.52%) for CVA6, 1.39% (95% CI, -1.14–3.91%) for CVA16 and 1.26% (95% CI, 0.08–2.43%) for panenterovirus.

Inter-assay variation of the monoplex and multiplex rRT-PCR assay were performed by testing for each standard dilution tested in three independent runs (Table 10). The mean CVs of inter-assay variability of the monoplex rRT-PCR were 2.91% (95% CI, 1.67–4.14%) for EV-A71, 2.48% (95% CI, 1.66–3.31%) for CVA6, 2.09% (95% CI, 0.32–3.87%) for CVA16 and 1.92% (95% CI, 0.36–3.48%) for panenterovirus. The mean CVs of inter-assay variability of the multiplex rRT-PCR were 2.24% (95% CI, -0.28–4.77%) for EV-A71, 3.11% (95% CI, 1.74–4.48%) for CVA6, 3.47% (95% CI, 1.77–5.16%) for CVA16 and 2.49% (95% CI, 1.54–3.43%) for panenterovirus. These results suggest that the singleplex and multiplex rRT-PCR assay were sufficiently reproducible.

Table 11. Intra- and inter-assay reproducibility of monoplex and multiplex real-time RT-PCR.

Virus Standard	Concentration (Copies/ $\mu$ l)	Intra-assay						Inter-assay					
		Monoplex RT-qPCR			Multiplex RT-qPCR			Monoplex RT-qPCR			Multiplex RT-qPCR		
		Mean Ct	SD	CV%	Mean Ct	SD	CV%	Mean Ct	SD	CV%	Mean Ct	SD	CV%
Enterovirus 71	1,000,000	18.53	0.15	0.81	20.47	0.49	2.39	20.13	0.67	3.33	17.4	0.6	3.45
	100,000	22.23	0.06	0.27	23.1	0.17	0.74	23.97	0.76	3.17	21.03	0.15	0.71
	10,000	27.17	0.12	0.44	27.23	0.55	2.02	28.2	0.95	3.37	25.1	0.46	1.83
	1,000	30.1	0.72	2.39	32.4	0.44	1.36	32	0.56	1.75	29.27	1.03	3.52
Coxsackievirus A6	1,000,000	18.9	0.1	0.53	21.47	0.72	3.35	19.2	0.61	3.18	17.53	0.59	3.37
	100,000	23.97	0.4	1.67	27.3	0.4	1.47	24.23	0.55	2.27	22.97	0.97	4.22
	10,000	27.5	0.56	2.04	31.37	0.32	1.02	28.13	0.55	1.96	24.63	0.59	2.40
	1,000	32.33	0.31	0.96	35.13	0.64	1.82	32.13	0.81	2.52	28.2	0.69	2.45
Coxsackievirus A16	1,000,000	19.7	0.1	0.51	20.53	0.06	0.29	20.2	0.52	2.57	17.67	0.83	4.70
	100,000	24.7	0.2	0.81	25.5	0.17	0.67	24.57	0.12	0.49	21.43	0.85	3.97
	10,000	28.6	0.17	0.59	29.33	0.25	0.85	29.47	0.67	2.27	25.8	0.61	2.36
	1,000	32.97	1.25	3.79	32.6	1.22	3.74	32.27	0.98	3.04	30.7	0.87	2.83
Panenterovirus	1,000,000	21.03	0.12	0.57	22.3	0.5	2.24	21.07	0.15	0.71	19.27	0.55	2.85
	100,000	24.33	0.06	0.25	26.03	0.15	0.58	25.07	0.71	2.83	22.37	0.42	1.88
	10,000	30.4	0.53	1.74	30.47	0.42	1.38	29.9	0.46	1.54	25.4	0.53	2.09
	1,000	33.87	0.42	1.24	35.23	0.29	0.82	34.67	0.9	2.60	28.87	0.9	3.12

### Performance of multiplex real-time RT-PCR against conventional RT-PCR

To evaluate the performance of the multiplex rRT-PCR assay, the clinical specimens were tested and its sensitivity and specificity were compared with conventional RT-PCRs (Table 12). A total of 1,312 samples from suspected HFMD and herpangina patients in hospitals and 100 other respiratory samples were tested using the multiplex rRT-PCR assay and conventional RT-PCRs. Of the 1,312 samples tested, 723 (55.1%) samples were detected positive by multiplex rRT-PCR and 602 (45.9%) samples positive by conventional RT-PCRs. Overall, concordance between both methods was 83.6%. Similarly, both methods identified specimens that were positive for EV-A71 (87 samples), CV-A6 (206 samples), CV-A16 (101 samples) and panenterovirus (161 samples). The overall diagnostic sensitivity, specificity, positive predictive value (PPV) and negative predictive value (NPV) of the multiplex rRT-PCR assay were greater than those of conventional RT-PCRs as shown in table 12. For example, the sensitivity and

specificity for EV-A71 using multiplex rRT-PCR were 99.0% (95% CI, 94.4 - 100.0%) and 100% (95% CI, 96.4 - 100.0%) and conventional RT-PCRs were 90.7% (95% CI, 83.1 - 95.7%) and 98.0% (95% CI, 93.0 - 99.8%) respectively. For CV-A6, sensitivity and specificity were 93.1% (95% CI, 89.2 - 95.8%) and 97.0% (95% CI, 91.5 - 99.4%) for multiplex rRT-PCR while sensitivity and specificity were 86.5% (95% CI, 81.7 - 90.4%) and 84.0% (95% CI, 75.3 - 90.6%) for conventional RT-PCRs.

Table 12. Diagnostic performance of one step multiplex real-time PCR and conventional RT-PCR identification of hand foot mouth viruses.

Virus	Assay Performance (95% CI)			
	Sensitivity (%)	Specificity (%)	PPV (%)	NPV (%)
<b>Enterovirus 71</b>				
multiplex rRT-PCR	99.0 (94.4 - 100.0)	100.0 (96.4 - 100.0)	100.0 (96.2 - 100.00)	99.0 (94.6 - 100.0)
cRT-PCR	90.7 (83.1 - 95.7)	98.0 (93.0 - 99.8)	97.8 (92.2 - 99.7)	91.6 (84.6 - 96.1)
<b>Coxsackievirus A6</b>				
multiplex rRT-PCR	93.1 (89.2 - 95.8)	97.0 (91.5 - 99.4)	98.8 (96.5 - 99.8)	84.4 (76.4 - 90.5)
cRT-PCR	86.5 (81.7 - 90.4)	84.0 (75.3 - 90.6)	93.3 (89.4 - 96.1)	70.6 (61.5 - 78.6)
<b>Coxsackievirus A16</b>				
multiplex rRT-PCR	92.8 (87.4 - 96.3)	100.0 (96.4 - 100.0)	100.0 (97.4 - 100.00)	90.1 (83.0 - 95.0)
cRT-PCR	73.7 (65.9 - 80.5)	100.0 (96.4 - 100.0)	100.0 (96.8 - 100.00)	71.4 (63.2 - 78.7)
<b>Panenterovirus</b>				
multiplex rRT-PCR	93.5 (89.8 - 96.2)	94.0 (87.4 - 97.8)	97.6 (94.9 - 99.1)	84.7 (76.6 - 90.8)
cRT-PCR	67.9 (61.9 - 73.6)	80.0 (70.8 - 87.3)	89.9 (84.8 - 93.7)	48.8 (40.9 - 56.7)

### Part 3: Molecular epidemiology and the evolution of human Coxsackievirus

#### A6

Coxsackievirus A6 (CV-A6) is a group of genetically diverse RNA viruses belonging to the Picornaviridae family and the enterovirus (EV) species. The enterovirus species contains important pathogenic viruses such as poliovirus, hepatitis A virus, and EV-A71 viruses (1). CV-A6 has been classified in the genus Enterovirus species A which currently comprises a total of 20 types. EVs possess a positive-stranded RNA genome of approximately ~7,400 nucleotides (or 7.4 kb), encased by a highly structured icosahedral capsid. The viral genome is translated into a large polyprotein that is subsequently cleaved into structural (VP1 to VP4) and non-structural proteins (2A to 2C and 3A to 3D). The VP1 is the immunodominant structural protein and contains the most important serotype-specific neutralization epitopes. The degree of similarity of nucleotides and amino acid sequences of the VP1 region provides the primary tool for identification and assignment of new types within a species; novel EV variants showing less than 75% nucleotide sequence identity are classified as new types (136).

Infection with CV-A6 is frequently asymptomatic, but may also manifest as influenza like syndrome or as a self-limiting hand, foot and mouth disease (HFMD). Previously, HFMD typically occurred in young children and was predominantly caused by enterovirus 71 (EV-A71) and CV-A16. HFMD has only sporadically associated with other members of EV species A (6, 114, 137). More recently, CV-A6 was first identified as the cause of epidemic HFMD with unusual clinical manifestation in Finland in 2008 (113). Since then, HFMD cases associated with CV-A6 have been reported in several countries in Europe, Asia and USA (116-119, 138, 139), reflecting the rapid emergence of a more pathogenic form of this species A serotype. Lately, CV-A6 has been the most common EV type identified in several outbreaks of HFMD that have typically been characterized by

a more severe clinical spectrum (eczema coxsackium and erosive lesions) as well as subsequent benign onychomadesis (115, 125, 140-145).

Since 2008, the predominant causative pathogen of HFMD in Thailand was either EV-A71 or CV-A16, which, however changed from year to year. In 2012, a large-scale outbreak of HFMD took place in Thailand with the highest incidence rate in a decade. Meanwhile, CV-A6 had replaced EV-A71 and CV-A16 as the major EV types, and was identified in 33.5% of surveillance samples in Thailand in 2012 (119). Moreover, there was a high number of CV-A6-infected patients presented with influenza like symptoms (126).

Recently, (146) described a potential correlation between the emergence of new CV-A6 variants with altered clinical phenotypes and the appearance of novel recombinant forms (RFs) of the virus. The latter possessed phylogenetically distinct 3Dpol region sequences likely acquired from other species A serotypes through recombination. They found that several different RFs have circulated over the past decade worldwide. Notably, the emergence of the new recombinant form (RF-H) has been associated with clinically reported cases of HFMD presenting as eczema herpeticum in Edinburgh in 2014.

How widely RF-H and its predecessor, RF-A and other recently emerged RFs circulate in Europe is unknown, nor is it clear whether the greater community circulation and spiking incidence of HFMD in Thailand reflects the more widely spread of such recombinants. To address these questions, we utilized molecular epidemiology by analyzing VP1 sequence divergence and 3Dpol sequence grouping of a total of 151 CV-A6 isolates and samples collected in several European countries (Germany, Spain, Sweden and Denmark) and Thailand between 2013 and 2014.

## Materials and Methods

### Samples.

A total of 151 anonymized CV-A6-positive clinical samples from Denmark, Germany, Spain, Sweden and Thailand collected between years 2013 and 2014 were selected for genetic characterization. Sequences were named using the following convention: two-letter country code/sample code/3Dpol clade/year of collection (e.g. DK/M22416/G/2014 for sample code M22416 referred from Denmark, collected in 2014, and belonging to the 3Dpol clade G). 3Dpol clade assignments were identified from the results of phylogeny (see below). Sequences obtained in the current study were supplemented with 79 previously published nucleotide sequences of complete genomes from 6 countries, including the CV-A6 prototype strain Gdula. The respective samples were collected between 1949 and 2014. Details of the sequences used in the study including the countries of origin, sampling dates and accession numbers are provided in Appendix A Table 1.

### Amplification of VP1 and 3Dpol regions.

Nested reverse transcription-PCRs (RT-PCRs) were carried out using newly designed primers listed in Appendix A table 2 to amplify a 1,331-bp region of the VP1 gene and a 1,200-bp region of the 3Dpol gene. The reverse transcription and first round PCR were performed using Superscript III One-Step RT-PCR system with Platinum Taq High Fidelity according to the manufacturer's instructions (Invitrogen, Carlsbad, CA). The following conditions were used: heating at 43 °C for 1 h, then 20 cycles of 53 °C for 1 min and 55 °C for 1 min, followed by 70 °C for 15 min and 94 °C for 2 min. PCR cycles included 40 cycles of 94 °C (30 s), 50 °C (30 s), and 68 °C (1 min 45 s) and a final extension at 68 °C for 5 min. One microliter of the first-round reaction was used as template in the second-round PCR containing second-round primers and GoTaq DNA polymerase (Promega,



Madison, WI) for 30 cycles of 94 °C for 30 s, 50 °C for 30 s and 72 °C for 90 s, followed by a final extension step for 5 min at 72 °C. Sequencing of the amplification products was carried out directly in both directions using ABI 7200 BigDye capillary sequencing (Applied Biosystems, Framingham, MA).

#### **Complete genome sequencing.**

The full-length genome of 39 CV-A6 variants representing four of the recombination groups were sequenced (RF-A, n = 21; RF-F, n = 10; RF-G, n = 2; and RF-H, n = 6) using primer sets (Appendix A Table 2) designed according to CV-A6-specific nucleotide sequences downloaded from GenBank. cDNA was synthesized with Superscript III reverse transcriptase (Invitrogen, Carlsbad, CA) and random hexamer primers and used as the template for nested PCR. The cycling conditions were identical to the second-round PCR mentioned above.

#### **Sequence analysis.**

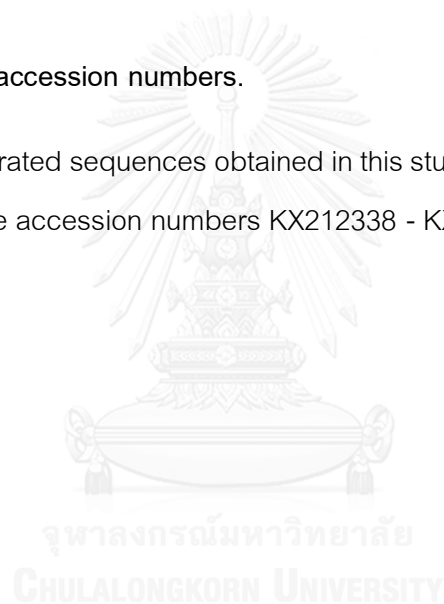
Sequences were formatted, assembled and aligned using the SSE 1.2 sequence editor package ([www.virus-evolution.org](http://www.virus-evolution.org)) (147). Phylogenetic trees were constructed using the Maximum-likelihood method and determined best-fit model of nucleotide substitution for each sequence data set using a correction value in the model selection procedure implemented in the MEGA program (v6) (148). In the analyses, Kimura two-parameter (K2P) with invariant sites (I) was selected as the substitution model for VP1 and 5UTR; K2P with I and gamma distribution (I-) for 3Dpol; K2P with I- for VP4/2 and 1000 bootstraps.

Rates of evolution and molecular clock phylogeny (149) were estimated from VP1 gene sequences using the Bayesian Markov Chain Monte Carlo (MCMC) method implemented in BEAST, version 1.8.0 (150). Bayesian MCMC analyses were performed

using a relaxed log-normal molecular clock model. The dynamic among study populations was estimated by performing a constant size and exponential growth models. Each Bayesian MCMC analysis was for 100,000,000 iterations and sampled every 10,000 states and discarding 10% of the chain as burn-in. Convergence of the chains and effective sample sizes of the estimates were checked using Tracer (<http://beast.bio.ed.ac.uk/Tracer>). The resulting tree of each run was summarized using Tree Annotator, and the maximum clade credibility tree was visualized with TreeAnnotator/FigTree.

#### **Nucleotide sequence accession numbers.**

All newly generated sequences obtained in this study were submitted to GenBank and were assigned the accession numbers KX212338 - KX212678.



## Results

### Phylogeny of CVA6 VP1 and 3Dpol genome regions

CV-A6 variants associated with HFMD presenting with eczema herpeticum in Edinburgh in 2014 were clustered in a novel appearance clade (RF-H) distinct from other previously characterized recombination groups assigned in the 3D region (146). These variants were also phylogenetically distinct in the VP1 region (146). In the current study we have extended the analysis of VP1 and 3D regions to CV-A6 variants identified in wider geographical area including Denmark (n = 22), Germany (n = 4), Spain (n = 14), Sweden (n = 6) and Thailand (n = 105). CV-A6 sequences for the VP1 region between positions 2485 and 3816 (numbering based on the Gdula prototype strain; GenBank accession number AY421764) were obtained.

VP1 sequences from Denmark and Spain (2014) clustered within the same lineage (lineage I) with those analysed previously from the patients with eczema herpeticum presenting in 2014 in Edinburgh but distinct from previous outbreaks in Taiwan (lineage II), Thailand (lineage III), China (lineage VI) and Finland (lineage V) (Figure 19-20).

In order to investigate the occurrence of recombination, sequences from the 3Dpol region were obtained and analyzed for each of the 151 isolates included in the VP1 analysis. The data set was supplemented by 39 (near-) complete genome sequences of CV-A6 variants from Denmark (n = 8), Germany (n = 3), Spain (n = 3) and Thailand (n = 25). CV-A6 3Dpol clades comprising groups A, B, C, D, E, F, G, H, I, J and K were designated through identification of bootstrap-supported clades as described previously for other enteroviruses (151-153). Designations follow the nomenclature established in our previous analysis of Edinburgh CV-A6 isolates (146). The majority of variants in the study clustered within two of the previously assigned recombinant forms, RF-A (99/151) and RF-F (37/151) (Table 13). Four Danish variants clustered within clade RF-H, as did two of the

variants from Spain. Three variants from Denmark and Spain were assigned as RF-G (Figure 21). No sequences within this study clustered within the previously described RF-B, RF-C, RF-D and RF-E. None of the CV-A6 3Dpol groups contained sequences from other species A serotypes.

Phylogenetic analysis of the VP1, VP4/2 and the 5'UTR produced broadly similar groupings of CV-A6 variants in each region (Figure 20, 22 and 23). However, there were several examples of incongruent groupings that indicate the existence of further recombination within CV-A6. For example, RF-E variants grouped with RF-A and -H in VP1 region but changed position in the 5'UTR and VP4/2. In contrast to VP1, RF-A were interspersed in the 5'UTR and VP4/2 regions with the member of RF-J. The phylogenetic group formed of RF-K was monophyletic in the VP1, VP4/2 and the 5'UTR regions but the only one exception grouped with RF-D. These findings indicate the occurrence of multiple recombinant events between VP1, VP4/2 and the 5'UTR.

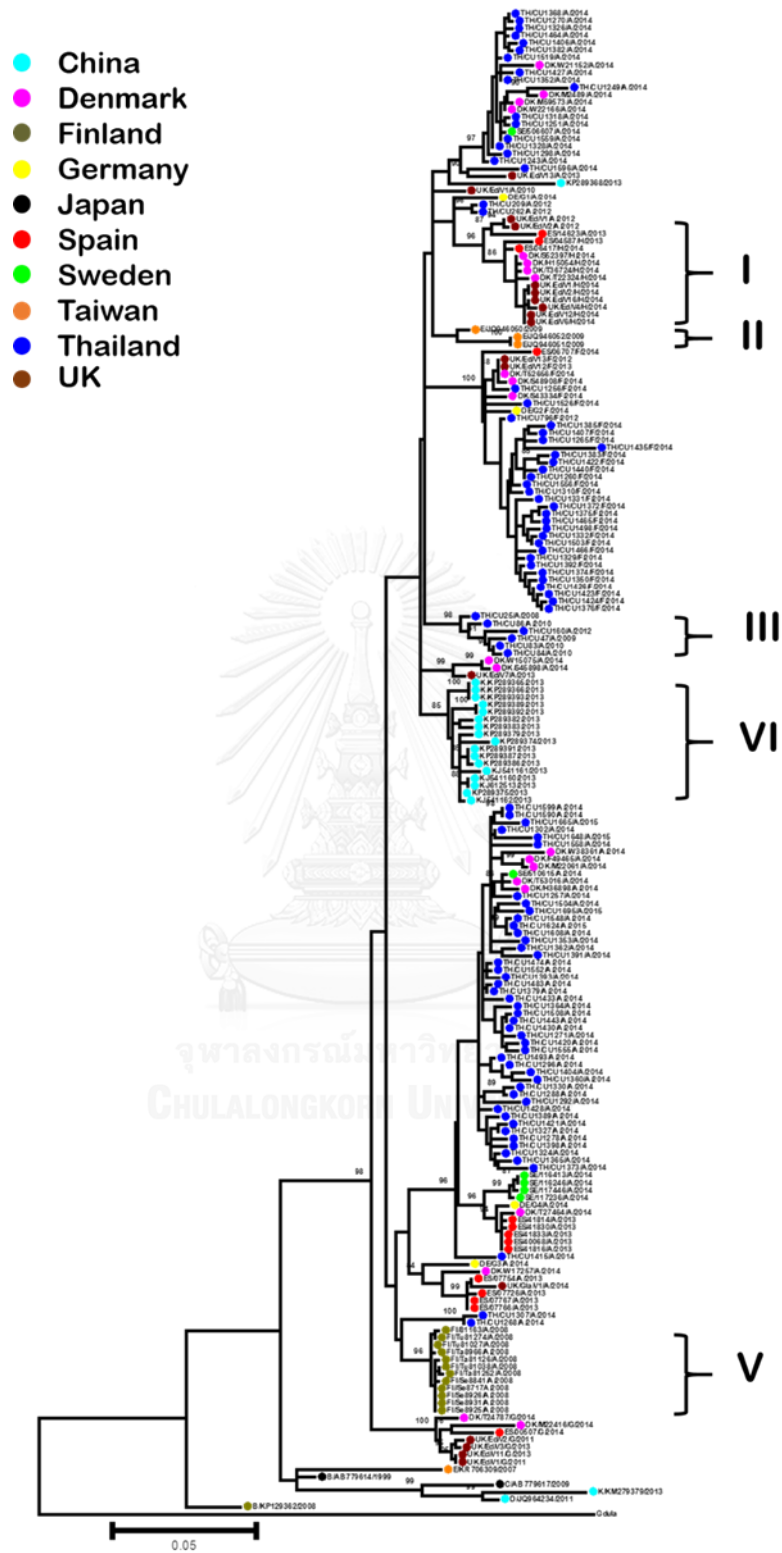


Figure 19. Phylogenetic analysis of VP1 sequences of CVA6 for study subjects and those previously determined. The tree display the color code for different countries.

Table 13. Recombination groups (RF-A to -K) based on phylogenetic analysis of the 3Dpol region.

Country	RF-A	RF-B	RF-C	RF-D	RF-E	RF-F	RF-G	RF-H	RF-J	RF-K	Total
All	105					37	3	6			151
Denmark	13					3	2	4			22
Germany	3					1					4
Spain	10					1	1	2			14
Sweden	6										6
Thailand	73					32					105



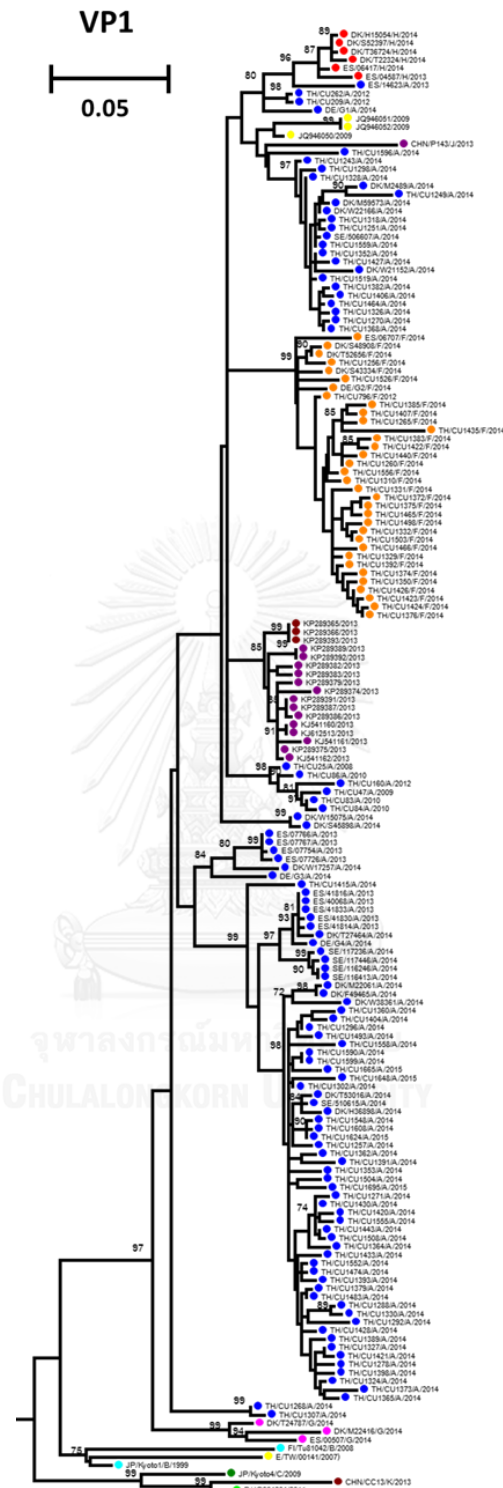


Figure 20. Phylogenetic analysis of VP1 sequences of CVA6 for study subjects and those previously determined (RF-B, -C, -D, and -E). Each sequence is labelled by country of origin, sample code, 3Dpol clade assignment and year of collection.

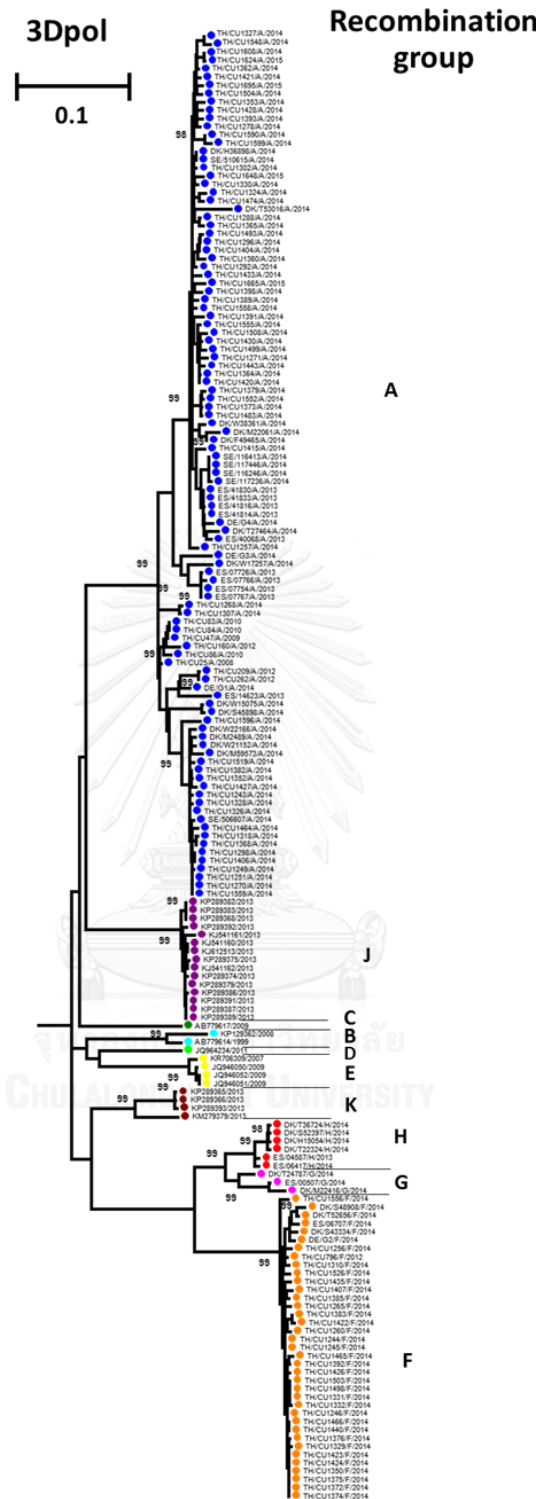


Figure 21. Phylogenetic analysis of 3D sequences of CVA6 for study subjects and those previously determined (RF-B, -C, -D, and -E). Each sequence is labelled by country of origin, sample code, 3Dpol clade assignment and year of collection.



## Sequence diversity of CVA6

Sequence divergence in VP1 provides a proxy measure for the time of divergence of CV-A6 variants from which estimates of the life spans of individual recombinant forms can be estimated. By pairwise comparison of each CV-A6 variant with each other, there was a precise correlation between VP1 sequence distances and assignment to the same or a different RF group in 3Dpol; a divergence threshold of 0.1 divided the two sets of comparisons (Figure 24).

CV-A6 VP1 variability was restricted primarily to synonymous sites, which indicates that most changes in sequences occurred through neutral drift. Through molecular clock analysis, the nucleotide substitution rate and times to the most recent common ancestor (tMRCAs) of different regions and the assignment of 3Dpol clades of the greatest RFs (RF-A and RF-F) were estimated. The substitution rate of the whole data set of all VP1 sequences was estimated to be  $8.1 \times 10^{-3}$  substitutions/site/year (high-probability distribution [HPD] range,  $6.0 \times 10^{-3}$  to  $10.5 \times 10^{-3}$ ); the date that the MRCA of all CV-A6 clusters existed was estimated to be 1947 (HPD, 1940 to 1949). The substitution rate for the whole data set of Asia VP1 sequence compared to Europe was more than 2.4 times faster at  $9.5 \times 10^{-3}$  substitutions/site/year (HPD,  $6.8 \times 10^{-3}$  to  $12.4 \times 10^{-3}$ ) (Table 14). Despite the greater sequence variability among Asia, the most recent common ancestor (MRCA) of this group occurred at almost the same time with that of Europe. The estimated date of the MRCA of RF-A was 1999 (HPD, 1995 to 2003); since then, RF-A lineage has diverged into five recombination groups (RF-E, -F, -H, -J and -K). The VP1 lineage containing the RF-G recombinant form was first documented in 2011 and thereafter underwent the recombination event that exchanged the 3Dpol region sequences between 2004 and 2011. VP1 lineage 1 contains CV-A6 variants belonging to RF-F with the

recombination event dated between 2009 and 2012. A further RF group (H) that appeared in 2013 probably recombined between 2011 and 2013.

Using the substitution rates estimated from VP1 sequence analysis, an estimation of approximate half-lives of CV-A6 lineages were calculated by combining the mean sequence divergence in VP1 at the 50% recombinant frequency threshold (0.05) with the substitution rate in VP1 ( $8.1 \times 10^{-3}$  substitutions/site/year). The RF half-lives of CV-A6 was approximately 3.1 years, thus within the range estimated from previous analyses of other enterovirus serotypes (Figure 25).



Table 14. Rates of sequence change and TMRCA by MCMC analysis.

RF group and geographic set	RF	n <sup>†</sup>	Divergence*				<i>dN/dS</i>		MCMC (BEAST)			
			Nucleotide		aa		VP1	3Dpol	Substitution rate (10 <sup>-3</sup> ) <sup>#</sup>		TMRCA <sup>‡</sup>	
			VP1	3Dpol	VP1	3Dpol			VP1	3Dpol	VP1	3Dpol
<b>Whole data set</b>												
All	All	244	0.052	ND	0.014	ND	0.035	ND	8.1 (6.0-10.5)	ND	68.2 (66.2-75.4)	ND
Europe	All	79	0.051	ND	0.011	ND	0.027	ND	3.9 (2.5-5.5)	ND	16.9 (9.7-25.4)	ND
Asia	All	164	0.049	ND	0.015	ND	0.041	ND	9.5 (6.8-12.4)	ND	18.9 (16.2-23.3)	ND
<b>Individual RF group</b>												
All	RF-A	160	0.046	0.047	0.012	0.020	0.036	0.057	10.4 (7.6-13.8)	11.0 (8.2-14.4)	15.9 (12.3-20.4)	12.9 (12.2-14.4)
Asia	RF-A	109	0.044	0.045	0.014	0.017	0.041	0.051	9.2 (6.4-12.3)	8.2 (5.7-10.9)	16.1 (12.2-20.8)	12.7 (12.2-13.9)
Europe	RF-A	51	0.044	0.049	0.009	0.025	0.027	0.068	6.8 (4.4-9.4)	10.9 (5.9-16.5)	7.5 (6.2-9.0)	7.9 (6.3-10.6)
All	RF-F	36	0.016	0.013	0.010	0.006	0.097	0.055	1.4 (0.03-3.0)	6.5 (3.6-10.2)	17.1 (3.0-42.1)	3.5 (2.7-4.4)

\* Mean pairwise P distances. ND, not determined.

† Number of sequences in each set analyzed.

# Mean value with the HPD interval in parentheses.

‡ Time before the present of the most recent common ancestor

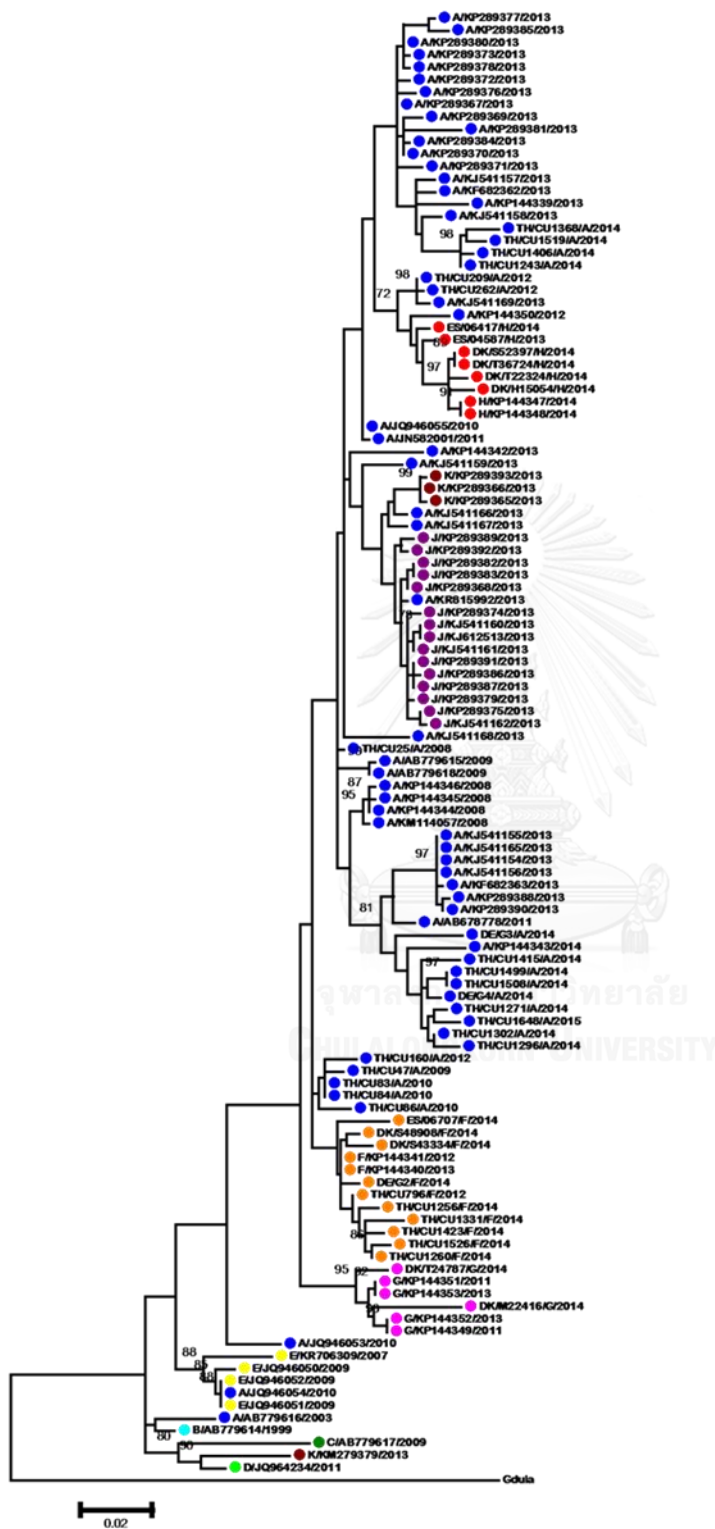


Figure 22. Phylogenetic analysis of 5' UTR of CVA6 for study subjects and those previously determined (RF-B, -C, -D, and -E).

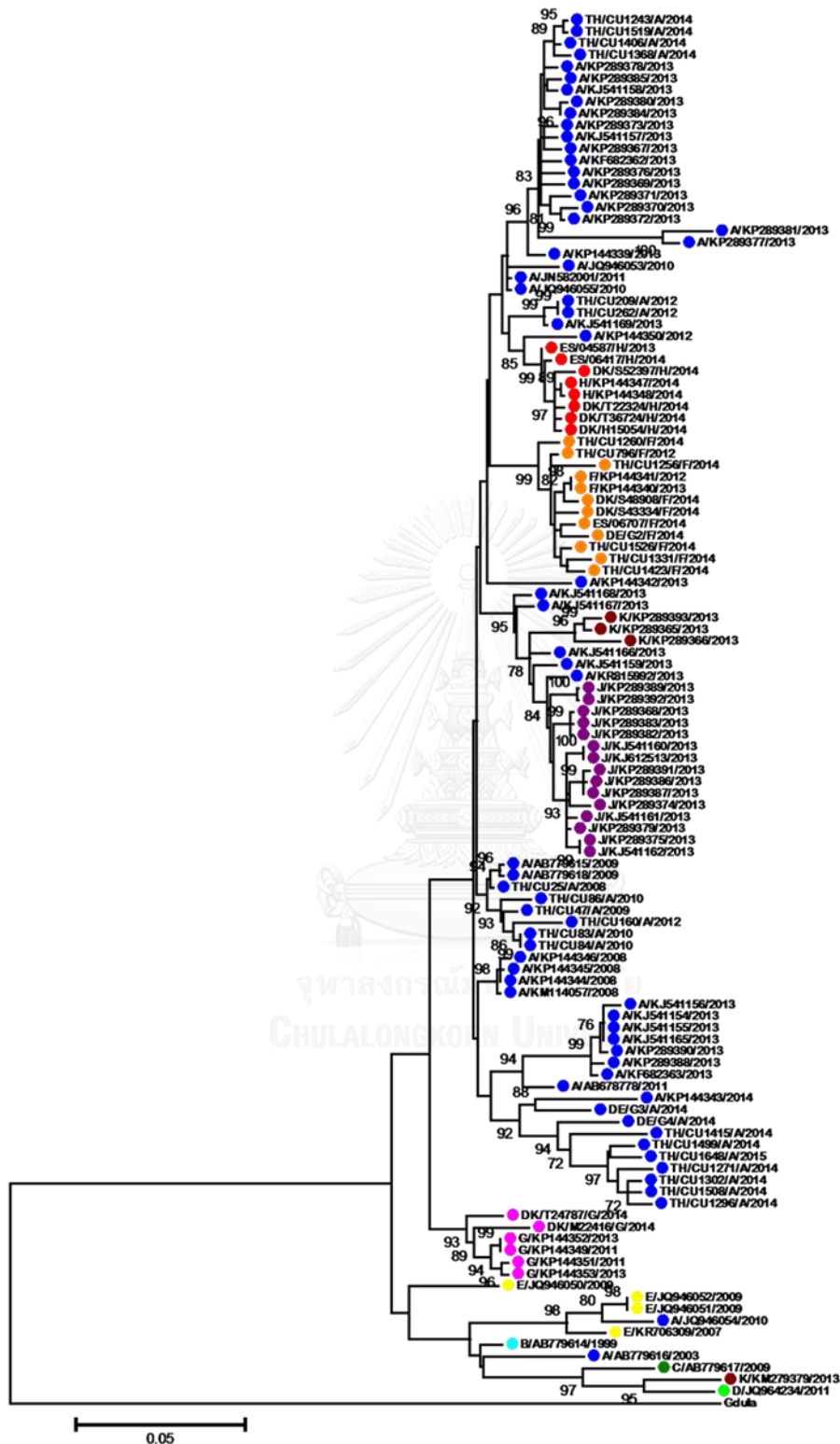


Figure 23. Phylogenetic analysis of VP4/2 sequences of CVA6 for study subjects and those previously determined (RF-B, -C, -D, and -E).

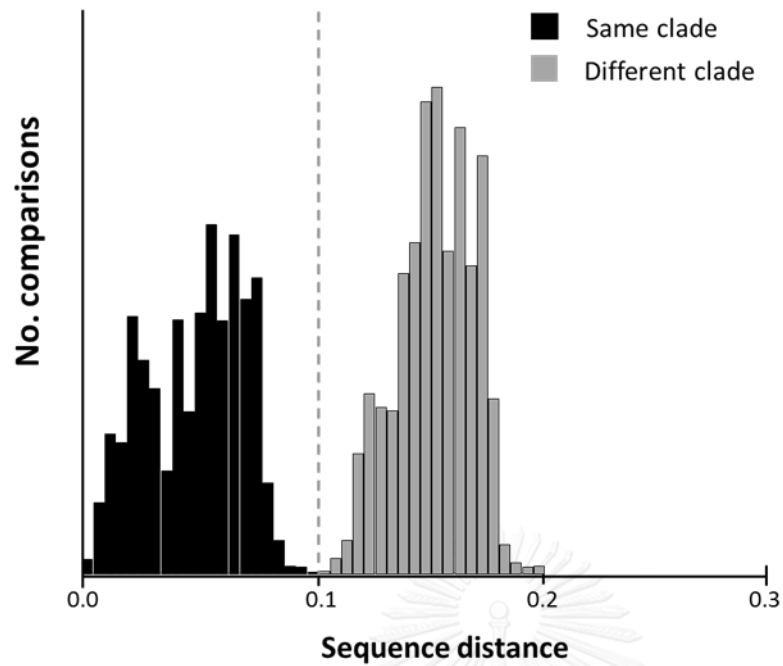


Figure 24. Histogram of genetic distances between CVA6 sequences.

The histogram shows the distribution of pairwise distances between sequences from this study and published CVA6 sequences in the 3Dpol region. The dashed line represents the threshold between a member of the same clades and between different clades.

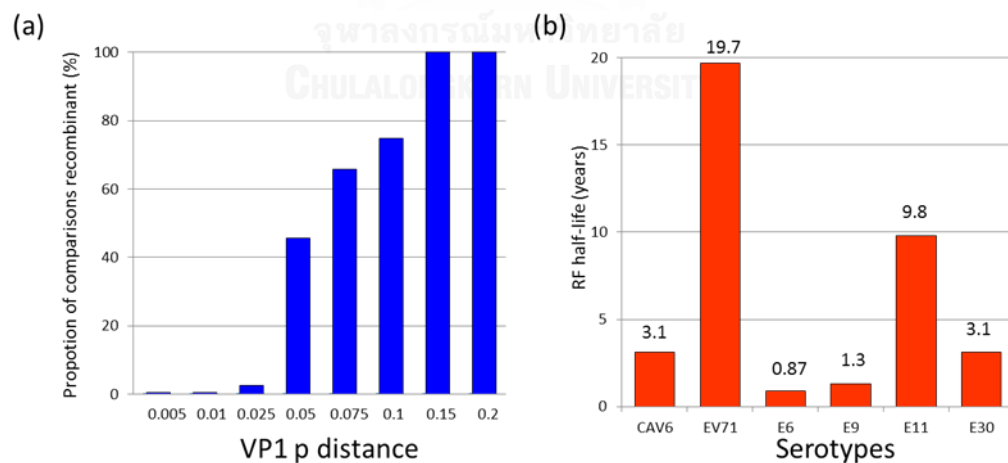


Figure 25. (A) Association between VP1 sequence divergence (shown on the x-axis) and the proportion of recombinant comparisons. (B) Comparison of mean half-lives of CVA6 with previously estimated by the same method.

To determine more precisely the timescale of recombination events underlying the appearance of each RF, datasets of VP1 gene sequences were analysed using the Bayesian Markov Chain Monte Carlo (MCMC) method to generate time-correlated phylogeny (Figure 26). While earlier recombination events could not be reconstructed in any detail due to inadequate sampling of CV-A6 before 2008, variants collected after this date were monophyletic falling into three further lineages with estimated dates of splitting between 2004 and 2005. The oldest lineage comprised purely RF-G samples while the other two lineages contained samples belonging to RF-A. One comprised solely RF-A and persisted for at least 11 years (2005 to 2015). The other lineage contains RF-A sequences and samples isolated subsequently belonging to other RF groups (E, F, H, J and K). Variants within lineage 2 (RF-A) were those detected in the first HFMD outbreak in Finland in 2008 along with variants detected subsequently in Europe and Asia over the following 1 to 5 years. In lineage 1, the oldest variants were those originally described in Asia (Thailand and Japan) before 2012 and then spread into Europe and Asia between 2013 and 2014. Within this lineage, several separate recombination events generated RFs including an RF-F group described in Thailand in 2012 (119). The RFs (F, G, H and K) were monophyletic and likely originated from single recombination events, unlike RF-E and RF-J which were detected in more than one VP1 lineage. With the exception of RF-F which was isolated from both Europe and Asia, other RFs groups were detected only from Europe or Asia; G and H (Europe), E (Taiwan), J and K (China).

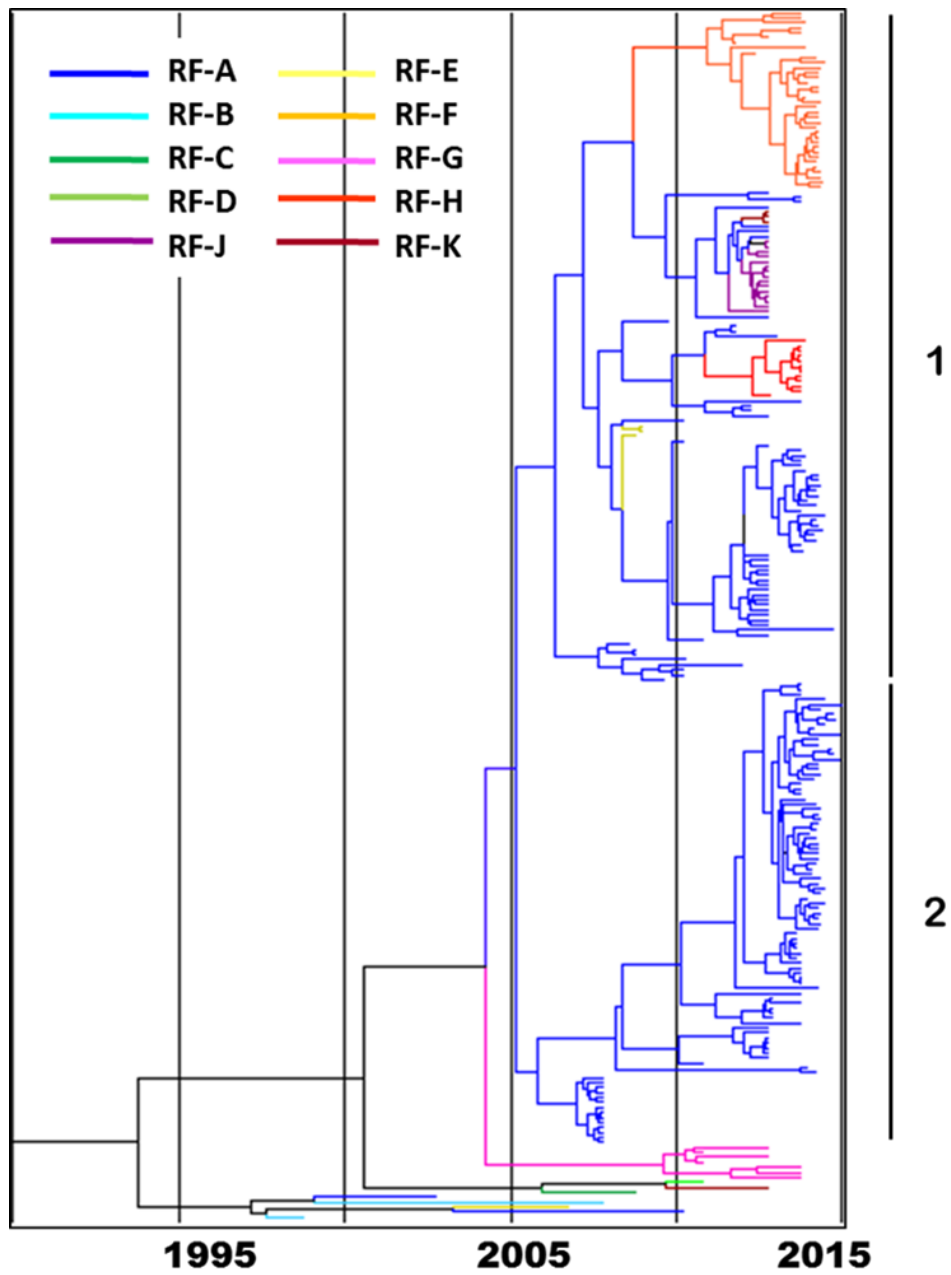


Figure 26. A dated phylogeny of VP1 sequences of CVA6 variants in this study and published sequences. Branch colors label recombination groups in each clade.



Having identified the likely time course and direction of the recombination events, divergence scan analyses were performed between the ancestral RF-A sequences with complete genome sequences generated in the current study (RF-F, -G, and -H) and the previous study (RF-J and RF-K) recombinant forms to identify recombination breakpoints (Figure 27). The sharp increase in sequence divergence at various points in the P2 region provided evidence for the occurrence of separate, individual recombination events for each RF. The first breakpoint was founded at the 2A protein-encoding region around nucleotide position 3500 (RF-G). The next breakpoints were located in 2B and at the border between 2B and 2C regions (RF-F, -J and -H). The last breakpoint of RF-K can be recognized at nucleotide position 5000 and included the 3' part of the 2C region.

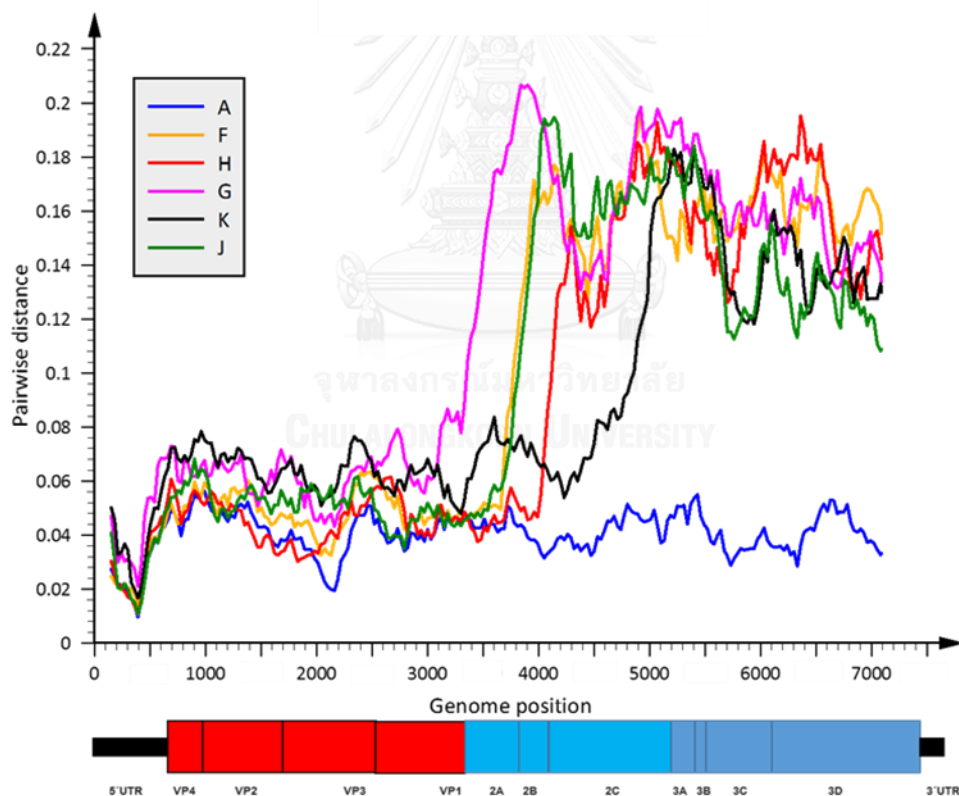


Figure 27. Divergence scan of nucleotide sequence between RF-A with other recombination groups (RF-F, H, G, K and J).

## Discussion and conclusion

In Thailand, HFMD usually occurs during the rainy season (June–August); average incidence during 2007–2011 was 20.2 cases per 100,000 population (5, 6). In 2012, an extensive outbreak of HFMD occurred; the incidence rate was 3-fold higher than the average incidence rate of 58.15 cases per 100,000 population or >36,000 cases; the 2012 outbreak included 2 fatal cases of EV71 encephalitis. Our study is the first report investigating epidemiology of multiple enterovirus infections among Thai patients with HFMD, herpangina and ILI who visited various hospitals in Thailand, 2012. In recent years, HFMD outbreaks caused by other types, especially CV-A6 have increasingly been reported in several countries worldwide (112, 113, 115-118). EV-A71 and CV-A16 are found predominantly in HFMD patients in Thailand (5, 6). Awareness of information on the epidemiological profiles, their pathogenic role, geographic distributions of other enteroviruses in Thailand are also still lacking.

Our study included 1964 suspected cases representing 35.8% (704/1,964), 8.5% (166/1,964) and 55.7% (1,094/1,964) of HFMD, herpangina and influenza-like illness, respectively. During the study period, 33.5% (657/1,964) patients presented with EV infection. HEV-A species were the most common HEV types among the pathogens causing HFMD (54.4%), herpangina (94.1%) and ILI (2.4%), followed by HEV-B and HEV-C species, while no HEV-C species were detected in herpangina. The number of HFMD/herpangina suspected cases in 2012 was up to six-fold higher than the yearly number of cases reported during the study period between 2008 and 2011 (6). The number of enterovirus infection increased abruptly during the rainy season in 2012, particularly in July 48.9%, which was consistent with reports from Korea in 2009 (154). Most strains in this study were detected during this period. This result suggests that epidemiological surveillance and prevention should mainly focus on the period of June-

August of each year. The majority of reported cases were children of 1-3 years of age. The incidence rate of HFMD in infants less than six months was low, which might be due to the protective role of maternal antibodies (155). All patients associated with HFMD/Herpangina included in this study presented with mild disease and did not develop any more severe symptoms.

According to previous studies, EV-A71 and CV-A16 were the major enteroviruses causing epidemics of HFMD in Thailand. EV-A71 subgenotype C4 was the predominant strain circulating during the 2008-2009 epidemic followed by CV-A16 and CV-A10 (5). Although CV-A16 was the most prevalent genotype in 2010, EV-A71 has been found to be an emerging causative agent in 2011 (6). In the present study, we found CV-A6 to be the dominant cause associated with HFMD. CV-A16 and EV-A71 are also very frequently identified types of human enterovirus. CV-A4, CV-A5, CV-A8-10, CV-A12, CV-B1, CV-B2, CV-B4 and CV-B5 are potential causes of HFMD. In Thailand, high prevalence of CV-A6 infections has not been reported yet. As reported in previous studies (112, 156-158), dual infections with CV-A6 and CV-A10 were predominant causes of HFMD/herpangina outbreaks in many countries during 2008-2010. Our study has established CV-A6 as the predominant cause of HFMD. Although CV-A6 has been a predominant emerging pathogen since 2012, no patients infected with CV-A6 died.

As reported in a previous study, herpangina is associated with different strains of enteroviruses, such as CV-A2 in Taipei 2008 (159), CV-A5 in Korea 2009 (160), CV-A6 and CV-A10 in France 2010 (158). In addition, in Japan during 2000-2005, there have been reports of enterovirus infections caused by CV-A2, CV-A4, CV-A6, CV-A8 and CV-A10 (103). Our study has established CV-A8 as the most prevalent cause of herpangina followed by CV-A6.

Our study investigated distinct clusters of CV-A6, EV-A71, CV-A6 and CV-B2 strains in relation to their geographic origins. Phylogenetic analysis showed that the Thai CV-A6 strains were closely related to strains isolated from Shanghai provinces of China 2012. Furthermore, on the basis of the VP1 sequences of EV-A71, the C4 subgenotype was previously identified as the most prominent EV-A71 subgenotype circulating in Thailand, and subgenotypes C1, C2 and B5 were also found (5, 6). Based on the results of phylogenetic analysis, we reported that most EV-A71 strains circulating in Thailand 2012 belonged to the B5 subgenotype, with 2 strains of subgenotype C4. Subgenotype B5 and subgenotype C4 were first described in Japan in 2003 and Taiwan in 1998 (86, 161). The Thai CV-A8 strains belonged to two evolutionary clusters with high nucleotide homology, closely related to the strains found in India and Japan, whereas all Thai CV-B2 strains were most closely related to the strains in China and Korea. Strains diversity may result from the diverse residues in the VP1 BC loop region, which is implicated with viral antigenicity. Substitutions resulting in conformational changes in this region may play an important role in the adaptation of enteroviruses (162, 163). We found amino acid sequence substitutions at 5 positions in CAV6 (89, 95, 97-99) and 5 positions in CAV8 (92, 93, 96, 97 and 100).

Conclusively, first, during the 2012 enterovirus outbreak, most HFMD was caused by CV-A6, whereas herpangina was mainly caused by CV-A8. Second, surveillance of epidemiology and monitoring of the HFMD/Herpangina outbreaks should be continued very carefully to see whether the circulating enterovirus genotypes have a serious impact on Thailand's public health. Third, this is the first report describing the circulation of multiple enteroviruses in Thailand.

Our previous study investigated the substantial increasing of CV-A6 infection among Thai children with HFMD in 2012 (119, 126). In recent years, sporadically detected

CV-A6 virus has been identified as causative agents in Europe, Asia and the USA since it has been reported with a change in its clinical phenotype in 2008 and declining EV-A71 and CV-A16. CV-A6 is becoming an increasingly crucial agent as it was the only pathogen documented differences in symptomatology from HFMD disease including frequently associated with high fever as shown in previous study (126). The benefits of using real time PCR technology in routine diagnostics include rapid, capacity for high throughput, high specificity and quantitative ability (164). Several conventional RT-PCR and real time PCR assays for EV-A71, CV-A6 and CV-A16 detection have also been reported, but none of them were not developed for simultaneous detection and differentiation of these viruses. In the current study, we developed and validated multiplex real-time PCR systems for rapid detection and typing of EV-A71, CV-A6 and CV-A16 associated with HFMD diseases.

The diagnostic tool for clinical tests need for rapid results with high enough sensitivity to identified the infectious agent in the early stage of disease to utilize in management and treatment of viral infection. With the multiplex rRT-PCR developed in this study, the amount of RNA transcript standard can be definitely detected at least 10 copies of EV-A71, CV-A6, CV-A16 and panenterovirus per reaction. The sensitivities of singleplex or multiplex real-time PCR assays can vary widely depending on the target region and EVs genotypes. Previous comparison of conventional gel electrophoresis based multiplex PCR and microarray to detect EVs RNA which had a detection limit of 100 copies and 1 copy respectively (129). Moreover, a GeXP analyzer-based multiplex RT-PCR assay also had the detection limit for EV-A71, CV-A16 and panenterovirus of 10 copies/ul (165). Despite the sensitivity of multiplex real-time PCR assay evaluated in this study has similar or higher values compared to other assays while can detect more pathogens.

The targets for the primers and probes for each of the selected agents were designed within viral protein 1 (VP1) for EV-A71, CV-A6, CV-A16 and 5'UTR for panenterovirus. Nevertheless, it is feasible that mutations in the primer and probe regions may evolve, due to the high evolutionary rates proper of RNA viruses (166). There was no amplification signals obtain from specimens of other RNA viruses such as influenza A (H3N2 and H1N1), influenza B, respiratory syncytial virus (RSV), adenovirus, rotavirus, parechovirus, indicating this method was dependable in specificity.

In conclusion, the multiplex rRT-PCR assays described above provide the highly sensitive detection and rapid simultaneous typing of EV-A71, CV-A6 and CV-A16 thus rendering it feasible and attractive for large scale surveillance of EVs associated with HFMD outbreaks.

CV-A6 infection represents a significant global public health concern and has become one of the most frequently detected enteroviral cause of HFMD. This study sought to understand how widespread the new recombinant forms of CV-A6 have become in Europe and other geographical regions through analysis of the molecular epidemiology and dynamics of recombination of CV-A6 variants collected within the last 8 years. Differences in the phylogenetic trees of VP1 and 3Dpol regions provided a strong evidence of recombination in several strains. Specifically, three CV-A6 variants did not cluster within the same recombinant group on the VP1 phylogenetic tree. The TW/00141/2007 strain was assigned as RF-E, but grouped with RF-B. The CHN/P143/2013 strain was assigned as RF-J, but grouped with RF-A. Finally, the CHN/CC13/2013 strain was assigned into RF-K, but grouped with RF-D. The patterns of phylogenetic discordance observed from this study suggests the occurrence of recombination in CV-A6 consistent with previous findings for other enteroviruses (151-153, 167-169).

As previously described (151), the RF lifespans of CV-A6 were calculated by measuring the relationship between VP1 divergence and the likelihood of recombination. The RF half-life of CV-A6 was closer to that estimated previously for E-30 (3.1 years), much shorter than that of EV-A71 and E-11 whereas the value was higher those of E-6 and E-9 (151-153, 167). Based on analysis of Bayesian MCMC methods, the rate of evolutionary change for CV-A6 in the VP1 region of  $8.1 \times 10^{-3}$  substitutions per site per year (Table 14) fell within the middle of the range described for other enteroviruses, as examples, CV-A24 ( $1.2 \times 10^{-3}$ ), CV-A21 ( $3.1 \times 10^{-3}$ ), EV-C96 ( $3.3 \times 10^{-3}$ ), EV-C99 ( $3.7 \times 10^{-3}$ ), CV-B5 ( $4.2 \times 10^{-3}$ ), E-11 ( $4.8 \times 10^{-3}$ ), EV-D68 ( $4.93 \times 10^{-3}$ ), EV-D70 ( $5 \times 10^{-3}$ ), CV-A4 ( $5.5 \times 10^{-3}$ ), E-9 ( $5.8 \times 10^{-3}$ ), EV-A71 ( $3.1-7.2 \times 10^{-3}$ ), CV-A2 ( $8.3 \times 10^{-3}$ ), E-30 ( $8.8 \times 10^{-3}$ ), CV-A16 ( $9.1 \times 10^{-3}$ ), poliovirus ( $10.3 \times 10^{-3}$ ), E-6 ( $11.2 \times 10^{-3}$ ), CV-A10 ( $14.1 \times 10^{-3}$ ) (151, 152, 167, 169-179).

Phylogenetic reconstruction was used to analyze trait evolution such as temporal and geographical correlates of individual recombination events. The most frequently detected recombinant form, RF-A, showed decades-long circulation and was the ancestor of five separate recombinant groups (RF-E, F, H, K and J) that have emerged in the past 5-10 years. The first outbreak of CV-A6-HFMD in Finland in 2008 was associated with RF-A with the subsequent appearance of this RF across of Europe and Asia between 2013 and 2014. The more recent emergence of RFs in Europe and Asia between 2013 and 2014 originated from descendants of multiple VP1 lineages that have diverged from RF-A variants circulating in Asia (Thailand and Japan) between 2008 and 2010. Recombination events have previously been recorded widely in other enteroviruses and were found to play a significant role in the evolution of these genomic viruses and the recombination breakpoints detected in this study (2A - 2C regions) are well-known recombination hotspots in enteroviruses (180). Regarding CV-A6, breakpoints within VP3

and between 5'UTR and VP1 have been detected in the genomes of RF-E variants in Taiwan (146).

This study reports a detailed, multi-centre investigation of the emergence of an enterovirus serotype associated with epidemics of HFMD. It catalogues the complexity of the evolutionary processes associated with its geographical expansion and the occurrence of a number of recombination events each involving replacement of close to complete non-structural gene blocks at varying times since the founder recombinant form, RF-A was first described in 2008 (113). Non-structural (NS) region sequences of most RFs have not been described in association with other species A serotypes including any of the RFs described for EV-A71 (152). However, there was some evidence for a limited degree of re-circulation within the recombination pool of NS region sequences; RFs -E and -K appear at two different positions in the VP1 phylogenetic tree (Fig. 1a). Furthermore, a limited degree of sharing of NS regions sequences between different species B serotypes has been documented (181).

Nevertheless, the typical pattern for an RF was its rapid emergence, variable penetrance into the sampled virus population and relatively rapid extinction, within years rather than decades, based on average recombination half-lives documented for CV-A6 and other EV types (Fig. 4b). This patterns is well attested in the turnover of RFs of CV-A6. While we remain relatively ignorant of the reasons for RF turnover, whether driven by immunological, host adaptive factors or transmissibility, or alternatively whether it occurs as a consequence of population bottlenecks and replacements without a fitness component, molecular epidemiological studies such as these will be of value in gaining a longer term, better understanding of the nature of enterovirus evolution and their clinical outcomes.



## APPENDIX A

Table S1: Sequences information

Isolate	Country	City	Year	RF group	Accession number		
					Complete genome	VP1	3D
Gdula	US	NS	1949	I	AY421764	-	-
Fin/Se8926	Finland	NS	2008	A	KP144346	-	-
TS6/Fin/Se8925/2008	Finland	NS	2008	A	-	KP129346	KP129366
Fin/Se8717	Finland	NS	2008	A	KP144344	-	-
V2/Fin/Ta81126/2008	Finland	NS	2008	A	-	KP129337	KP129357
Fin/Se8841	Finland	NS	2008	A	KP144345	-	-
TS5/Fin/Se8931/2008	Finland	NS	2008	A	-	KP129344	KP129364
TS2/Fin/Tu81038/2008	Finland	NS	2008	A	-	KP129341	KP129361
TS1/Fin/Ta81252/2008	Finland	NS	2008	A	-	KP129336	KP129356
TA1/Fin/Ta8966/2008	Finland	NS	2008	A	-	KP129339	KP129359
V4/Fin/Tu81274/2008	Finland	NS	2008	A	-	KP129340	KP129360
V1/Fin/81163/2008	Finland	NS	2008	A	-	KP129335	KP129355
V5/Fin/Se8928/2008	Finland	NS	2008	A	-	KP129345	KP129365
TS4/Fin/Tu81027/2008	Finland	NS	2008	A	-	KP129343	KP129363
Finland/2008	Finland	NS	2008	A	KM114057	-	-
Shizuoka 18	Japan	Shizuoka	2011	A	AB678778	-	-
V1/Gla/UK/2014	UK	Glasgow	2014	A	KP144343	-	-
Kyoto2	Japan	Kyoto	2003	A	AB779616	-	-
Kyoto3	Japan	Kyoto	2009	A	AB779615	-	-
Kyoto5	Japan	Kyoto	2009	A	AB779618	-	-
V1/Ed/UK/2012	UK	Edinburgh	2012	A	KP144350	-	-
V2/Ed/UK/2012	UK	Edinburgh	2012	A	-	KP129347	KP129367
V1/Ed/UK/2010	UK	Edinburgh	2010	A	-	KP129348	KP129368
TW/409/10	Taiwan	NS	2010	A	JQ946055	-	-
TW/1537/2011	Taiwan	NS	2011	A	JN582001	-	-
TW/391/10	Taiwan	NS	2010	A	JQ946053	-	-
TW/399/10	Taiwan	NS	2010	A	JQ946054	-	-
V7/Ed/UK/2013	UK	Edinburgh	2013	A	KP144342	-	-
V13/Ed/UK/2013	UK	Edinburgh	2013	A	KP144339	-	-

CU25/THA/2008	Thailand	Bangkok	2008	A	KX212500	KX212346	KX212536
CU47/THA/2009	Thailand	Bangkok	2009	A	KX212498	KX212344	KX212534
CU83/THA/2010	Thailand	Bangkok	2010	A	KX212495	KX212341	KX212531
CU84/THA/2010	Thailand	Bangkok	2010	A	KX212496	KX212342	KX212532
CU86/THA/2010	Thailand	Bangkok	2010	A	KX212499	KX212345	KX212535
TH/CU1499/A/2014	Thailand	Bangkok	2014	A	KX212503	KX212338	KX212528
TH/CU1508/A/2014	Thailand	Bangkok	2014	A	KX212504	KX212403	KX212593
TH/CU1420/A/2014	Thailand	Bangkok	2014	A	-	KX212380	KX212570
TH/CU1555/A/2014	Thailand	Khon kaen	2014	A	-	KX212404	KX212594
TH/CU1430/A/2014	Thailand	Bangkok	2014	A	-	KX212384	KX212574
TH/CU1271/A/2014	Thailand	Bangkok	2014	A	KX212505	KX212405	KX212595
TH/CU1443/A/2014	Thailand	Bangkok	2014	A	-	KX212385	KX212575
TH/CU1364/A/2014	Thailand	Bangkok	2014	A	-	KX212379	KX212569
TH/CU1379/A/2014	Thailand	Khon kaen	2014	A	-	KX212409	KX212599
TH/CU1483/A/2014	Thailand	Khon kaen	2014	A	-	KX212410	KX212600
TH/CU1552/A/2014	Thailand	Khon kaen	2014	A	-	KX212408	KX212598
TH/CU1433/A/2014	Thailand	Bangkok	2014	A	-	KX212417	KX212607
TH/CU1474/A/2014	Thailand	Bangkok	2014	A	-	KX212387	KX212577
TH/CU1393/A/2014	Thailand	Bangkok	2014	A	-	KX212378	KX212568
TH/CU1327/A/2014	Thailand	Bangkok	2014	A	-	KX212391	KX212581
TH/CU1421/A/2014	Thailand	Bangkok	2014	A	-	KX212396	KX212586
TH/CU1695/A/2015	Thailand	Bangkok	2015	A	-	KX212422	KX212612
TH/CU1278/A/2014	Thailand	Bangkok	2014	A	-	KX212419	KX212609
TH/CU1428/A/2014	Thailand	Bangkok	2014	A	-	KX212399	KX212589
TH/CU1389/A/2014	Thailand	Bangkok	2014	A	-	KX212381	KX212571
TH/CU1288/A/2014	Thailand	Bangkok	2014	A	-	KX212373	KX212563
TH/CU1330/A/2014	Thailand	Bangkok	2014	A	-	KX212375	KX212565
TH/CU1365/A/2014	Thailand	Bangkok	2014	A	-	KX212374	KX212564
TH/CU1398/A/2014	Thailand	Bangkok	2014	A	-	KX212418	KX212608
TH/CU1324/A/2014	Thailand	Bangkok	2014	A	-	KX212386	KX212576
TH/CU1373/A/2014	Thailand	Khon kaen	2014	A	-	KX212407	KX212597
TH/CU1292/A/2014	Thailand	Bangkok	2014	A	-	KX212402	KX212592
TH/CU1257/A/2014	Thailand	Bangkok	2014	A	-	KX212383	KX212573
DK/M22061/A/2014	Denmark	NS	2014	A	-	KX212411	KX212601
DK/F49465/A/2014	Denmark	NS	2014	A	-	KX212412	KX212602
DK/W38361/A/2014	Denmark	NS	2014	A	-	KX212413	KX212603
TH/CU1353/A/2014	Thailand	Khon kaen	2014	A	-	KX212420	KX212610
TH/CU1362/A/2014	Thailand	Bangkok	2014	A	-	KX212395	KX212585

TH/CU1391/A/2014	Thailand	Bangkok	2014	A	-	KX212406	KX212596
TH/CU1504/A/2014	Thailand	Bangkok	2014	A	-	KX212421	KX212611
DK/H36898/A/2014	Denmark	NS	2014	A	-	KX212416	KX212606
DK/T53016/A/2014	Denmark	NS	2014	A	-	KX212414	KX212604
TH/CU1608/A/2014	Thailand	Bangkok	2014	A	-	KX212393	KX212583
TH/CU1624/A/2015	Thailand	Bangkok	2015	A	-	KX212394	KX212584
TH/CU1548/A/2014	Thailand	Bangkok	2014	A	-	KX212392	KX212582
TH/CU1590/A/2014	Thailand	Bangkok	2014	A	-	KX212397	KX212587
TH/CU1599/A/2014	Thailand	Bangkok	2014	A	-	KX212398	KX212588
TH/CU1665/A/2015	Thailand	Bangkok	2015	A	-	KX212388	KX212578
TH/CU1302/A/2014	Thailand	Bangkok	2014	A	KX212501	KX212389	KX212579
TH/CU1648/A/2015	Thailand	Bangkok	2015	A	KX212502	KX212415	KX212605
TH/CU1558/A/2014	Thailand	Khon kaen	2014	A	-	KX212390	KX212580
TH/CU1296/A/2014	Thailand	Bangkok	2014	A	KX212506	KX212400	KX212590
TH/CU1493/A/2014	Thailand	Bangkok	2014	A	-	KX212401	KX212591
TH/CU1360/A/2014	Thailand	Bangkok	2014	A	-	KX212376	KX212566
TH/CU1404/A/2014	Thailand	Bangkok	2014	A	-	KX212377	KX212567
DK/T27464/A/2014	Denmark	NS	2014	A	-	KX212426	KX212616
ES/41833/A/2013	Spain	Teruel	2013	A	-	KX212425	KX212615
ES/40068/A/2013	Spain	Mallorca	2013	A	-	KX212427	KX212617
ES/41830/A/2013	Spain	Teruel	2013	A	-	KX212424	KX212614
ES/41816/A/2013	Spain	Teruel	2013	A	-	KX212423	KX212613
ES/41814/A/2013	Spain	Teruel	2013	A	-	KX212429	KX212619
DE/G4/A/2014	Germany	NS	2014	A	KX212508	KX212428	KX212618
TH/CU1415/A/2014	Thailand	Bangkok	2014	A	KX212507	KX212382	KX212572
ES/07754/A/2013	Spain	Salamanca	2013	A	-	KX212430	KX212620
ES/07766/A/2013	Spain	Salamanca	2013	A	-	KX212433	KX212623
ES/07767/A/2013	Spain	Salamanca	2013	A	-	KX212431	KX212621
ES/07726/A/2013	Spain	Salamanca	2013	A	-	KX212432	KX212622
DK/W17257/A/2014	Denmark	NS	2014	A	-	KX212434	KX212624
DE/G3/A/2014	Germany	NS	2014	A	KX212509	KX212435	KX212625
TH/CU1268/A/2014	Thailand	Bangkok	2014	A	-	KX212436	KX212626
TH/CU1307/A/2014	Thailand	Bangkok	2014	A	-	KX212437	KX212627
ES/14623/A/2013	Spain	Mallorca	2013	A	-	KX212351	KX212541
DE/G1/A/2014	Germany	NS	2014	A	-	KX212350	KX212540
DK/M2489/A/2014	Denmark	NS	2014	A	-	KX212354	KX212544
TH/CU1249/A/2014	Thailand	Bangkok	2014	A	-	KX212365	KX212555
DK/M59573/A/2014	Denmark	NS	2014	A	-	KX212352	KX212542

DK/W22166/A/2014	Denmark	NS	2014	A	-	KX212371	KX212561
TH/CU1251/A/2014	Thailand	Bangkok	2014	A	-	KX212357	KX212547
TH/CU1559/A/2014	Thailand	Bangkok	2014	A	-	KX212366	KX212556
DK/W21152/A/2014	Denmark	NS	2014	A	-	KX212353	KX212543
TH/CU1368/A/2014	Thailand	Bangkok	2014	A	KX212494	KX212368	KX212558
TH/CU1464/A/2014	Thailand	Bangkok	2014	A	-	KX212358	KX212548
TH/CU1270/A/2014	Thailand	Bangkok	2014	A	-	KX212369	KX212559
TH/CU1326/A/2014	Thailand	Bangkok	2014	A	-	KX212361	KX212551
TH/CU1382/A/2014	Thailand	Bangkok	2014	A	-	KX212359	KX212549
TH/CU1406/A/2014	Thailand	Bangkok	2014	A	KX212493	KX212364	KX212554
TH/CU1352/A/2014	Thailand	Bangkok	2014	A	-	KX212360	KX212550
TH/CU1427/A/2014	Thailand	Khon kaen	2014	A	-	KX212356	KX212546
TH/CU1519/A/2014	Thailand	Bangkok	2014	A	KX212492	KX212370	KX212560
TH/CU1318/A/2014	Thailand	Bangkok	2014	A	-	KX212367	KX212557
TH/CU1328/A/2014	Thailand	Bangkok	2014	A	-	KX212362	KX212552
TH/CU1298/A/2014	Thailand	Bangkok	2014	A	-	KX212363	KX212553
TH/CU1243/A/2014	Thailand	Bangkok	2014	A	KX212491	KX212355	KX212545
TH/CU1596/A/2014	Thailand	Bangkok	2014	A	-	KX212372	KX212562
DK/W15075/A/2014	Denmark	NS	2014	A	-	KX212348	KX212538
DK/S45898/A/2014	Denmark	NS	2014	A	-	KX212349	KX212539
TH/CU160/A/2012	Thailand	Bangkok	2012	A	KX212497	KX212343	KX212533
TH/CU209/A/2012	Thailand	Bangkok	2012	A	KX212489	KX212339	KX212529
TH/CU262/A/2012	Thailand	Bangkok	2012	A	KX212490	KX212340	KX212530
SE/116246/A/2014	Sweden	Stockholm	2014	A	-	KX212488	KX212673
SE/116413/A/2014	Sweden	Stockholm	2014	A	-	KX212483	KX212674
SE/117236/A/2014	Sweden	Stockholm	2014	A	-	KX212484	KX212675
SE/117446/A/2014	Sweden	Stockholm	2014	A	-	KX212485	KX212676
SE/506607/A/2014	Sweden	Stockholm	2014	A	-	KX212486	KX212677
SE/510615/A/2014	Sweden	Stockholm	2014	A	-	KX212487	KX212678
P115/2013/China	China	Wenzhou	2013	A	KP289367	-	-
P169/2013/China	China	Wenzhou	2013	A	KP289369	-	-
P2/2013/China	China	Wenzhou	2013	A	KP289370	-	-
P223/2013/China	China	Wenzhou	2013	A	KP289371	-	-
P225/2013/China	China	Wenzhou	2013	A	KP289372	-	-
P246/2013/China	China	Wenzhou	2013	A	KP289373	-	-
P345/2013/China	China	Wenzhou	2013	A	KP289376	-	-
P358/2013/China	China	Wenzhou	2013	A	KP289377	-	-
P360/2013/China	China	Wenzhou	2013	A	KP289378	-	-

P362/2013/China	China	Wenzhou	2013	A	KP289380	-	-
P366/2013/China	China	Wenzhou	2013	A	KP289381	-	-
P6/2013/China	China	Wenzhou	2013	A	KP289384	-	-
P66/2013/China	China	Wenzhou	2013	A	KP289385	-	-
P702/2013/China	China	Wenzhou	2013	A	KP289388	-	-
P731/2013/China	China	Wenzhou	2013	A	KP289390	-	-
SZc173/13	China	Shenzhen	2013	A	KF682362	-	-
SZc294/13	China	Shenzhen	2013	A	KF682363	-	-
5084/SH/CHN/2013	China	Shanghai	2013	A	KJ541154	-	-
PF19/SH/CHN/2013	China	Shanghai	2013	A	KJ541155	-	-
5047/SH/CHN/2013	China	Shanghai	2013	A	KJ541156	-	-
4645/SH/CHN/2013	China	Shanghai	2013	A	KJ541157	-	-
5069/SH/CHN/2013	China	Shanghai	2013	A	KJ541158	-	-
4592/SH/CHN/2013	China	Shanghai	2013	A	KJ541159	-	-
PF001/SH/CHN/2013	China	Shanghai	2013	A	KJ541165	-	-
1827/SH/CHN/2013	China	Shanghai	2013	A	KJ541166	-	-
1232/SH/CHN/2013	China	Shanghai	2013	A	KJ541167	-	-
3913/SH/CHN/2013	China	Shanghai	2013	A	KJ541168	-	-
4368/SH/CHN/2013	China	Shanghai	2013	A	KJ541169	-	-
12743/GZ/CHN/2013	China	Guangzhou	2013	A	KR815992	-	-
TS3/Fin/Tu81042/2008	Finland	NS	2008	B	-	KP129342	KP129362
Kyoto1	Japan	Kyoto	1999	B	AB779614	-	-
Kyoto4	Japan	Kyoto	2009	C	AB779617	-	-
HN421	China	Henan	2011	D	JQ964234	-	-
TW/295/09	Taiwan	NS	2009	E	JQ946052	-	-
TW/273/09	Taiwan	NS	2009	E	JQ946051	-	-
TW/20/09	Taiwan	NS	2009	E	JQ946050	-	-
TW-2007-00141	Taiwan	NS	2007	E	KR706309	-	-
V13/Ed/UK/2012	UK	Edinburgh	2012	F	KP144341	-	-
V12/Ed/UK/2013	UK	Edinburgh	2013	F	KP144340	-	-
DK/S48908/F/2014	Denmark	NS	2014	F	KX212510	KX212438	KX212628
DK/T52656/F/2014	Denmark	NS	2014	F	-	KX212439	KX212629
TH/CU1256/F/2014	Thailand	Bangkok	2014	F	KX212519	KX212460	KX212650
DK/S43334/F/2014	Denmark	NS	2014	F	KX212511	KX212441	KX212631
DE/G2/F/2014	Germany	NS	2014	F	KX212512	KX212442	KX212632
ES/06707/F/2014	Spain	Mallorca	2014	F	KX212513	KX212440	KX212630
TH/CU1383/F/2014	Thailand	Bangkok	2014	F	-	KX212463	KX212653
TH/CU1422/F/2014	Thailand	Bangkok	2014	F	-	KX212464	KX212654

TH/CU1440/F/2014	Thailand	Bangkok	2014	F	-	KX212467	KX212657
TH/CU1260/F/2014	Thailand	Bangkok	2014	F	KX212518	KX212462	KX212652
TH/CU1385/F/2014	Thailand	Bangkok	2014	F	-	KX212461	KX212651
TH/CU1407/F/2014	Thailand	Bangkok	2014	F	-	KX212470	KX212660
TH/CU1435/F/2014	Thailand	Bangkok	2014	F	-	KX212471	KX212661
TH/CU1265/F/2014	Thailand	Bangkok	2014	F	-	KX212469	KX212659
TH/CU1310/F/2014	Thailand	Bangkok	2014	F	-	KX212468	KX212658
TH/CU1526/F/2014	Thailand	Bangkok	2014	F	KX212517	KX212473	KX212663
TH/CU1392/F/2014	Thailand	Bangkok	2014	F	-	KX212447	KX212637
TH/CU1466/F/2014	Thailand	Bangkok	2014	F	-	KX212446	KX212636
TH/CU1329/F/2014	Thailand	Bangkok	2014	F	-	KX212458	KX212648
TH/CU1331/F/2014	Thailand	Bangkok	2014	F	KX212515	KX212448	KX212638
TH/CU1498/F/2014	Thailand	Bangkok	2014	F	-	KX212452	KX212642
TH/CU1332/F/2014	Thailand	Bangkok	2014	F	-	KX212451	KX212641
TH/CU1503/F/2014	Thailand	Bangkok	2014	F	-	KX212453	KX212643
TH/CU1465/F/2014	Thailand	Bangkok	2014	F	-	KX212445	KX212635
TH/CU1423/F/2014	Thailand	Khon kaen	2014	F	KX212516	KX212459	KX212649
TH/CU1426/F/2014	Thailand	Khon kaen	2014	F	-	KX212450	KX212640
TH/CU1424/F/2014	Thailand	Khon kaen	2014	F	-	KX212449	KX212639
TH/CU1350/F/2014	Thailand	Bangkok	2014	F	-	KX212455	KX212645
TH/CU1376/F/2014	Thailand	Bangkok	2014	F	-	KX212457	KX212647
TH/CU1372/F/2014	Thailand	Bangkok	2014	F	-	KX212465	KX212655
TH/CU1375/F/2014	Thailand	Bangkok	2014	F	-	KX212456	KX212646
TH/CU1374/F/2014	Thailand	Bangkok	2014	F	-	KX212466	KX212656
TH/CU1556/F/2014	Thailand	Khon kaen	2014	F	-	KX212472	KX212662
TH/CU796/F/2012	Thailand	Bangkok	2012	F	KX212514	KX212347	KX212537
V2/Ed/UK/2011	UK	Edinburgh	2011	G	KP144351	-	-
V3/Ed/UK/2013	UK	Edinburgh	2013	G	KP144353	-	-
V11/Ed/UK/2013	UK	Edinburgh	2013	G	KP144352	-	-
V1/Ed/UK/2011	UK	Edinburgh	2011	G	KP144349	-	-
DK/M22416/G/2014	Denmark	NS	2014	G	KX212526	KX212475	KX212665
ES/00507/G/2014	Spain	Mallorca	2014	G	-	KX212474	KX212664
DK/T24787/G/2014	Denmark	NS	2014	G	KX212527	KX212476	KX212666
V12/Ed/UK/2014	UK	Edinburgh	2014	H	-	KP129352	KP129374
V1/Ed/UK/2014	UK	Edinburgh	2014	H	-	KP129354	KP129373
V2/Ed/UK/2014	UK	Edinburgh	2014	H	-	KP129353	KP129372
V16/Ed/UK/2014	UK	Edinburgh	2014	H	KP144347	-	-
V4/Ed/UK/2014	UK	Edinburgh	2014	H	KP144348	-	-

V6/Ed/UK/2014	UK	Edinburgh	2014	H	KP129370	-	-
DK/S52397/H/2014	Denmark	NS	2014	H	KX212524	KX212477	KX212667
DK/T22324/H/2014	Denmark	NS	2014	H	KX212525	KX212480	KX212670
DK/H15054/H/2014	Denmark	NS	2014	H	KX212522	KX212479	KX212669
DK/T36724/H/2014	Denmark	NS	2014	H	KX212523	KX212478	KX212668
ES/06417/H/2014	Spain	Vigo	2014	H	KX212521	KX212482	KX212672
ES/04587/H/2013	Spain	Madrid	2013	H	KX212520	KX212481	KX212671
P143/2013/China	China	Wenzhou	2013	J	KP289368	-	-
P278/2013/China	China	Wenzhou	2013	J	KP289374	-	-
P309/2013/China	China	Wenzhou	2013	J	KP289375	-	-
P361/2013/China	China	Wenzhou	2013	J	KP289379	-	-
P406/2013/China	China	Wenzhou	2013	J	KP289382	-	-
P426/2013/China	China	Wenzhou	2013	J	KP289383	-	-
P674/2013/China	China	Wenzhou	2013	J	KP289386	-	-
P695/2013/China	China	Wenzhou	2013	J	KP289387	-	-
P728/2013/China	China	Wenzhou	2013	J	KP289389	-	-
P786/2013/China	China	Wenzhou	2013	J	KP289391	-	-
P794/2013/China	China	Wenzhou	2013	J	KP289392	-	-
5039/SH/CHN/2013	China	Shanghai	2013	J	KJ541160	-	-
5056/SH/CHN/2013	China	Shanghai	2013	J	KJ541161	-	-
PF3/SH/CHN/2013	China	Shanghai	2013	J	KJ541162	-	-
PF1/SH/CHN/2013	China	Shanghai	2013	J	KJ612513	-	-
P289/2013/China	China	Wenzhou	2013	K	KP289365	-	-
P423/2013/China	China	Wenzhou	2013	K	KP289366	-	-
P874/2013/China	China	Wenzhou	2013	K	KP289393	-	-
CC13/57	China	Changchun	2013	K	KM279379	-	-

NS: non specified

Table S2: Primer set used for whole genome amplification of human coxsackievirus A6 by nested RT-PCR

No.	Primer	Sequence (5' to 3')	Position
1	CAV6-F39/OS	ACT GGG CGC YAG CAC ACT GAT TC	39 - 61
	CAV6-R1673/OAS	AGT TAR TGT RAT TGG YAC YTC TGT	1650 - 1673
	CAV6-F55/IS	CTG ATT CTA YGG AAY CTT TGT GCG	55 - 78
	CAV6-R1567/IAS	GGA AGY GCR TTR ACA TAT GGC AT	1545 - 1567
2	CAV6-F1266/OS	TCG GGY TTC TGY ATG CAY GTT CA	1266 - 1288
	CAV6-R2806/OAS	GAY AGT TCT AGY TTG CGC CGC TG	2784 - 2806
	CAV6-F1290/IS	TGY AAY GCR AGC AAR TTC CAT CA	1290 - 1312
	CAV6-R2727/IAS	CCG AGT CCT TYA CCT CCA CAA C	2706 - 2727
3	CAV6-F2458/OS	CRA ATG CDG TGG AAA GYG CTG T	2458 - 2479
	CAV6-R3832/OAS	CCT TTG ATR TAA TCW GAY ACD CC	3810 - 3832
	CAV6-F2485/IS	GCR CTY GCT GAY ACC ACA ATA TC	2485 - 2506
	CAV6-R3816/IAS	GAC ACC CTG YTC CAT RGC TTC	3795 - 3816
4	CAV6-F3498/OS	GCT CAR GGA TGT GAY ACY ATT GC	3498 - 3520
	CAV6-R4564/OAS	CTA GAG TGR TAY TTR TCR GCT AT	4542 - 4564
	CAV6-F3603/IS	GTC TTY GTG GAA GCT AGT GAG TA	3603 - 3625
	CAV6-R4463/IAS	ACG GTG TTT GCT CTT GAA CTG CAT	4440 - 4463
5	CAV6-F4107/OS	AGY GCA TCN TGG CTH AAG AAG TT	4107 - 4129
	CAV6-R5482/OAS	TGA TCY GTY TGV ACY TGC CTR AT	5460 - 5482
	CAV6-F4214/IS	TRT ACC AGC AGC TAA AGA GAA GGT	4214 - 4237
	CAV6-R5330/IAS	GTA GAT RAC ATA CAC CAR TGA RAC	5307 - 5330
6	CAV6-F4994/OS	ATC CAA RGT BAG RTA YAG TGT GGA	4994 - 5017
	CAV6-R6422/OAS	GAG RTC AAR DCC ATA CTT RTC CAT	6399 - 6422
	CAV6-F5061/IS	GCY ATT GGN AAC ACA ATC GAA GC	5061 - 5083
	CAV6-R6364/IAS	GGG TCY AAR ATG TCY CTC TTC TT	6342 - 6364



## REFERENCES

1. Knowles NJ, Hovi, T., Hyypia, T., King, A. M. Q., Lindberg, A. M., Pallansch, M. A., Palmenberg, A. C., Simmonds, P., Skern, T. & other authors. Family Picornaviridae. In *Virus Taxonomy: Ninth Report of the International Committee on Taxonomy of Viruses*, pp. 855–880. Edited by A M Q King, M J Adams, E B Carstens & E J Lefkowitz London: Academic Press. 2012.
2. Solomon T, Lewthwaite P, Perera D, Cardoso MJ, McMinn P, Ooi MH. Virology, epidemiology, pathogenesis, and control of enterovirus 71. *Lancet Infect Dis*. 2010;10(11):778-90.
3. Horwood PF, Andronico A, Tarantola A, Salje H, Duong V, Mey C, et al. Seroepidemiology of Human Enterovirus 71 Infection among Children, Cambodia. *Emerg Infect Dis*. 2016;22(1):92-5.
4. Wang JF, Guo YS, Christakos G, Yang WZ, Liao YL, Li ZJ, et al. Hand, foot and mouth disease: spatiotemporal transmission and climate. *Int J Health Geogr*. 2011;10:25.
5. Chatproedprai S, Theamboonlers A, Korkong S, Thongmee C, Wanankul S, Poovorawan Y. Clinical and molecular characterization of hand-foot-and-mouth disease in Thailand, 2008-2009. *Jpn J Infect Dis*. 2010;63(4):229-33.
6. Puenpa J, Theamboonlers A, Korkong S, Linsuwanon P, Thongmee C, Chatproedprai S, et al. Molecular characterization and complete genome analysis of human enterovirus 71 and coxsackievirus A16 from children with hand, foot and mouth disease in Thailand during 2008-2011. *Arch Virol*. 2011;156(11):2007-13.
7. Hyypia T, Kallajoki M, Maaronen M, Stanway G, Kandolf R, Auvinen P, et al. Pathogenetic differences between coxsackie A and B virus infections in newborn mice. *Virus Res*. 1993;27(1):71-8.
8. van der Linden L, Wolthers KC, van Kuppeveld FJ. Replication and Inhibitors of Enteroviruses and Parechoviruses. *Viruses*. 2015;7(8):4529-62.
9. Rossmann MG. Viral cell recognition and entry. *Protein Sci*. 1994;3(10):1712-25.

10. Tuthill TJ, Groppe E, Hogle JM, Rowlands DJ. Picornaviruses. *Curr Top Microbiol Immunol*. 2010;343:43-89.
11. Hogle JM. Poliovirus cell entry: common structural themes in viral cell entry pathways. *Annu Rev Microbiol*. 2002;56:677-702.
12. Rossmann MG, Arnold E, Erickson JW, Frankenberger EA, Griffith JP, Hecht HJ, et al. Structure of a human common cold virus and functional relationship to other picornaviruses. *Nature*. 1985;317(6033):145-53.
13. Xiao C, Bator-Kelly CM, Rieder E, Chipman PR, Craig A, Kuhn RJ, et al. The crystal structure of coxsackievirus A21 and its interaction with ICAM-1. *Structure*. 2005;13(7):1019-33.
14. Yoder JD, Cifuentes JO, Pan J, Bergelson JM, Hafenstein S. The crystal structure of a coxsackievirus B3-RD variant and a refined 9-angstrom cryo-electron microscopy reconstruction of the virus complexed with decay-accelerating factor (DAF) provide a new footprint of DAF on the virus surface. *J Virol*. 2012;86(23):12571-81.
15. Ren J, Wang X, Hu Z, Gao Q, Sun Y, Li X, et al. Picornavirus uncoating intermediate captured in atomic detail. *Nat Commun*. 2013;4:1929.
16. Cifuentes JO, Lee H, Yoder JD, Shingler KL, Carnegie MS, Yoder JL, et al. Structures of the procapsid and mature virion of enterovirus 71 strain 1095. *J Virol*. 2013;87(13):7637-45.
17. Plevka P, Perera R, Cardoso J, Kuhn RJ, Rossmann MG. Crystal structure of human enterovirus 71. *Science*. 2012;336(6086):1274.
18. Wang X, Peng W, Ren J, Hu Z, Xu J, Lou Z, et al. A sensor-adaptor mechanism for enterovirus uncoating from structures of EV71. *Nat Struct Mol Biol*. 2012;19(4):424-9.
19. Pevear DC, Tull TM, Seipel ME, Groarke JM. Activity of pleconaril against enteroviruses. *Antimicrob Agents Chemother*. 1999;43(9):2109-15.
20. Jiang P, Liu Y, Ma HC, Paul AV, Wimmer E. Picornavirus morphogenesis. *Microbiol Mol Biol Rev*. 2014;78(3):418-37.
21. Wimmer E, Hellen CU, Cao X. Genetics of poliovirus. *Annu Rev Genet*. 1993;27:353-436.

22. Barnabei MS, Sjaastad FV, Townsend D, Bedada FB, Metzger JM. Severe dystrophic cardiomyopathy caused by the enteroviral protease 2A-mediated C-terminal dystrophin cleavage fragment. *Sci Transl Med.* 2015;7(294):294ra106.
23. Hanson PJ, Ye X, Qiu Y, Zhang HM, Hemida MG, Wang F, et al. Cleavage of DAP5 by coxsackievirus B3 2A protease facilitates viral replication and enhances apoptosis by altering translation of IRES-containing genes. *Cell Death Differ.* 2016;23(5):828-40.
24. Mu Z, Wang B, Zhang X, Gao X, Qin B, Zhao Z, et al. Crystal structure of 2A proteinase from hand, foot and mouth disease virus. *J Mol Biol.* 2013;425(22):4530-43.
25. de Jong AS, de Mattia F, Van Dommelen MM, Lanke K, Melchers WJ, Willems PH, et al. Functional analysis of picornavirus 2B proteins: effects on calcium homeostasis and intracellular protein trafficking. *J Virol.* 2008;82(7):3782-90.
26. Echeverri A, Banerjee R, Dasgupta A. Amino-terminal region of poliovirus 2C protein is sufficient for membrane binding. *Virus Res.* 1998;54(2):217-23.
27. Rodriguez PL, Carrasco L. Poliovirus protein 2C contains two regions involved in RNA binding activity. *J Biol Chem.* 1995;270(17):10105-12.
28. Doedens JR, Kirkegaard K. Inhibition of cellular protein secretion by poliovirus proteins 2B and 3A. *EMBO J.* 1995;14(5):894-907.
29. Wessels E, Duijsings D, Lanke KH, van Dooren SH, Jackson CL, Melchers WJ, et al. Effects of picornavirus 3A Proteins on Protein Transport and GBF1-dependent COP-I recruitment. *J Virol.* 2006;80(23):11852-60.
30. Paul AV, van Boom JH, Filippov D, Wimmer E. Protein-primed RNA synthesis by purified poliovirus RNA polymerase. *Nature.* 1998;393(6682):280-4.
31. Takegami T, Kuhn RJ, Anderson CW, Wimmer E. Membrane-dependent uridylylation of the genome-linked protein VPg of poliovirus. *Proc Natl Acad Sci U S A.* 1983;80(24):7447-51.
32. Lin JY, Chen TC, Weng KF, Chang SC, Chen LL, Shih SR. Viral and host proteins involved in picornavirus life cycle. *J Biomed Sci.* 2009;16:103.

33. Norder H, De Palma AM, Selisko B, Costenaro L, Papageorgiou N, Arnan C, et al. Picornavirus non-structural proteins as targets for new anti-virals with broad activity. *Antiviral Res.* 2011;89(3):204-18.
34. Pallansch MA, Roos R. Enteroviruses: polioviruses, coxsackieviruses, echoviruses, and newer enteroviruses. In: *Fields Virology (Volume 1)* Lippincott, Williams & Wilkins, MD, USA. 2001:840-84.
35. Reczek D, Schwake M, Schroder J, Hughes H, Blanz J, Jin X, et al. LIMP-2 is a receptor for lysosomal mannose-6-phosphate-independent targeting of beta-glucocerebrosidase. *Cell.* 2007;131(4):770-83.
36. Lin YW, Yu SL, Shao HY, Lin HY, Liu CC, Hsiao KN, et al. Human SCARB2 transgenic mice as an infectious animal model for enterovirus 71. *PLoS One.* 2013;8(2):e57591.
37. Yamayoshi S, Koike S. Identification of a human SCARB2 region that is important for enterovirus 71 binding and infection. *J Virol.* 2011;85(10):4937-46.
38. Yamayoshi S, Ohka S, Fujii K, Koike S. Functional comparison of SCARB2 and PSGL1 as receptors for enterovirus 71. *J Virol.* 2013;87(6):3335-47.
39. Yamayoshi S, Iizuka S, Yamashita T, Minagawa H, Mizuta K, Okamoto M, et al. Human SCARB2-dependent infection by coxsackievirus A7, A14, and A16 and enterovirus 71. *J Virol.* 2012;86(10):5686-96.
40. Nishimura Y, Shimojima M, Tano Y, Miyamura T, Wakita T, Shimizu H. Human P-selectin glycoprotein ligand-1 is a functional receptor for enterovirus 71. *Nat Med.* 2009;15(7):794-7.
41. Somers WS, Tang J, Shaw GD, Camphausen RT. Insights into the molecular basis of leukocyte tethering and rolling revealed by structures of P- and E-selectin bound to SLe(X) and PSGL-1. *Cell.* 2000;103(3):467-79.
42. Nishimura Y, Wakita T, Shimizu H. Tyrosine sulfation of the amino terminus of PSGL-1 is critical for enterovirus 71 infection. *PLoS Pathog.* 2010;6(11):e1001174.
43. Hajjar KA, Acharya SS. Annexin II and regulation of cell surface fibrinolysis. *Ann N Y Acad Sci.* 2000;902:265-71.

44. Yang SL, Chou YT, Wu CN, Ho MS. Annexin II binds to capsid protein VP1 of enterovirus 71 and enhances viral infectivity. *J Virol*. 2011;85(22):11809-20.
45. Yang B, Chuang H, Yang KD. Sialylated glycans as receptor and inhibitor of enterovirus 71 infection to DLD-1 intestinal cells. *Viol J*. 2009;6:141.
46. Chung PW, Huang YC, Chang LY, Lin TY, Ning HC. Duration of enterovirus shedding in stool. *J Microbiol Immunol Infect*. 2001;34(3):167-70.
47. Chen CS, Yao YC, Lin SC, Lee YP, Wang YF, Wang JR, et al. Retrograde axonal transport: a major transmission route of enterovirus 71 in mice. *J Virol*. 2007;81(17):8996-9003.
48. Saraste A, Arola A, Vuorinen T, Kyto V, Kallajoki M, Pulkki K, et al. Cardiomyocyte apoptosis in experimental coxsackievirus B3 myocarditis. *Cardiovasc Pathol*. 2003;12(5):255-62.
49. Ooi MH, Wong SC, Clear D, Perera D, Krishnan S, Preston T, et al. Adenovirus type 21-associated acute flaccid paralysis during an outbreak of hand-foot-and-mouth disease in Sarawak, Malaysia. *Clin Infect Dis*. 2003;36(5):550-9.
50. Lin YW, Wang SW, Tung YY, Chen SH. Enterovirus 71 infection of human dendritic cells. *Exp Biol Med (Maywood)*. 2009;234(10):1166-73.
51. Chen LC, Shyu HW, Chen SH, Lei HY, Yu CK, Yeh TM. Enterovirus 71 infection induces Fas ligand expression and apoptosis of Jurkat cells. *J Med Virol*. 2006;78(6):780-6.
52. Bergelson JM, Shepley MP, Chan BM, Hemler ME, Finberg RW. Identification of the integrin VLA-2 as a receptor for echovirus 1. *Science*. 1992;255(5052):1718-20.
53. Freimuth P, Philipson L, Carson SD. The coxsackievirus and adenovirus receptor. *Curr Top Microbiol Immunol*. 2008;323:67-87.
54. Fry EE, Newman JW, Curry S, Najjam S, Jackson T, Blakemore W, et al. Structure of Foot-and-mouth disease virus serotype A10 61 alone and complexed with oligosaccharide receptor: receptor conservation in the face of antigenic variation. *J Gen Virol*. 2005;86(Pt 7):1909-20.

55. Greve JM, Davis G, Meyer AM, Forte CP, Yost SC, Marlor CW, et al. The major human rhinovirus receptor is ICAM-1. *Cell*. 1989;56(5):839-47.
56. He Y, Mueller S, Chipman PR, Bator CM, Peng X, Bowman VD, et al. Complexes of poliovirus serotypes with their common cellular receptor, CD155. *J Virol*. 2003;77(8):4827-35.
57. Hofer F, Gruenberger M, Kowalski H, Machat H, Huettinger M, Kuechler E, et al. Members of the low density lipoprotein receptor family mediate cell entry of a minor-group common cold virus. *Proc Natl Acad Sci U S A*. 1994;91(5):1839-42.
58. Huber SA. VCAM-1 is a receptor for encephalomyocarditis virus on murine vascular endothelial cells. *J Virol*. 1994;68(6):3453-8.
59. Israelsson S, Gullberg M, Jonsson N, Roivainen M, Edman K, Lindberg AM. Studies of Echovirus 5 interactions with the cell surface: heparan sulfate mediates attachment to the host cell. *Virus Res*. 2010;151(2):170-6.
60. Powell RM, Ward T, Goodfellow I, Almond JW, Evans DJ. Mapping the binding domains on decay accelerating factor (DAF) for haemagglutinating enteroviruses: implications for the evolution of a DAF-binding phenotype. *J Gen Virol*. 1999;80 ( Pt 12):3145-52.
61. Triantafilou K, Triantafilou M, Takada Y, Fernandez N. Human parechovirus 1 utilizes integrins  $\alpha$ v $\beta$ 3 and  $\alpha$ v $\beta$ 1 as receptors. *J Virol*. 2000;74(13):5856-62.
62. Vlasak M, Goesler I, Blaas D. Human rhinovirus type 89 variants use heparan sulfate proteoglycan for cell attachment. *J Virol*. 2005;79(10):5963-70.
63. Williams CH, Kajander T, Hyypia T, Jackson T, Sheppard D, Stanway G. Integrin  $\alpha$ v $\beta$ 6 is an RGD-dependent receptor for coxsackievirus A9. *J Virol*. 2004;78(13):6967-73.
64. Calandria C, Irurzun A, Barco A, Carrasco L. Individual expression of poliovirus 2A<sub>pro</sub> and 3C<sub>pro</sub> induces activation of caspase-3 and PARP cleavage in HeLa cells. *Virus Res*. 2004;104(1):39-49.

65. Henke A, Launhardt H, Klement K, Stelzner A, Zell R, Munder T. Apoptosis in coxsackievirus B3-caused diseases: interaction between the capsid protein VP2 and the proapoptotic protein siva. *J Virol.* 2000;74(9):4284-90.
66. Li ML, Hsu TA, Chen TC, Chang SC, Lee JC, Chen CC, et al. The 3C protease activity of enterovirus 71 induces human neural cell apoptosis. *Virology.* 2002;293(2):386-95.
67. Liang CC, Sun MJ, Lei HY, Chen SH, Yu CK, Liu CC, et al. Human endothelial cell activation and apoptosis induced by enterovirus 71 infection. *J Med Virol.* 2004;74(4):597-603.
68. Wang YF, Chou CT, Lei HY, Liu CC, Wang SM, Yan JJ, et al. A mouse-adapted enterovirus 71 strain causes neurological disease in mice after oral infection. *J Virol.* 2004;78(15):7916-24.
69. Kuo RL, Kung SH, Hsu YY, Liu WT. Infection with enterovirus 71 or expression of its 2A protease induces apoptotic cell death. *J Gen Virol.* 2002;83(Pt 6):1367-76.
70. Chen SC, Chang LY, Wang YW, Chen YC, Weng KF, Shih SR, et al. Sumoylation-promoted enterovirus 71 3C degradation correlates with a reduction in viral replication and cell apoptosis. *J Biol Chem.* 2011;286(36):31373-84.
71. Buenz EJ, Howe CL. Picornaviruses and cell death. *Trends Microbiol.* 2006;14(1):28-36.
72. Rodriguez PL, Carrasco L. Poliovirus protein 2C has ATPase and GTPase activities. *J Biol Chem.* 1993;268(11):8105-10.
73. Racaniello VR. Picornaviridae: the viruses and their replication. In *Fields Virology*, 5th Ed D M Knipe, and P M Howley, eds, eds Lippincott Williams & Wilkins, Philadelphia. 2007:796–839.
74. Banerjee R, Dasgupta A. Interaction of picornavirus 2C polypeptide with the viral negative-strand RNA. *J Gen Virol.* 2001;82(Pt 11):2621-7.
75. Liu Y, Wang C, Mueller S, Paul AV, Wimmer E, Jiang P. Direct interaction between two viral proteins, the nonstructural protein 2C and the capsid protein VP3, is required for enterovirus morphogenesis. *PLoS Pathog.* 2010 Aug 26;6(8):e1001066.

76. Liu J, Wei T, Kwang J. Avian encephalomyelitis virus nonstructural protein 2C induces apoptosis by activating cytochrome c/caspase-9 pathway. *Virology*. 2004;318(1):169-82.
77. Tang WF, Yang SY, Wu BW, Jheng JR, Chen YL, Shih CH, et al. Reticulon 3 binds the 2C protein of enterovirus 71 and is required for viral replication. *J Biol Chem*. 2007;282(8):5888-98.
78. Zheng Z, Li H, Zhang Z, Meng J, Mao D, Bai B, et al. Enterovirus 71 2C protein inhibits TNF- $\alpha$ -mediated activation of NF- $\kappa$ B by suppressing I $\kappa$ B kinase  $\beta$  phosphorylation. *J Immunol*. 2011 Sep 1;187(5):2202-12.
79. Schmidt NJ, Lennette EH, Ho HH. An apparently new enterovirus isolated from patients with disease of the central nervous system. *J Infect Dis*. 1974;129(3):304-9.
80. van der Sanden S, Koopmans M, Uslu G, van der Avoort H, Dutch Working Group for Clinical V. Epidemiology of enterovirus 71 in the Netherlands, 1963 to 2008. *J Clin Microbiol*. 2009;47(9):2826-33.
81. Ryu WS, Kang B, Hong J, Hwang S, Kim A, Kim J, et al. Enterovirus 71 infection with central nervous system involvement, South Korea. *Emerg Infect Dis*. 2010;16(11):1764-6.
82. Wang SM, Liu CC, Tseng HW, Wang JR, Huang CC, Chen YJ, et al. Clinical spectrum of enterovirus 71 infection in children in southern Taiwan, with an emphasis on neurological complications. *Clin Infect Dis*. 1999;29(1):184-90.
83. Zhang Y, Zhu Z, Yang W, Ren J, Tan X, Wang Y, et al. An emerging recombinant human enterovirus 71 responsible for the 2008 outbreak of hand foot and mouth disease in Fuyang city of China. *Virology*. 2010;7:94.
84. Huang SW, Hsu YW, Smith DJ, Kiang D, Tsai HP, Lin KH, et al. Reemergence of enterovirus 71 in 2008 in taiwan: dynamics of genetic and antigenic evolution from 1998 to 2008. *J Clin Microbiol*. 2009;47(11):3653-62.
85. Herrero LJ, Lee CS, Hurrelbrink RJ, Chua BH, Chua KB, McMinn PC. Molecular epidemiology of enterovirus 71 in peninsular Malaysia, 1997-2000. *Arch Virol*. 2003;148(7):1369-85.



86. Mizuta K, Abiko C, Murata T, Matsuzaki Y, Itagaki T, Sanjoh K, et al. Frequent importation of enterovirus 71 from surrounding countries into the local community of Yamagata, Japan, between 1998 and 2003. *J Clin Microbiol.* 2005;43(12):6171-5.
87. Chan KP, Goh KT, Chong CY, Teo ES, Lau G, Ling AE. Epidemic hand, foot and mouth disease caused by human enterovirus 71, Singapore. *Emerg Infect Dis.* 2003;9(1):78-85.
88. Binford SL, Maldonado F, Brothers MA, Weady PT, Zalman LS, Meador JW, 3rd, et al. Conservation of amino acids in human rhinovirus 3C protease correlates with broad-spectrum antiviral activity of rupintrivir, a novel human rhinovirus 3C protease inhibitor. *Antimicrob Agents Chemother.* 2005;49(2):619-26.
89. De Palma AM, Heggermont W, Lanke K, Coutard B, Bergmann M, Monforte AM, et al. The thiazolobenzimidazole TBZE-029 inhibits enterovirus replication by targeting a short region immediately downstream from motif C in the nonstructural protein 2C. *J Virol.* 2008;82(10):4720-30.
90. De Palma AM, Purstinger G, Wimmer E, Patick AK, Andries K, Rombaut B, et al. Potential use of antiviral agents in polio eradication. *Emerg Infect Dis.* 2008;14(4):545-51.
91. De Palma AM, Vliegen I, De Clercq E, Neyts J. Selective inhibitors of picornavirus replication. *Med Res Rev.* 2008;28(6):823-84.
92. Patick AK. Rhinovirus chemotherapy. *Antiviral Res.* 2006;71(2-3):391-6.
93. Senior K. FDA panel rejects common cold treatment. *Lancet Infect Dis.* 2002;2(5):264.
94. Mao LX, Wu B, Bao WX, Han FA, Xu L, Ge QJ, et al. Epidemiology of hand, foot, and mouth disease and genotype characterization of Enterovirus 71 in Jiangsu, China. *J Clin Virol.* 2010;49(2):100-4.
95. Shah VA, Chong CY, Chan KP, Ng W, Ling AE. Clinical characteristics of an outbreak of hand, foot and mouth disease in Singapore. *Ann Acad Med Singapore.* 2003;32(3):381-7.

96. Wong SS, Yip CC, Lau SK, Yuen KY. Human enterovirus 71 and hand, foot and mouth disease. *Epidemiol Infect.* 2010;138(8):1071-89.
97. Gopalkrishna V, Patil PR, Patil GP, Chitambar SD. Circulation of multiple enterovirus serotypes causing hand, foot and mouth disease in India. *J Med Microbiol.* 2012;61(Pt 3):420-5.
98. Hu YF, Yang F, Du J, Dong J, Zhang T, Wu ZQ, et al. Complete genome analysis of coxsackievirus A2, A4, A5, and A10 strains isolated from hand, foot, and mouth disease patients in China revealing frequent recombination of human enterovirus A. *J Clin Microbiol.* 2011;49(7):2426-34.
99. Ryu WS, Kang B, Hong J, Hwang S, Kim J, Cheon DS. Clinical and etiological characteristics of enterovirus 71-related diseases during a recent 2-year period in Korea. *J Clin Microbiol.* 2010;48(7):2490-4.
100. Tryfonos C, Richter J, Koptides D, Yiangou M, Christodoulou CG. Molecular typing and epidemiology of enteroviruses in Cyprus, 2003-2007. *J Med Microbiol.* 2011;60(Pt 10):1433-40.
101. Chen KT, Chang HL, Wang ST, Cheng YT, Yang JY. Epidemiologic features of hand-foot-mouth disease and herpangina caused by enterovirus 71 in Taiwan, 1998-2005. *Pediatrics.* 2007;120(2):e244-52.
102. Tseng FC, Huang HC, Chi CY, Lin TL, Liu CC, Jian JW, et al. Epidemiological survey of enterovirus infections occurring in Taiwan between 2000 and 2005: analysis of sentinel physician surveillance data. *J Med Virol.* 2007;79(12):1850-60.
103. Yamashita T, Ito M, Taniguchi A, Sakae K. Prevalence of coxsackievirus A5, A6, and A10 in patients with herpangina in Aichi Prefecture, 2005. *Jpn J Infect Dis.* 2005;58(6):390-1.
104. Liu MY, Liu W, Luo J, Liu Y, Zhu Y, Berman H, et al. Characterization of an outbreak of hand, foot, and mouth disease in Nanchang, China in 2010. *PLoS One.* 2011;6(9):e25287.

105. Thoa le PK, Chiang PS, Khanh TH, Luo ST, Dan TN, Wang YF, et al. Genetic and antigenic characterization of enterovirus 71 in Ho Chi Minh City, Vietnam, 2011. *PLoS One*. 2013;8(7):e69895.
106. Wang X, Zhu C, Bao W, Zhao K, Niu J, Yu XF, et al. Characterization of full-length enterovirus 71 strains from severe and mild disease patients in northeastern China. *PLoS One*. 2012;7(3):e32405.
107. Zhang Y, Tan XJ, Wang HY, Yan DM, Zhu SL, Wang DY, et al. An outbreak of hand, foot, and mouth disease associated with subgenotype C4 of human enterovirus 71 in Shandong, China. *J Clin Virol*. 2009;44(4):262-7.
108. Zhao K, Han X, Wang G, Hu W, Zhang W, Yu XF. Circulating coxsackievirus A16 identified as recombinant type A human enterovirus, China. *Emerg Infect Dis*. 2011 Aug;17(8):1537-40.
109. Huang YP, Lin TL, Kuo CY, Lin MW, Yao CY, Liao HW, et al. The circulation of subgenogroups B5 and C5 of enterovirus 71 in Taiwan from 2006 to 2007. *Virus Res*. 2008;137(2):206-12.
110. Chan LG, Parashar UD, Lye MS, Ong FG, Zaki SR, Alexander JP, et al. Deaths of children during an outbreak of hand, foot, and mouth disease in sarawak, malaysia: clinical and pathological characteristics of the disease. For the Outbreak Study Group. *Clin Infect Dis*. 2000;31(3):678-83.
111. Khanh TH, Sabanathan S, Thanh TT, Thoa le PK, Thuong TC, Hang V, et al. Enterovirus 71-associated hand, foot, and mouth disease, Southern Vietnam, 2011. *Emerg Infect Dis*. 2012;18(12):2002-5.
112. Blomqvist S, Klemola P, Kaijalainen S, Paananen A, Simonen ML, Vuorinen T, et al. Co-circulation of coxsackieviruses A6 and A10 in hand, foot and mouth disease outbreak in Finland. *J Clin Virol*. 2010;48(1):49-54.
113. Osterback R, Vuorinen T, Linna M, Susi P, Hyypia T, Waris M. Coxsackievirus A6 and hand, foot, and mouth disease, Finland. *Emerg Infect Dis*. 2009;15(9):1485-8.

114. Wu Y, Yeo A, Phoon MC, Tan EL, Poh CL, Quak SH, et al. The largest outbreak of hand; foot and mouth disease in Singapore in 2008: the role of enterovirus 71 and coxsackievirus A strains. *Int J Infect Dis.* 2010;14(12):e1076-81.
115. Wei SH, Huang YP, Liu MC, Tsou TP, Lin HC, Lin TL, et al. An outbreak of coxsackievirus A6 hand, foot, and mouth disease associated with onychomadesis in Taiwan, 2010. *BMC Infect Dis.* 2011;11:346.
116. Fujimoto T, Iizuka S, Enomoto M, Abe K, Yamashita K, Hanaoka N, et al. Hand, foot, and mouth disease caused by coxsackievirus A6, Japan, 2011. *Emerg Infect Dis.* 2012;18(2):337-9.
117. Montes M, Artieda J, Pineiro LD, Gastesi M, Diez-Nieves I, Cilla G. Hand, foot, and mouth disease outbreak and coxsackievirus A6, northern Spain, 2011. *Emerg Infect Dis.* 2013;19(4).
118. Flett K, Youngster I, Huang J, McAdam A, Sandora TJ, Rennick M, et al. Hand, foot, and mouth disease caused by coxsackievirus a6. *Emerg Infect Dis.* 2012;18(10):1702-4.
119. Puenpa J, Chieochansin T, Linsuwanon P, Korkong S, Thongkomplew S, Vichaiwattana P, et al. Hand, foot, and mouth disease caused by coxsackievirus A6, Thailand, 2012. *Emerg Infect Dis.* 2013;19(4):641-3.
120. Nix WA, Oberste MS, Pallansch MA. Sensitive, seminested PCR amplification of VP1 sequences for direct identification of all enterovirus serotypes from original clinical specimens. *J Clin Microbiol.* 2006;44(8):2698-704.
121. Tamura K, Peterson D, Peterson N, Stecher G, Nei M, Kumar S. MEGA5: molecular evolutionary genetics analysis using maximum likelihood, evolutionary distance, and maximum parsimony methods. *Mol Biol Evol.* 2011;28(10):2731-9.
122. Laxmivandana R, Yergolkar P, Gopalkrishna V, Chitambar SD. Characterization of the non-polio enterovirus infections associated with acute flaccid paralysis in South-Western India. *PLoS One.* 2013;8(4):e61650.

123. Xiang Z, Gonzalez R, Wang Z, Ren L, Xiao Y, Li J, et al. Coxsackievirus A21, enterovirus 68, and acute respiratory tract infection, China. *Emerg Infect Dis*. 2012;18(5):821-4.
124. Di B, Zhang Y, Xie H, Li X, Chen C, Ding P, et al. Circulation of Coxsackievirus A6 in hand-foot-mouth disease in Guangzhou, 2010-2012. *Virology*. 2014;11:157.
125. Sinclair C, Gaunt E, Simmonds P, Broomfield D, Nwafor N, Wellington L, et al. Atypical hand, foot, and mouth disease associated with coxsackievirus A6 infection, Edinburgh, United Kingdom, January to February 2014. *Euro Surveill*. 2014;19(12):20745.
126. Puenpa J, Mauleekoonphairoj J, Linsuwanon P, Suwannakarn K, Chieochansin T, Korkong S, et al. Prevalence and characterization of enterovirus infections among pediatric patients with hand foot mouth disease, herpangina and influenza like illness in Thailand, 2012. *PLoS One*. 2014;9(6):e98888.
127. Bendig JW, O'Brien PS, Muir P. Serotype-specific detection of coxsackievirus A16 in clinical specimens by reverse transcription-nested PCR. *J Clin Microbiol*. 2001;39(10):3690-2.
128. Brown BA, Kilpatrick DR, Oberste MS, Pallansch MA. Serotype-specific identification of enterovirus 71 by PCR. *J Clin Virol*. 2000;16(2):107-12.
129. Chen TC, Chen GW, Hsiung CA, Yang JY, Shih SR, Lai YK, et al. Combining multiplex reverse transcription-PCR and a diagnostic microarray to detect and differentiate enterovirus 71 and coxsackievirus A16. *J Clin Microbiol*. 2006;44(6):2212-9.
130. Cui A, Xu C, Tan X, Zhang Y, Zhu Z, Mao N, et al. The development and application of the two real-time RT-PCR assays to detect the pathogen of HFMD. *PLoS One*. 2013;8(4):e61451.
131. Tan EL, Chow VT, Quak SH, Yeo WC, Poh CL. Development of multiplex real-time hybridization probe reverse transcriptase polymerase chain reaction for specific detection and differentiation of Enterovirus 71 and Coxsackievirus A16. *Diagn Microbiol Infect Dis*. 2008;61(3):294-301.

132. Xiao XL, He YQ, Yu YG, Yang H, Chen G, Li HF, et al. Simultaneous detection of human enterovirus 71 and coxsackievirus A16 in clinical specimens by multiplex real-time PCR with an internal amplification control. *Arch Virol*. 2009;154(1):121-5.
133. Zhang S, Wang J, Yan Q, He S, Zhou W, Ge S, et al. A one-step, triplex, real-time RT-PCR assay for the simultaneous detection of enterovirus 71, coxsackie A16 and pan-enterovirus in a single tube. *PLoS One*. 2014;9(7):e102724.
134. Zhang L, Wang X, Zhang Y, Gong L, Mao H, Feng C, et al. Rapid and sensitive identification of RNA from the emerging pathogen, coxsackievirus A6. *Virology*. 2012;9:298.
135. Payungporn S, Chutinimitkul S, Chaisingh A, Damrongwattanapokin S, Buranathai C, Amonsin A, et al. Single step multiplex real-time RT-PCR for H5N1 influenza A virus detection. *J Virol Methods*. 2006;131(2):143-7.
136. Oberste MS, Maher K, Kilpatrick DR, Pallansch MA. Molecular evolution of the human enteroviruses: correlation of serotype with VP1 sequence and application to picornavirus classification. *J Virol*. 1999;73(3):1941-8.
137. Schuffenecker I, Mirand A, Antona D, Henquell C, Chomel JJ, Archimbaud C, et al. Epidemiology of human enterovirus 71 infections in France, 2000-2009. *J Clin Virol*. 2011;50(1):50-6.
138. Hayman R, Shepherd M, Tarring C, Best E. Outbreak of variant hand-foot-and-mouth disease caused by coxsackievirus A6 in Auckland, New Zealand. *J Paediatr Child Health*. 2014;50(10):751-5.
139. Tan X, Li L, Zhang B, Jorba J, Su X, Ji T, et al. Molecular epidemiology of coxsackievirus A6 associated with outbreaks of hand, foot, and mouth disease in Tianjin, China, in 2013. *Arch Virol*. 2015;160(4):1097-104.
140. Ben-Chetrit E, Wiener-Well Y, Shulman LM, Cohen MJ, Elinav H, Sofer D, et al. Coxsackievirus A6-related hand foot and mouth disease: skin manifestations in a cluster of adult patients. *J Clin Virol*. 2014;59(3):201-3.

141. Buttery VW, Kenyon C, Grunewald S, Oberste MS, Nix WA. Atypical Presentations of Hand, Foot, and Mouth Disease Caused by Coxsackievirus A6-- Minnesota, 2014. *MMWR Morb Mortal Wkly Rep.* 2015;64(29):805.
142. Chatproedprai S, Tempark T, Wanlapakorn N, Puenpa J, Wananukul S, Poovorawan Y. Unusual skin manifestation of hand, foot and mouth disease associated with coxsackievirus A6: cases report. *Springerplus.* 2015;4:362.
143. Feder HM, Jr., Bennett N, Modlin JF. Atypical hand, foot, and mouth disease: a vesiculobullous eruption caused by Coxsackie virus A6. *Lancet Infect Dis.* 2014;14(1):83-6.
144. Lott JP, Liu K, Landry ML, Nix WA, Oberste MS, Bolognia J, et al. Atypical hand-foot-and-mouth disease associated with coxsackievirus A6 infection. *J Am Acad Dermatol.* 2013;69(5):736-41.
145. Yasui Y, Makino T, Hanaoka N, Owa K, Horikoshi A, Tanaka A, et al. A case of atypical hand-foot-and-mouth disease caused by coxsackievirus A6: differential diagnosis from varicella in a pediatric intensive care unit. *Jpn J Infect Dis.* 2013;66(6):564-6.
146. Gaunt E, Harvala H, Osterback R, Sreenu VB, Thomson E, Waris M, et al. Genetic characterization of human coxsackievirus A6 variants associated with atypical hand, foot and mouth disease: a potential role of recombination in emergence and pathogenicity. *J Gen Virol.* 2015;96(Pt 5):1067-79.
147. Simmonds P. SSE: a nucleotide and amino acid sequence analysis platform. *BMC Res Notes.* 2012;5:50.
148. Tamura K, Stecher G, Peterson D, Filipski A, Kumar S. MEGA6: Molecular Evolutionary Genetics Analysis version 6.0. *Mol Biol Evol.* 2013;30(12):2725-9.
149. Drummond AJ, Rambaut A. BEAST: Bayesian evolutionary analysis by sampling trees. *BMC Evol Biol.* 2007;7:214.
150. Drummond AJ, Suchard MA, Xie D, Rambaut A. Bayesian phylogenetics with BEAUti and the BEAST 1.7. *Mol Biol Evol.* 2012;29(8):1969-73.

151. McWilliam Leitch EC, Bendig J, Cabrerizo M, Cardoso J, Hyypia T, Ivanova OE, et al. Transmission networks and population turnover of echovirus 30. *J Virol.* 2009;83(5):2109-18.
152. McWilliam Leitch EC, Cabrerizo M, Cardoso J, Harvala H, Ivanova OE, Koike S, et al. The association of recombination events in the founding and emergence of subgenogroup evolutionary lineages of human enterovirus 71. *J Virol.* 2012;86(5):2676-85.
153. McWilliam Leitch EC, Cabrerizo M, Cardoso J, Harvala H, Ivanova OE, Kroes AC, et al. Evolutionary dynamics and temporal/geographical correlates of recombination in the human enterovirus echovirus types 9, 11, and 30. *J Virol.* 2010;84(18):9292-300.
154. Baek K, Yeo S, Lee B, Park K, Song J, Yu J, et al. Epidemics of enterovirus infection in Chungnam Korea, 2008 and 2009. *Virol J.* 2011;8:297.
155. Zeng M, El Khatib NF, Tu S, Ren P, Xu S, Zhu Q, et al. Seroepidemiology of Enterovirus 71 infection prior to the 2011 season in children in Shanghai. *J Clin Virol.* 2012;53(4):285-9.
156. He YQ, Chen L, Xu WB, Yang H, Wang HZ, Zong WP, et al. Emergence, circulation, and spatiotemporal phylogenetic analysis of coxsackievirus a6- and coxsackievirus a10-associated hand, foot, and mouth disease infections from 2008 to 2012 in Shenzhen, China. *J Clin Microbiol.* 2013;51(11):3560-6.
157. Lu QB, Zhang XA, Wo Y, Xu HM, Li XJ, Wang XJ, et al. Circulation of Coxsackievirus A10 and A6 in hand-foot-mouth disease in China, 2009-2011. *PLoS One.* 2012;7(12):e52073.
158. Mirand A, Henquell C, Archimbaud C, Ughetto S, Antona D, Bailly JL, et al. Outbreak of hand, foot and mouth disease/herpangina associated with coxsackievirus A6 and A10 infections in 2010, France: a large citywide, prospective observational study. *Clin Microbiol Infect.* 2012;18(5):E110-8.
159. Lee MH, Huang LM, Wong WW, Wu TZ, Chiu TF, Chang LY. Molecular diagnosis and clinical presentations of enteroviral infections in Taipei during the 2008 epidemic. *J Microbiol Immunol Infect.* 2011;44(3):178-83.



160. Park K, Lee B, Baek K, Cheon D, Yeo S, Park J, et al. Enteroviruses isolated from herpangina and hand-foot-and-mouth disease in Korean children. *Virology*. 2012;9:205.
161. Lin KH, Hwang KP, Ke GM, Wang CF, Ke LY, Hsu YT, et al. Evolution of EV71 genogroup in Taiwan from 1998 to 2005: an emerging of subgenogroup C4 of EV71. *J Med Virol*. 2006;78(2):254-62.
162. Norder H, Bjerregaard L, Magnius L, Lina B, Aymard M, Chomel JJ. Sequencing of 'untypable' enteroviruses reveals two new types, EV-77 and EV-78, within human enterovirus type B and substitutions in the BC loop of the VP1 protein for known types. *J Gen Virol*. 2003;84(Pt 4):827-36.
163. Stirk HJ, Thornton JM. The BC loop in poliovirus coat protein VP1: an ideal acceptor site for major insertions. *Protein Eng*. 1994;7(1):47-56.
164. Claas ECJ, Melchers WJG, van den Brule AJC. The role of real-time PCR in routine microbial diagnostics. . In *Real-time PCR in microbiology: From diagnosis to characterization* Edited by Mackay IM Norfolk: Caister Academic Presse Med 2007:231–67.
165. Hu X, Zhang Y, Zhou X, Xu B, Yang M, Wang M, et al. Simultaneously typing nine serotypes of enteroviruses associated with hand, foot, and mouth disease by a GeXP analyzer-based multiplex reverse transcription-PCR assay. *J Clin Microbiol*. 2012;50(2):288-93.
166. Holmes EC. Molecular clocks and the puzzle of RNA virus origins. *J Virol*. 2003;77(7):3893-7.
167. Cabrerizo M, Trallero G, Simmonds P. Recombination and evolutionary dynamics of human echovirus 6. *J Med Virol*. 2014;86(5):857-64.
168. Calvert J, Chieochansin T, Benschop KS, McWilliam Leitch EC, Drexler JF, Grywna K, et al. Recombination dynamics of human parechoviruses: investigation of type-specific differences in frequency and epidemiological correlates. *J Gen Virol*. 2010;91(Pt 5):1229-38.

169. McIntyre CL, McWilliam Leitch EC, Savolainen-Kopra C, Hovi T, Simmonds P. Analysis of genetic diversity and sites of recombination in human rhinovirus species C. *J Virol.* 2010;84(19):10297-310.
170. Gullberg M, Tolf C, Jonsson N, Mulders MN, Savolainen-Kopra C, Hovi T, et al. Characterization of a putative ancestor of coxsackievirus B5. *J Virol.* 2010;84(19):9695-708.
171. Jenkins GM, Rambaut A, Pybus OG, Holmes EC. Rates of molecular evolution in RNA viruses: a quantitative phylogenetic analysis. *J Mol Evol.* 2002;54(2):156-65.
172. Linsuwanon P, Puenpa J, Suwannakarn K, Auksornkitti V, Vichiwattana P, Korkong S, et al. Molecular epidemiology and evolution of human enterovirus serotype 68 in Thailand, 2006-2011. *PLoS One.* 2012;7(5):e35190.
173. Lukashev AN, Shumilina EY, Belalov IS, Ivanova OE, Eremeeva TP, Reznik VI, et al. Recombination strategies and evolutionary dynamics of the Human enterovirus A global gene pool. *J Gen Virol.* 2014;95(Pt 4):868-73.
174. Mirand A, Schuffenecker I, Henquell C, Billaud G, Jugie G, Falcon D, et al. Phylogenetic evidence for a recent spread of two populations of human enterovirus 71 in European countries. *J Gen Virol.* 2010;91(Pt 9):2263-77.
175. Smura T, Blomqvist S, Vuorinen T, Ivanova O, Samoilovich E, Al-Hello H, et al. The evolution of Vp1 gene in enterovirus C species sub-group that contains types CVA-21, CVA-24, EV-C95, EV-C96 and EV-C99. *PLoS One.* 2014;9(4):e93737.
176. Takeda N, Tanimura M, Miyamura K. Molecular evolution of the major capsid protein VP1 of enterovirus 70. *J Virol.* 1994;68(2):854-62.
177. Tee KK, Lam TT, Chan YF, Bible JM, Kamarulzaman A, Tong CY, et al. Evolutionary genetics of human enterovirus 71: origin, population dynamics, natural selection, and seasonal periodicity of the VP1 gene. *J Virol.* 2010;84(7):3339-50.
178. Yip CC, Lau SK, Lo JY, Chan KH, Woo PC, Yuen KY. Genetic characterization of EV71 isolates from 2004 to 2010 reveals predominance and persistent circulation of the newly proposed genotype D and recent emergence of a distinct lineage of subgenotype C2 in Hong Kong. *Virol J.* 2013;10:222.

179. Zhang Y, Wang D, Yan D, Zhu S, Liu J, Wang H, et al. Molecular evidence of persistent epidemic and evolution of subgenotype B1 coxsackievirus A16-associated hand, foot, and mouth disease in China. *J Clin Microbiol.* 2010;48(2):619-22.
180. Lukashev AN, Lashkevich VA, Ivanova OE, Koroleva GA, Hinkkanen AE, Ilonen J. Recombination in circulating Human enterovirus B: independent evolution of structural and non-structural genome regions. *J Gen Virol.* 2005;86(Pt 12):3281-90.
181. Bailly JL, Mirand A, Henquell C, Archimbaud C, Chambon M, Charbonne F, et al. Phylogeography of circulating populations of human echovirus 30 over 50 years: nucleotide polymorphism and signature of purifying selection in the VP1 capsid protein gene. *Infect Genet Evol.* 2009;9(4):699-708.



## VITA

Name: Miss Jiratchaya Puenpa

Birthday: August 8, 1987 Birth place: Bangkok, Thailand

Education:

2013-2016 Ph.D., Biomedical Science, Faculty of Medicine, Chulalongkorn University

2010-2012 M.Sc., Biomedical Science, Faculty of Medicine, Chulalongkorn University

2005-2008 B.Sc., Biochemistry, Faculty of Science, Chulalongkorn University

Research Experiences:

2015 Visiting scholar at the Roslin Institute, University of Edinburgh, UK

## Publications:

1. Puenpa J, Vongpunsawad S, Osterback R, Waris M, Eriksson E, Albert J, Midgley S, Fischer TK, Eis-Hübinger AM, Cabrerizo M, Gaunt E, Simmonds P, Poovorawan Y. Molecular epidemiology and the evolution of human coxsackievirus A6. *J Gen Virol.* (pending)
2. Puenpa J, Suwannakarn K, Chansaenroj J, Korkong S, Poovorawan Y. Development of the single step multiplex real-time RT-PCR assays for rapid and differentiation of Enterovirus 71, Coxsackievirus A16 and Coxsackievirus A6. (pending)
3. Mauleekoonphairoj J, Puenpa J, Korkong S, Vongpunsawad S, Poovorawan Y. Prevalence of human enterovirus among patients with hand, foot, and mouth disease and herpangina in Thailand, 2013. *Southeast Asian J Trop Med Public Health.* 2015 Nov;46(6):1013-20.
4. Mauleekoonphairoj J, Vongpunsawad S, Puenpa J, Korkong S, Poovorawan Y. Complete genome sequence analysis of enterovirus 71 isolated from children with hand, foot, and mouth disease in Thailand, 2012-2014. *Virus Genes.* 2015 Oct;51(2):290-3.
5. Chatproedprai S, Tempark T, Wanlapakorn N, Puenpa J, Wananukul S, Poovorawan Y. Unusual skin manifestation of hand, foot and mouth disease associated with coxsackievirus A6: cases report. *Springerplus.* 2015 Jul 17;4:362.
6. Chansaenroj J, Vongpunsawad S, Puenpa J, Theamboonlers A, Vuthitanachot V, Chattakul P, Areechokchai D, Poovorawan Y. Epidemic outbreak of acute haemorrhagic conjunctivitis caused by coxsackievirus A24 in Thailand, 2014. *Epidemiol Infect.* 2015 Oct;143(14):3087-93.
7. Puenpa J, Mauleekoonphairoj J, Linsuwanon P, Suwannakarn K, Chieochansin T, Korkong S, Theamboonlers A, Poovorawan Y. Prevalence and characterization of enterovirus infections among pediatric patients with hand foot mouth disease, herpangina and influenza like illness in Thailand, 2012. *PLoS One.* 2014 Jun 2;9(6):e98888.
8. Linsuwanon P, Puenpa J, Huang SW, Wang YF, Mauleekoonphairoj J, Wang JR, Poovorawan Y. Epidemiology and seroepidemiology of human enterovirus 71 among Thai populations. *J Biomed Sci.* 2014 Feb 18;21:16.
9. Puenpa J, Chieochansin T, Linsuwanon P, Korkong S, Thongkomplew S, Vichaiwattana P, Theamboonlers A, Poovorawan Y. Hand, foot, and mouth disease caused by coxsackievirus A6, Thailand, 2012. *Emerg Infect Dis.* 2013 Apr;19(4):641-3.
10. Linsuwanon P, Puenpa J, Suwannakarn K, Auksornkitti V, Vichaiwattana P, Korkong S, Theamboonlers A, Poovorawan Y. Molecular epidemiology and evolution of human enterovirus serotype 68 in Thailand, 2006-2011. *PLoS One.* 2012;7(5):e35190.
11. Puenpa J, Theamboonlers A, Korkong S, Linsuwanon P, Thongmee C, Chatproedprai S, Poovorawan Y. Molecular characterization and complete genome analysis of human enterovirus 71 and coxsackievirus A16 from children with hand, foot and mouth disease in Thailand during 2008-2011. *Arch Virol.* 2011 Nov;156(11):2007-13.